INVESTIGATION OF PERFORMANCE AND CHARACTERISTICS OF A MULTI-CYLINDER GASOLINE ENGINE WITH CONTROLLED AUTO-IGNITION COMBUSTION IN NATURALLY ASPIRATED AND BOOSTED OPERATION

A thesis submitted for the degree of Doctor of Philosophy

by

Mario Eduardo Santos Martins

School of Engineering and Design
Brunel University
United Kingdom

August 2007

Brunel University
School of Engineering and Design
United Kingdom

Mario Eduardo Santos Martins

Investigation of Performance and Characteristics of a Multi-Cylinder Gasoline Engine with Controlled Auto-Ignition Combustion in Naturally Aspirated and Boosted Operation

August 2007

Abstract

Controlled Auto-Ignition (CAI) also known as Homogeneous Charge Compression Ignition (HCCI) is increasingly seen as a very effective way of lowering both fuel consumption and emissions. Hence, it is regarded as one of the best ways to meet stringent future emissions legislation. It has however, still many problems to overcome, such as limited operating range.

This combustion concept was achieved in a production type, 4-cylinder gasoline engine, in two separated tests: naturally aspirated and turbocharged. Very few modifications to the original engine were needed. These consisted basically of a new set of camshafts for the naturally aspirated test and new camshafts plus turbocharger for the boosted test.

The first part of investigation shows that naturally aspirated CAI could be readily achieved from 1000 to 3500rpm. The load range, however, decreased noticeably with engine speed due to flow restrictions imposed by the low lift camshafts. Ultra-low levels of NO_x emissions and reduced fuel consumption were observed.

After baseline experiments with naturally aspirated operation, the capability of turbocharging for extended CAI operation was investigated. The results show that the CAI range could achieve higher load and speed with the addition of the turbocharger. The engine showed increased fuel consumption due to excessive pumping losses. Emissions, however, have been reduced substantially in comparison to the original engine. NO_x levels could be reduced by up to 98% when compared to a standard SI production engine.

Acknowledgements

I would like to express, first and foremost, my deep gratitude to Professor Hua Zhao for all his help and support during the course of this project. I owe to him all the knowledge and experience acquired during the past 4 years. By accepting me as his PhD Student, he also made possible my stay in UK, which was a wonderful life experience.

I would like to thank CAPES for the financial support that made possible my stay in this country.

I would like to acknowledge Ford and Mr. Tabrez Mughis for all the support and information during this research.

I would like to express my gratitude to the continual assistance of various technicians for their expertise and assistance for commissioning the test cell and for several other problems that they have helped me with. Special thanks go to Clive Barrett, Andy Sellway, Ken Anstiss, John Langdon and Bob Webb.

I would like to thank my colleagues and friends Kiranjeev Gill, Navin Kalian, Jake (Changho) Yang and Kayiu Man for their continuous help and support in solving the problems that happen during this period and for their friendship that always helped me to keep motivated during difficult moments.

I would also like to thank all my other colleagues and friends for their company, friendship and moral support that made this a joyful time.

Finally, my most sincere gratitude goes to my family, which gave me the conditions to be here and which always helped me to keep my faith and motivation high, giving me the strength and support to overcome the difficulties and to make the most of this experience.

Nomenclature

General Abbreviations

AC	Alternate Current
ACEA	European Automobile Manufacturers' Association
AFR	Air/Fuel Ratio
AFRS	Stoichiometric Air/Fuel Ratio
ARC	Active Radical Combustion
ATAC	Active Thermo Atmosphere Combustion
ATDC	After Top Dead Center
BDC	Bottom Dead Center
BMEP	Brake Mean Effective Pressure
BSCO	Brake Specific Carbon Monoxide
BSFC	Brake Specific Fuel Consumption
BSHC	Brake Specific Hydro-Carbons
BSNO	Brake Specific Nitrogen Oxides
BTDC	Before Top Dead Center
CA	Crank Angle
CA	Crank Angle
CAAA	Clean Air Act Amendments
CAI	Controlled Auto-Ignition
CARB	Californian Air Resource Board
CI	Compression Ignition
CR	Compression Ratio
DAQ	Data Acquisition Board
DI	Direct Injection
ECU	Electronic Control Unit
EGR	Exhaust Gas Re-circulation
EPA	Environmental Protection Agency-USA
EVC	Exhaust Valve Closing
EVO	Exhaust Valve Opening
FID	Flame Ionization Detection
FTP	Federal Test Procedure
GDI	Gasoline Direct Injection
HCCI	Homogeneous Charge Compression Ignition

HEV	Hybrid Electric Vehicle
IC	Internal Combustion
IMEP	Indicated Mean Effective Pressure
ISCO	Indicated Specific Carbon Monoxide
ISFC	Indicated Specific Fuel Consumption
ISHC	Indicated Specific Hydro-carbons
ISNO	Indicated Specific Nitrogen Oxides
IVC	Intake Valve Closing
IVO	Intake Valve Opening
JAMA	Japan Automobile Manufacturers' Association
KAMA	Korean Automobile Manufacturers' Association
LEV	Low Emission Vehicle
MBT	Minimum Spark Advance for Best Torque
MFB	Mass Fraction Burn
MHI	Mitsubishi Heavy Industries
MPD	Magneto-Pneumatic Detection
NDIR	Non-Dispersive Infrared
NIMEP	Net Indicated Mean Effective Pressure
NOx	Nitrogen Oxides
NVO	Negative Valve Overlap
NVO	Negative Valve Overlap
PC	Personal Computer
PM	Particulate Matter
PMEP	Pumping Mean Effective Pressure
ppm	Parts per Million
PRF	Primary Reference Fuel
PZEV	Partial Zero Emissions Vehicle
RESS	Rechargeable Energy Storage System
RON	Research Octane Number
rpm	Revolutions per Minute
SAE	Society of Automotive Engineers
SCR	Selective Catalyst Reduction
SI	Spark Ignition
SULEV	Super Low Emissions Vehicle
TDC	Top Dead Center

TLEV	Transitional Low Emissions Vehicle
TPS	Throttle Position Sensor
uHC	Unburned Hydrocarbons
ULEV	Ultra Low Emissions Vehicle
VBA	Visual Basic for Applications
VCT	Variable Compression Ratio
VCT	Variable Cam Timing
VGT	Variable Geometry Turbocharger
VOC	Variable Organic Compounds
VR	Variable Reluctance
VVA	Variable Valve Actuation
WOT	Wide Open Throttle
ZEV	Zero Emission Vehicle

Contents **Page**

1. Introduction

Mobility has always played a crucial role for humanity. In all eras, man is always trying to find ways to transport people and goods for long distances and at the highest possible speeds. The advent of the motorcar has transformed the way man interacts with the world. It is actually hard to imagine the world without it. This invention, however, would not have been possible without the contribution of the internal combustion engine, which dates back to 1870 when Nicholaus Otto built the first four-stroke internal combustion engine.

Once applied to the automobile, the internal combustion engine has changed the way people travel and move goods in a revolutionary way. Just as the steam engine had made railroads possible, the internal combustion engine has made moving heavy loads without rails much easier and more practical. This is a transportation technology acting as a catalyst to modern consumer culture whose importance cannot be overstated.

The technology of IC engine has been continuously evolving ever since it was first developed. Cleaner and more fuel efficient engines have been built. Environmental awareness has led to the development of legislation to limit emissions. At the same time, global warming and the need to reduce fossil fuel burn has become a major concern, requiring further developments in fuel efficiency and taking the emissions legislation to much stricter levels.

New technologies and alternatives for IC engines have been proposed and researched for the last century. Concepts such as electric and hybrid vehicles, fuel cell powered cars, hydrogen fuel, etc. are considered possible solutions.

However, until now there is no readily available replacement for the internal combustion engine. All other alternatives suffer from high cost, efficiency issues, low power density, energy storage difficulties, lack of infrastructure, etc.

Thus, measures that could make the current IC engine more environmentally friendly would certainly be very welcome. In this sense, new after-treatment systems have been

developed and even more efficient engines have been produced. Concepts such as downsizing, variable valve operation, turbocharging, cylinder deactivation, etc. have become more common.

A new technology that has proved to be very effective in achieving both low emissions and fuel consumption is an alternative combustion technology known as Controlled Auto-Ignition (CAI) or Homogeneous Charge Compression Ignition (HCCI). This combustion method produces very low levels of NO_x and has been seen as a way forward in engines technology. It is able to achieve the emissions levels determined by future legislation without the need for expensive and complicated exhaust after-treatment.

CAI combustion is a concept that relies on controlling the temperature, pressure and composition of the intake charge so the mixture auto-ignites. Up to now, researchers have been using various methods for achieving CAI combustion. One of the most feasible ways seems to be the use of variable valve timing systems to trap large amount of exhaust residuals and provide the energy needed for auto-ignition. This also has the advantage of controlling the heat release. However the use of trapped residuals to promote CAI and the changes needed in the valve train end up limiting the achievable power range. In order to have an engine suitable for automotive applications, any way to extend the power range is very desirable.

Thus, it is envisaged that forced induction through a turbocharger would extend the operating range to higher loads and produce an engine closer to the expected automotive applications.

Initially, baseline research will be carried out in a naturally aspirated engine running on CAI. The engine has custom built camshafts for running in a negative valve overlap configuration. It will be tested to establish its operating range, and to analyze its performance, emissions and fuel consumption. After that, the engine will be equipped with a turbocharger and a new intake camshaft for the turbocharged operation. The impacts of boost and several other variables over the SI and CAI operation will be investigated.

1.1 Objectives of the Project

The objectives of the project are:

(i) To improve the understanding of CAI combustion operation in a multi-cylinder engine with residual gas trapping via negative valve overlap and to determine its operating range.

(ii) To carry out a detailed analysis of the NA CAI engine performance, emissions and combustion to generate baseline parameters for comparing with the turbocharged part of the experiment and to identify areas of improvement.

(iii) To investigate CAI combustion under forced induction via turbocharging and to determine the possible CAI range increase that can be achieved with boosting, as well as to analyze performance, emissions, fuel consumption and combustion.

(iv) To study the variables affecting the Turbocharged CAI operation, to investigate the problems and pitfalls of, and to propose measures for improvement and future work routes.

1.2 Outline of Thesis

Following introduction, Chapter 2 provides a review of relevant literature relating to the project. Its first part is an overview of global warming and climate change, together with a description on how emissions legislation begun and evolved with time. The second part gives information about the state-of-the art engine technology. The third part introduces a novel combustion system called Controlled Auto-Ignition (CAI/HCCI) and explains the basics of it. The final part shows its limits and potential problems to overcome before the technology goes to road and summarizes this section.

Chapter 3 describes the general set-up of the test facility. The details of dynamometer are presented. The two different set-ups (naturally aspirated and turbocharged) are explained.

The ECU is described, as well as the variable camshaft timing mechanism. The equipment and sensors used for monitoring the engine data acquisition system are listed.

Chapter 4 describes the data acquisition system used to obtain pressure data, its operating principle, and methods used to validate acquired data. In addition, load, specific fuel consumption as well as specific emission calculations are listed. Finally, the method used to obtain the heat release rate and the 10%, 50% and 90% MFB is also detailed.

Chapter 5 describes the naturally aspirated CAI experiments. The concept of negative valve overlap is introduced and the way to obtain it is explained. The operation and test procedure for the NA CAI engine is explained. Data of performance and emissions is analyzed and compared to data from a standard SI engine. Detailed in-cylinder conditions and combustion analysis are carried out to provide a baseline for the turbocharged operation.

Chapter 6 investigates the potential of turbocharging for enlarging the CAI operational range. It describes the methodology used during the Turbocharged CAI test. Turbocharged operation with NVO is explained. The engine operation and test procedure are described. A performance and emissions overview is carried out, followed by a comparative analysis with the NA CAI engine and the standard SI engine. The effects of boost and trapped residuals on engine performance and economy are explored, as well as the effects of spark timing and air/fuel ratio. Operating variables for best fuel economy are outlined. In-cylinder conditions and combustion analysis are presented and discussed.

Chapter 7 presents the conclusions obtained from the experimental work during this project. It describes the potential, drawbacks and areas of possible improvement for Turbocharged CAI. This chapter also contains some guidelines and recommendations for future work.

2. Literature Review

2.1 Introduction

By the year 2000, the 1990s was considered the warmest decade in the warmest century of the last millennium [1]. Most scientists agree that human activities such as burning fossil fuels are the main source of greenhouse gas emissions and hence climate change. Moreover, since instrumental records began in 1861, the ten warmest years have all occurred since 1994. 1998 was the warmest year and 2005 reached almost the same level. If no action is taken to reduce greenhouse gas emissions, global temperatures are expected to rise from 1.4 to 5.8°C by 2100 and sea level could also rise by between 9 and 88 centimetres compared to 1990 levels [2].

In the UK, the greenhouse emissions from the transport sector, which are Carbon Dioxide (CO_2), Volatile Organic Compounds (VOC), and Oxides of Nitrogen (NO_x) are currently 25% of the total. The increase in people's prosperity tends to make them travel in ways that use more carbon. For this reason, road transport CO_2 emissions grew by 8% between 1990 and 2000 even though average new car fuel efficiency has improved around 10% since 1997. Although the link between traffic growth and economic growth has weakened in the past few years, forecasts still indicate an emissions growth of 8% between 2000 and 2010 [2,3].

Reflecting the concern about the steep growth in CO_2 emissions levels, the Kyoto Protocol was open to signature and signed by many nations since 1997, setting up individual targets for emissions reduction. Under this protocol, the UK has agreed to a reduction of 12% in total CO_2 emissions by 2010. The protocol came into force in 2005. [4]. In addition, the European Union, under the European Community Strategy to reduce CO_2 emissions from cars, has negotiated voluntary agreements to reduce CO_2 emissions with car manufacturers. Commitments have been concluded with the European (European Automobile Manufacturers' Association - ACEA), the Japanese (Japan Automobile Manufacturers' Association - JAMA) and Korean (Korean Automobile Manufacturers' Association - KAMA) automobile industries.

All three commitments are equivalent and have as objective to reduce average new car CO_2 emissions to 140g/km by 2008-9, mainly through technological development. The

other two pillars are to improve consumer information on the fuel-economy of automobiles and to develop marketing strategies to influence motorists' choice towards more fuel efficient vehicles [5].

In UK, further measure to deliver savings by 2010 include the Renewable Transport Fuel Obligation which will require 5% of all UK fuel sales to come from renewable sources by 2010-11 and further improving the efficiency of new vehicles through fiscal incentives and by working to develop options on how to move forward beyond the first phase of the EU voluntary agreements with automotive manufacturers after 2008 [6].

The above mentioned protocols and agreements are, therefore, putting enormous pressure over the automotive industry, which is trying to comply with them by using several alternatives. Its main goal, when it comes to IC engines, is to make them more fuel-efficient and less pollutant, in an effort to reduce their environmental impact.

Burning fossil fuels has predominantly two types of emissions: global effect and local effect emissions. CO_2 has mainly global effects. The main impact of carbon dioxide on the environment is as a greenhouse gas, leading to global warming. The concentration of carbon dioxide in the atmosphere has increased by around 30% since the industrial revolution, mainly as a result of the combustion of fossil fuels. Carbon dioxide represents almost 80% of the total UK global warming emissions contribution, the other major contributions being from methane and nitrous oxide.

The local effect emissions are the ground level generated NO_x and VOC, which react with oxygen in the presence of sunlight to produce ozone and photochemical smog, potential causes of respiratory problems, as well as acid rain. CO resulting from incomplete carbon oxidation can cause minor headaches and dizziness up to unconsciousness and respiratory failure, if inhaled in concentrations sufficiently high. In addition, the production of particulate matter (PM) in fuel rich combustion can cause lung problems and has carcinogenic effects.

Vehicle emissions have fallen dramatically over the past decades, largely through the use of exhaust gas after treatment, such as catalytic converters and developments in engine control systems. This has been motivated by increasingly tight emissions regulations all

over the world. Emissions legislation came in force in United States, European Union, Japan and several other countries to set-up targets leading to less pollutant vehicles.

Although having local specific legislation, many countries have their regulations inspired by USA and European standards.

European emissions regulation first appeared in the 1970s. Nowadays, regulation covers CO (carbon monoxide), HC (hydrocarbons), NOx (nitrogen oxides) and PM (particulate matter). Five steps of legislative emissions reduction took place before the 1990s, when the first of the Euro standards was adopted. Euro IV came into force on 1st of January 2006 for new types and 1st of January 2007 for all new registrations, leading to an additional 50% cut in emissions compared to Euro III (Table 2.1). It can be noticed the significant reduction in emissions limits from EURO I to EURO IV and, moreover, from the present EURO IV to the 2009 coming EURO V and proposed EURO VI in 2014.

In the United States, under the Clean Air Act Amendments (CAAA) of 1990 and on enforcement by EPA, two sets of standards have been defined for light-duty vehicles: Tier 1 standards, which were published as a final rule on June 5, 1991 and implemented progressively between 1994 and 1997; Tier 2 standards, which were adopted on December 21, 1999, with a implementation schedule from 2004 to 2009. Tier 2 emissions can be from 50 to 95% lower than Tier 1, depending on vehicle class [7].

In California, the Californian Air Research Board (CARB) has specified additional standards to Tier 1 regulations. Although been traditionally more stringent than the EPA requirements, CARB legislation is similar in structure to that of the federal legislation: Tier 1/LEV California emission standards extended through the year 2003 and LEV II California regulations became effective in 2004 (Table 2.1).

Hence, in order to comply with the upcoming very stringent emissions legislations, it is necessary to drastically change the current SI and CI engines, finding alternatives leading to lower emissions, especially of NO_x.

Table 2.1 Current and future EU and CARB legislated emissions levels for passenger cars [8],[9]

Euro Standard	Year of Approval	Durability Vehicle Basis	Engine type	CO (g/km)	HC/NMOG (g/km)	NO_x (g/km)	$HC+NO_x$ (g/km)	PM (g/km)
Euro I	1992		SI	2.72	-	-	0.97	
			CI	2.72	-	-	0.97	0.14
Euro II	1996		SI	2.20	-	-	0.50	
			CI	1.00	-	-	0.70	0.08
Euro III	2000		SI	2.30	0.2	0.15	-	-
			CI	0.64	-	0.50	0.56	0.05
Euro IV	2005		SI	1.00	0.1	0.08	-	-
			CI	0.50	-	0.25	0.30	0.03
Euro V	2009		SI	1.00	0.10[a]	0.06	-	0.005[b, c]
			CI	0.50	0.05	0.18	-	0.005[c]
Euro VI (proposed)	2014		SI	1.0	0.10[c]	0.06	-	0.005[b, c]
			CI	0.50	-	0.08	0.17	0.005[e]
CARB (Tier I-LEV I)	2001-03	100,000mi						
TLEV			Any	2.61	0.097	0.37	0.00	0.05
LEV			Any	2.61	0.056	0.19	0.00	0.05
ULEV			Any	1.30	0.034	0.19	0.00	0.02
CARB (LEV II)	2004-10	120,000mi						
LEV			Any	2.61	0.056	0.04	0.00	0.01
ULEV			Any	1.30	0.034	0.04	0.00	0.01
SULEV			Any	0.06	0.006	0.01	0.00	0.01

a - and NMHC = 0.068 g/km

b - applicable only to vehicles using DI engines

c - proposed to be changed to 0.003 g/km using the PMP measurement procedure

The final goal of emissions legislation would be to lead to the development of affordable and practical zero emission vehicles (ZEV), with good performance levels. Although still very much at a conceptual level, there are technologies already available for such vehicle like the fuel cell technology. However, this vehicle will only by a ZEV if the hydrogen is obtained using energy coming from renewable sources (such as sunlight) or through "reforming" methanol or other hydrogen-containing substance. There are, however, many obstacles still for the use of fuel cell in mass transportation, such as hydrogen on-board storage at very high pressure, putting safety concerns, mass production of hydrogen, fuel supply infra-structure, etc. All these make hydrogen fuel cells an unlikely option for mass transportation in short to medium term.

A more feasible option at the present time seems to be the Hybrid Electric Vehicle (HEV), which combines a battery-driven electric motor and an IC engine. The electric motor is powered by electric batteries or other rechargeable energy storage system (RESS) whose charge is primarily produced by an engine-driven generator. This system, rather than changing the concept of the IC engine, relies on the possibility of making a more efficient use of it, by preventing long idling times and improving the vehicle's start-and-stop capability since the electric motor is much more efficient in this range. Also, regenerative braking can be used by having generators installed in the wheels, since the battery can store the energy recovered during braking. At the present time, there are already such vehicles being mass produced by Toyota and Honda.

Although being advantageous from exhaust emissions point of view, HEV's efficiency as a whole is still uncertain. There are still many issues that need to be addressed, such as battery technology. The current batteries employ many substances that have a big environmental impact, such as heavy metals. Their power density is still low and their weight is too high. There are also questions concerning their reliability, life cycle, hot and cold temperature performance, safety, recycling, etc. Also, the extra weight added by batteries and electric motor to the whole car contributes to the production of extra CO_2, which might offset the other emissions related advantages. And finally, their price is still not competitive in comparison to regular IC engine vehicles.

2.2 Internal Combustion Engines Technology– State of the art

Recent advances in engine technology have enabled substantial improvements in fuel consumption and exhaust emissions reduction. The use of 3-way catalysts enables the reduction of CO, HC and NO_x by more than 90%. However, the 3-way catalysts are only efficient provided the AFR is kept very close to stoichiometric operation.

In SI engines load is controlled by throttling the intake air, thus controlling air flow, and metering the fuel accordingly to keep stoichiometric combustion for high efficiency catalyst operation. Intake throttling however contributes to the reduction of the engine's efficiency by over 20%, increasing fuel consumption and CO_2 emissions. Conversely, in Diesel engines the main parameter for load control is fuel flow rate. This permits air and fuel flow to vary independently, enabling lean-burn and unthrottled operation and hence

significant reductions in fuel consumption, particularly at part load. However, their operation away from stoichiometric prevents the use of a 3-way catalyst for effectively reducing their higher levels of NO_x emissions.

Diesel engines also have the tendency to produce high levels of particulate matter (PM). The present and coming emissions legislations can only be achieved with the use of exhaust particulate filters that require periodic purging events by fuel post-injection, in order to raise their temperature to around 550°C and oxidize the carbon particles into CO_2. Besides being expensive, these systems also have a fuel consumption penalty of 3-4% that might offset the lean-burn advantages [10].

In addition, the technology for NO_x emissions aftertreatment is available but still very expensive and not durable enough. With devices such as De-NOx lean traps, the major challenge would be durability, as required "de-SO_x events" involve raising the temperature to levels (about 600 °C) that are critical for the catalyst coating. For SCR (selective catalytic reduction), which is a technology for heavy-duty vehicles that is under investigation for different and more transient application on passenger cars, technical difficulties would include packaging (e.g. urea tank system, dosing unit, catalyst), control of fast transient behaviour (dosing of urea and mixing), and the need for a supporting network [11].

A different technological approach that allows substantial reduction in NO_x emissions and improved efficiency is Controlled Auto-Ignition (CAI), also called Homogeneous Charge Compression Ignition (HCCI). CAI combustion is a process that combines characteristics of both SI and CI engines. It relies on the compression to promote auto-ignition of a premixed charge and a subsequent homogeneous combustion. Controlling temperature and composition of the charge enables the auto-ignition of very lean or highly diluted mixtures, at low combustion temperatures, substantially reducing NOx emissions. Since the engine operates at WOT, no throttling losses are present and the fuel economy of a gasoline engine at part load can have significant improvement.

2.3 Controlled Auto-Ignition Combustion (CAI)

The CAI combustion method was first studied in the late 1970s by Onishi et al [12] and Nogushi et al [13] working on 2-stroke gasoline engines. The researchers found out a different combustion process that allowed remarkable improvements in both fuel consumption and exhaust emissions on a 2-stroke engine. Onishi et al [12] called it Active Thermo-Atmosphere Combustion (ATAC). ATAC is different from a conventional SI combustion in the sense that ignition happens simultaneously in many locations within the combustion chamber. It was noticed that no flame propagation was present, unlike what happens in SI engines. They also found that it was different from Diesel combustion since fuel and air were uniformly mixed. They concluded therefore that ATAC was a third combustion process of the internal combustion engine. They noticed as well that stable lean combustion could be achieved at part-throttle operation. This culminated with the first automotive production CAI engine, the two-stroke ARC250 introduced by Honda [14], who claims it reduces fuel consumption by up to 29% and significantly reduces HC emissions.

Even with the apparent advantages of this engine, it suffers from problems common to two-stroke engines that make them unsuitable for current automotive applications. The first problem is the need of the fresh charge to be pumped into the cylinder due to the absence of low intake pressure, which can be overcome by the traditional two-stroke crankcase induction. This configuration prevents the existence of a closed lubrication system, and the oil has to be mixed (and burned) with the fuel, greatly increasing the emissions. Alternatively, an external pump could be used, which in turn would increase parasite losses and weight, therefore affecting fuel consumption, and would add complexity and cost to the vehicle. Moreover, the strong influence of gas flow dynamics on the gas exchange process makes the torque very dependent on engine speed. Also, having intake and exhaust ports open simultaneously, during high load operations, permits some fuel to cross over unburned, elevating HC emissions to extremely high and unacceptable levels.

After noticing the improvements in fuel consumption and emissions on two-stroke engines, researchers started to investigate CAI possibility for four-stroke engines. The first reported experiment on a 4-stroke gasoline engine was carried out by Najt and Foster [15]. CAI was achieved by means of intake charge heating. The heat release was

controlled (to avoid knock) using highly diluted charge. Many fundamental studies were performed and characteristics of CAI were studied. However, this approach was very limited due to the small speeds and load range achievable. Moreover, the need for intake heating and its large thermal inertia makes it very unsuitable for the very transient characteristics of automotive applications. Also, if the energy needed for the intake heating is not taken from the engine's wasted energy into the exhaust, extra energy would need to be added to the system, which would increase the fuel consumption. Nevertheless, despite the difficulties found, Najt and Foster [15] proved the potential of the CAI combustion.

Christensen et al [16] tested CAI with various fuels with different compression ratios and intake temperatures. Contrary to what should be expected, increased compression ratio was found to adversely affect combustion efficiency, lowering the engine's indicated efficiency. They also showed that almost any liquid fuel could be used in a CAI engine and that NO_x emissions were generally very low.

Thring [17] was the pioneer of using external exhaust gas recirculation (EGR) as one of the means to achieve CAI, together with intake heating. The effects of A/F ratio, EGR rate, fuel type, and compression ratio on emissions and the attainable CAI range were studied. It was found that CAI needs a high amount of EGR in order to control the heat release rate. He proposed that a possible application for CAI would be a passenger car engine using CAI at idle and light load and switching to conventional SI combustion at full load. He stated that this would offer fuel economy similar to a Diesel engine at idle and light load, alongside very smooth operation. In addition, specific power output significantly better than Diesel could be achieved.

Pucher et al [18] has successfully achieved CAI by increasing compression ratio to the point where the required temperature for ignition could be achieved through compression only. This method, however, has the disadvantage of producing a very narrow CAI operational range. Ultra-lean mixtures had to be used hence limiting the load range. Another drawback of this concept is that it could not be used in a switching SI/CAI mode, as the compression ratio is too high to allow safe SI operation.

Lavy et al [19] presented results about the first 4-stroke engine that was able to achieve CAI, over a limited load and speed range, solely by means of exhaust gas trapping via a

negative valve overlap strategy (NVO). This strategy consists in closing the exhaust valve early to trap a certain amount of exhaust gas and a late intake valve opening to avoid back flow to the intake ports. To enable this strategy, they used an engine supplied with a set of camshafts with reduced cam profiles. In such a strategy, the more advanced EVC is, the larger the amount of trapped residuals.

The advent of FVVT systems in research engines made possible a much greater degree of freedom when studying CAI, as demonstrated by Law et al. [20] and Milovanovic [21], who, besides other variables, studied the influence of valve timing events on controlling CAI combustion achieved via NVO.

Despite not having the FVVT facility, production engines can also achieve CAI combustion via NVO, as showed by Li et al. [22] and Zhao et al. [23]. NVO was made possible by using bespoke camshafts with low lift and shorter duration, which would allow early EVC with EVO still in acceptable limits and late IVO without impacting too much IVC. It was realised in a production engine that had VCT (Variable Cam Timing) sprockets in each cam, enabling a greater degree of flexibility when investigating CAI and improved engine start. They also achieved NO_x emissions 90-98% lower than a standard SI engine and up to 30% reduction in fuel consumption.

The fact that CAI/HCCI combustion uses large amounts of charge dilutions enables a substantial reduction in peak cylinder temperatures, which, in turn, reduces the heat losses and increases the indicated thermal efficiency to levels close to the ones of Diesel engines, hence reducing fuel consumption [24].

Fuerhapter et al. [25] investigated CAI combustion control and transient response using the exhaust gas rebreathing method and confirmed the potential of CAI on reducing fuel consumption and emissions by having unthrottled operation and highly efficient combustion.

With the increasingly flexible valve trains for both research and production engines, Internal EGR has become very popular among researchers in the past few years. It is seen as the most feasible way for achieving CAI in automotive applications. Also, this method requires the minimum amount of changes to the current production engines.

2.4 Limits and Challenges of CAI Combustion

While it is a fact that CAI combustion offers a great potential in reducing emissions and fuel consumption of IC engines, it is also a fact that there are still many limitations and challenges to be overcome before it can be considered applicable in the automotive industry. Some of these challenges will be discussed in this section.

2.4.1 Combustion Control

Regarding combustion control, ignition timing and heat release are the chief concerns. With CAI operation, there is no direct control over ignition timing. While in SI and CI engines there is either a spark or injection event to trigger ignition, CAI combustion is solely governed by chemical kinetics. CAI Combustion is "self-triggered" depending on temperature, pressure and mixture composition. In addition, there is no direct control either over the heat release after ignition. As exposed by Christensen et al [26], there are several potential parameters that determine CAI combustion autoignition timing: compression ratio, inlet mixture temperature, inlet manifold pressure, fuel type, AFR, EGR rate, engine speed and coolant temperature. If gasoline direct injection (GDI) is to be used, variable injection timing can also be included in this list.

Some of these controlling parameters were investigated by Oakley [27], [28], who studied CAI for many different EGR rates and discovered that AFR had very little effect on ignition timing, except for EGR rates higher than 40% when reducing AFR would then significantly retard ignition timing. While testing different fuels, he also found that methanol outperforms gasoline in systems that rely on EGR to promote auto-ignition. The combinations of parameters that promote auto-ignition for gasoline are fewer than for methanol.

As already mentioned, the preferred way to achieve CAI nowadays is through NVO with VCT (Variable Camshaft Timing) or VVT (Variable Valve Timing) systems. These systems, at the same time can be used to trap exhaust residuals and to change the engine's effective compression ratio. Therefore, together with other parameters, precisely controlling valve timing would therefore enable a greater degree of control over CAI ignition timing [29-32].

2.4.2 Exhaust emissions

From the emissions point of view, one of the drawbacks of CAI is that HC and sometimes CO emissions levels can be much higher than the ones from SI engines. These emissions are normally associated with incomplete combustion, low temperature bulk quenching and cycle-by-cycle variations [33]. According to Martinesz-Frias et al. [34] these conditions happen at the boundaries of the CAI range as a result from cold mass in crevices and boundary layers, which are too cold to burn completely. The higher HC and CO emissions of CAI combustion, however, do not constitute a major challenge, since a relatively cheap 3-way catalyst can convert them to acceptable levels.

2.4.3 Operational Range

Currently one of the major challenges of CAI combustion is its very limited operating range when compared to standard SI or CI engines. With large amounts of trapped residuals, there comes a zone of highly diluted charge in which combustion is mainly determined by the EGR percentage and the AFR. A study done by Thring et al. [17] in a single cylinder engine at fixed speed identified 3 different regions that limit CAI combustion: the "misfire region", "the power-limited region" and "the knock region". In the misfire region, either the mixture is too rich or the EGR rate is too high for stable combustion. In the power limited region, either the mixture is too lean or the EGR rate is excessive to generate enough power to overcome friction losses. Finally, in the knock region, rich conditions and low EGR rate makes combustion extremely fast, allowing for high levels of combustion noise of knock to happen.

The knock limit was further explored by Oakley et al. [35] and Yelvington et al.[36] who described that with low AFR and low EGR rates (therefore high loads) the in-cylinder pressure traces show very strong oscillations that are similar to the ones of knock in SI engines. They reason that CAI/HCCI knock originates due to local inter-pressure gradients resultant from very fast chemical heat release. It becomes evident that any measure to further control heat release and avoid knock could help expand the CAI range.

On a 4-cylinder engine at various speeds, Li et al. [22] described an operational range from 1000rpm up to 3500rpm and load ranging from 0.5 to 4bar BMEP, as shown in Figure 2.1.

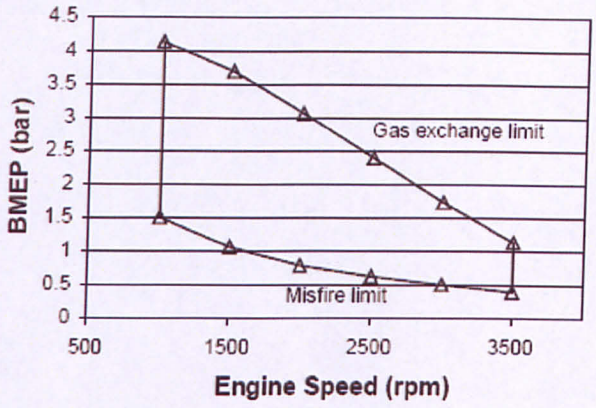

Figure 2.1 CAI Load range at various speeds in a 4-cylinder engine [22]

It identified only two main limits for stable operation: the gas exchange limit and the misfire limit. Knock was not present due to the high amounts of exhaust residuals. The maximum load is determined by the gas exchange limit, which is caused by restrictions in the air flow due to the use of low lift/duration camshafts for NVO configuration. The minimum load is determined by misfire since at this condition exhaust gas temperatures are too low to initiate CAI combustion. Since the CAI range achieved is much smaller than the ones of standard production engines, it becomes evident that measures to enlarge it are highly necessary.

At the boundaries of the CAI range, cycle-by-cycle variations tend to increase substantially, eventually leading the engine to misfire. In such a critical situation, it has been shown by several researchers that spark assistance could help trigger CAI [37-40]. It has been found that spark assistance has a clear effect on CAI combustion initiation for lambda values up to 3. Also, it is reasoned that when the in-cylinder conditions alone are not able to initiate CAI combustion, an extra source of energy is needed, which can be provided by the spark. As a result, it was found that having the spark on is an effective way to enlarge the CAI range.

Another technique which has been shown to increase the CAI range is by actively controlling cooling water temperature, as demonstrated by Milovanovic et al. [41]. The coolant temperature was decreased from the nominal operational value of 90 °C to 65 °C to extend the upper operating range limit, while it was increased from 90 °C to 125°C to reduce the lower operating range limit. The results obtained indicate that with reducing the coolant temperature, the upper limit can be extended up to 14%, while with increasing the coolant temperature the lower limit can be extended up to 28% whilst keeping the combustion stability, the rate of pressure rise and peak cylinder pressure in acceptable levels. The fuel economy showed improvements for the upper limit with reduced coolant temperature, but it deteriorated for the lower limit with increased coolant temperature. NO_x and HC emissions showed reduced levels for the lower limit when running at high temperature.

Another challenge for CAI operation is to find ways to improve volumetric efficiency. The use of trapped residuals or external EGR to promote CAI has the disadvantage of reducing the volume available for the fresh charge to fill in the cylinder, severely impairing, therefore, the volumetric efficiency. This gives CAI engines very low power density.

2.4.4 Boosted CAI

A good way to tackle the low volumetric efficiency (low power density) problem issue could be the use of forced induction. Indeed, boosting is regarded as an effective way to increase the engine's load range while on CAI operation. It is, however, accompanied by high cylinder pressure which may limit its advantages.

Stanglmaier, et al. [42] stated that highly boosted, fuel-lean HCCI engines appear to be a promising option for producing full power output in stationary and marine applications.

Christensen et al. [43] showed that supercharging can dramatically increase the attainable IMEP for HCCI/CAI operation. The maximum IMEP achieved was 14bar with natural gas as fuel. The engine was running under 2 bar boost pressure with a compression ratio of 17:1, when the maximum cylinder pressure was controlled to be lower than 250bar in order to avoid engine damage. With a lower compression ratio and higher boost pressure,

higher IMEP would be achieved, but this caused a reduction in thermal efficiency. HC emissions tended to decrease with an increase in boost pressure and load. CO emissions showed to be very dependent on AFR and pre-heating. If operated near the rich limit but with hot inlet air, CO emission is negligible. NO_x emissions were overall extremely low.

Christensen et al. [44] also studied supercharged HCCI in a single cylinder engine with variable compression ratio (VCR), modified from a truck engine. The engine was fuelled with natural gas and had pilot injection of iso-octane to improve ignition properties of the mixture at high loads. This setup also had cooled external EGR. It was found that supercharging in combination with cooled EGR extends the load limit while keeping maximum cylinder pressures at the same level as the original diesel engine. Substantial reductions of NO_x were achieved at a gross IMEP of 16bar.

Olson et al. [45] investigated CAI/HCCI performance of a 6-cylinder truck engine modified to use a turbocharger with dual-fuel HCCI operation. Two different fuels were used, ethanol and n-heptane, to better control auto-ignition timing. The main goals of this study were to demonstrate high load operation of a full-sized HCCI engine and to explore some of the typical constraints associated with turbocharged HCCI operation. The possibility of achieving high loads, up to 16 bar BMEP, as well as ultra low NO_x emissions with turbocharging and dual fuel was proved. Despite the great potential shown by the system, the lack of inlet air pre-heating impaired the performance at low load, reducing the efficiency. At high loads, the low exhaust temperatures were found to provide little energy to the turbocharger, hence causing pumping losses higher than levels from a comparable conventional diesel engine. Even with these limitations, brake thermal efficiencies and power rating were close to those of the original diesel engine, but with significant reduction in NO_x emissions. The maximum efficiency was found to be slightly lower than for the original engine. It was concluded that turbocharger matching is a key issue for achieving high-load operation combined with high efficiency.

In another study, Olson et al. [46] discussed the effects of cooled EGR on a turbocharged multi-cylinder HCCI engine modified from a 12 litre truck engine. The engine had port fuel injection of ethanol and n-heptane. The effects of EGR on boost, combustion duration and emissions were investigated. It was found that in all cases EGR improves combustion efficiency. It was found that in turbocharged mode the results are very much dependent on how the system is implemented. The presence of external EGR introduces

a pressure drop and exhaust mass flow loss after compression, which was found to negatively affect the performance of the turbocharger. NO_x, CO and HC emissions proved to be reduced in most cases.

Olson et al. [47] also investigated forced induction over HCCI combustion on an ethanol and n-heptane fuelled engine by comparing the impacts of a mechanically driven compressor to a traditional turbocharger. Simulation and experimental results were matched to provide more reliable data. It was found that the best solution for boosting depends very much on the particular application. A mechanically driven compressor is shown to be beneficial only if it is of a positive displacement type and if brake thermal efficiency is not very important at peak load. A turbocharger with two stages of boosting and inter-stage cooling is found to be very attractive for HCCI applications, especially when high boost is required. Turbocharging efficiency is found to be of high importance, therefore the best match for the turbocharger needs to be found. For this reason, the use of a VGT turbocharger seems to be very advantageous.

Yap, et al. [48], [49] investigated the effects of boost on a gasoline engine with residual gas trapping (iEGR). Boost was supplied from an external air compressor. A substantial increase in the upper limit of load range could be achieved without auxiliary intake heating, while NO_x emissions were characteristically low. It was found that there is a maximum amount of boost that can be applied without intake heating for any given amount of trapped residuals due to the limitations of their heating effect. It was concluded that increasing the trapped residuals amount together with a higher boost to maintain load can lower NOx further, but specific fuel consumption and CO emissions will increase due to increased pumping losses and lower combustion efficiency. It was also found that there is optimum intake valve timing for reducing NO_x.

Wilhelmsson, et al. [51] studied an operational strategy suitable for HCCI operation in a heavy duty turbocharged duel fuelled port injected engine. The fuels used were n-heptane and natural gas and the engine was under feedback combustion control during the experiments. It is stated that the low exhaust temperature of HCCI engines limits the benefits of turbocharging by causing pumping losses, meaning that maximum boost does not necessarily mean maximum efficiency in HCCI engines. It is also said that an

optimization problem emerges when one considers the need for boost and at the same time avoiding excessive noise, emissions and pumping losses. It is concluded that turbocharging does come at a cost, which is increased pumping losses. It was found that the best strategy in terms of turbocharging is to apply as little boost as possible while still meeting the NO_x requirements. In addition, natural gas seemed to be an ill-suited fuel for pure HCCI operation due to its high ignition temperature and rapid combustion.

With all the above, it is proved the potential for boosting to extend the CAI/HCCI load and speed range. There are still many drawbacks and pitfalls to overcome, and therefore, further research and development is needed.

2.5 Summary

Saving the environment against mankind's abuse is of paramount importance if we intend to have good living conditions in the future. In this sense, tackling global warming by changing the ways we use energy is one of the means forward. While other technologies still are not available, combustion of fossil fuels will still be a major source of energy, especially when it comes to the transport sector. Therefore, it is extremely important to improve the ways we burn fuels. We need to burn less and with lower emissions levels.

There are many alternatives under study for the transport sector, which offer lower emissions. However, all of them have associate drawbacks that need to be overcome if they are to be used in automotive applications.

One of the most promising technologies is CAI/HCCI combustion, which has been under intense investigation by engine researchers. This technology shows a great potential in lowering fuel consumption and emissions levels, while still retaining a substantially standard engine concept. In additions, by providing very low emissions levels, it does not need expensive and complicated exhaust after-treatment systems.

Despite of all the potential advantages, it still has several issues that must be tackled for this technology to be available on the road. One of the major challenges is to enlarge its operational range, which is still very limited and not suitable for automotive applications. Researchers have shown that the use of forced induction has proved to be very effective in increasing the load range of CAI/HCCI engines. However, it still needs investigation and there are many issues that have to be addressed to make it less of a laboratory concept and more of a road one. This research will concentrate on the study of a turbocharged CAI/HCCI engine with substantially standard components, where issues relating fuel consumption and emissions will be investigated with the help of in-cylinder conditions and combustion analysis.

3. Experimental Set-up and Test Facility

3.1 Introduction

The aim of this chapter is to provide a description of the engine test cell and all the measuring devices used to collect the data. Also, a full description of the engine and ancillaries, its management system (ECU) and all the sensors is given. The engine was set-up initially as a naturally aspirated unit, as supplied, and latter received a turbocharger for the boosted operation.

3.2 Ford Duratec 1.6 L Ti-VCT Gasoline Engine

In order to carry out the research a Ford Duratec 1.6 L Ti-VCT (Twin Independent Variable Cam Timing) Gasoline Engine has been used. This engine (Table 3.1) is designed for Ford road cars, such as Fiesta™ and Focus™. Some modifications have been done in a standard engine in order to meet the requirements of each one of the tests done (naturally aspirated and turbocharged).

Table 3.1 Ford Duratec 1.6L Ti-VCT Engine Specifications

Engine Type	Inline 4-cylinder
Bore (mm)	79
Stroke (mm)	81.4
Displacement (cm^3)	1596
Fuel Supply	Port Injection
Power @ RPM	85 kW @ 6000
Compression Ratio	11:1
Fuel	Gasoline 95 RON

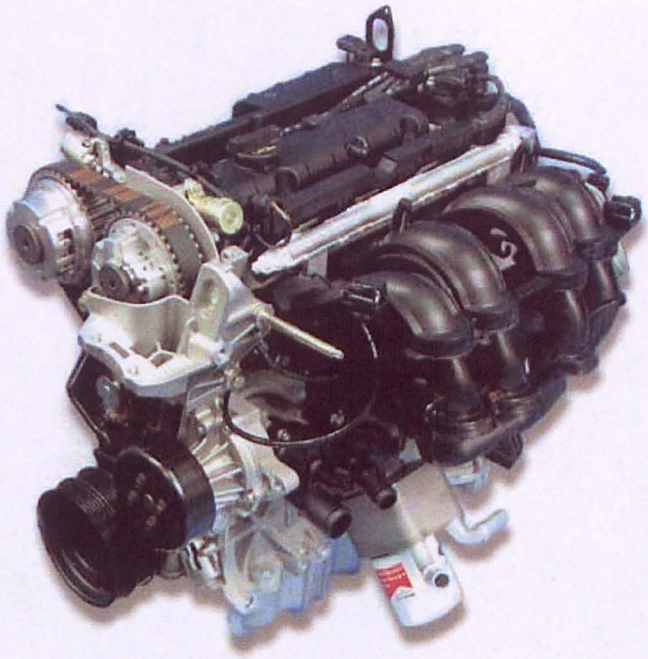

Figure 3.1 Ford Duratec 1.6L Ti-VCT Engine [53]

The cylinder head had to be modified to install the pressure transducers. This procedure proved to be very time consuming, since it had many pitfalls to overcome. For the transducers to be installed in the cylinder head, they need mounting sleeves since the water jacket has to be crossed to reach the combustion chamber. For the cylinder head to accommodate the mounting sleeves, it needs to be drilled through according to the sleeves' geometry. In addition, since the sleeves have to cross a water jacket plug, other plugs need to be machined to match the sleeves' geometry.

The mounting sleeves are not commercially available and have to be custom made since for each engine the cylinder head will have a particular geometry. The first sleeves were designed with a tapered end to rest on the cylinder head wall. After many changes, this design was found inappropriate, since it would not seal against the cylinder head wall and could not succeed the leak test. It was decided to change the sleeves' design, in which it would have a treaded end. After passing the leak test, it was decided that this design was suitable for running the engine with. Since only one cylinder would be monitored at a time, "dummy" sensors were fabricated in order to close the sensor holes of the other cylinders.

Therefore, to install the pressure transducers in the engine, the cylinder head had to be drilled and tapped, whereas sleeves, plugs and dummy transducers had to be fabricated (Appendix A).

3.3 Naturally Aspirated test set-up

In order to suit the needs of the experiment, this set-up (Figure 3.1) required few modifications on the standard engine, which will be further described in this section.

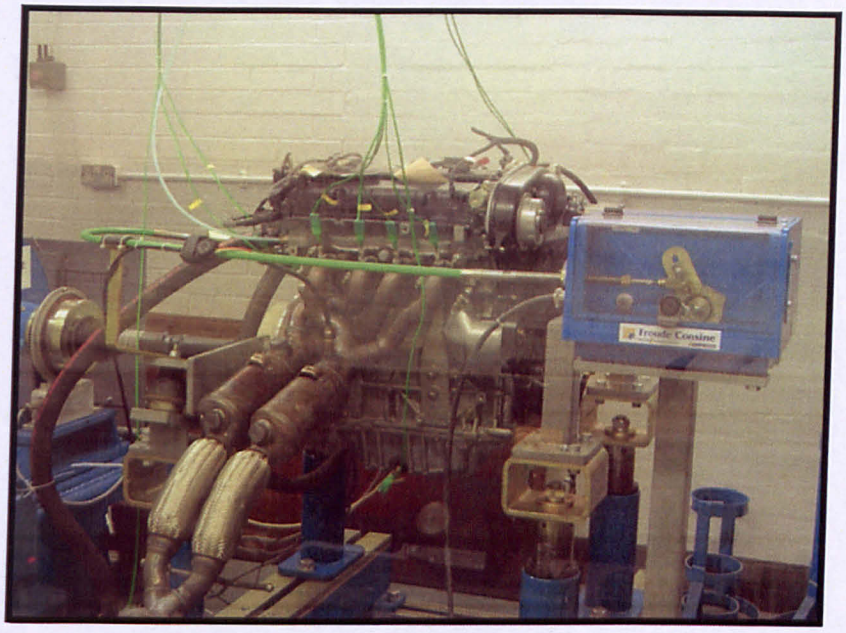

Figure 3.2 Naturally aspirated set-up

3.3.1 Intake System

The intake system had some changes in comparison to the original engine's arrangement. The original air filter was replaced by a simple conical unit, attached directly to the throttle body, in order to simplify installation.

A mechanical throttle replaced the original electronic unit, so that it could be connected and controlled by a throttle that is part of the engine test facility. This device, however, apart from at engine start, was hardly used for the CAI engine experiments, as to be shown later.

3.3.2 Valve Train

The engine is originally fitted with two hydraulically controlled VCT (Variable Cam Timing) units, which are able to shift the cams by a range of 52 °CA on the intake and 47 °CA on the exhaust side. The phase shifting is controlled by the ECU (electronic control unit) by means of two solenoid valves (Figure 3.3) which regulate the oil flow (Figure 3.4) to the VCT units.

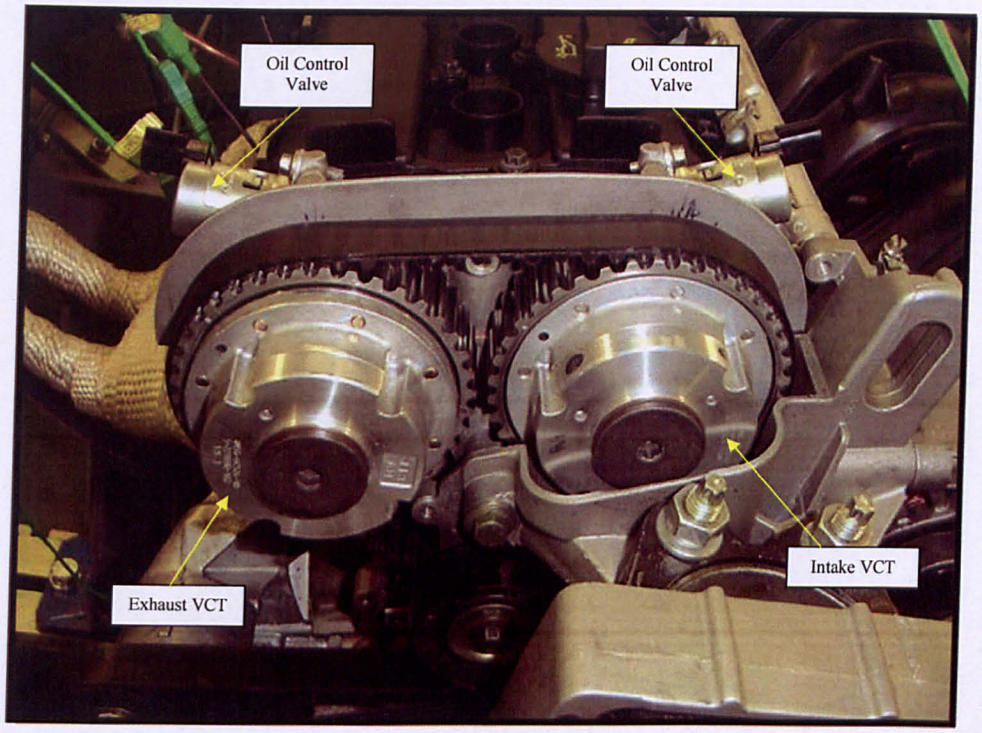

Figure 3.3 VCT units and oil control valves

The two original camshafts were replaced by two other low lift camshafts, in order to meet the requirements of the experiment. Their details will be discussed in depth in the following chapters.

When the engine is off, during the engine start and at idle the cam phasing units are blocked mechanically by a locking pin in a defined base position. This locking pin prevents the uncontrolled phasing of the VCT units while starting the engine. For a controlled cam phasing during engine operation, the locking pin is automatically released

when pressurizing the VCT units with engine oil. During engine shut down, the VCT unit on the intake side is depressurized and then moved into the base position by drag torque of the camshaft. A torsion spring is integrated into the exhaust cam-phasing unit moving the exhaust camshaft in the base position as soon as the VCT unit is depressurized. The torsion spring is strong enough to work against the drag moment even if the engine is running.

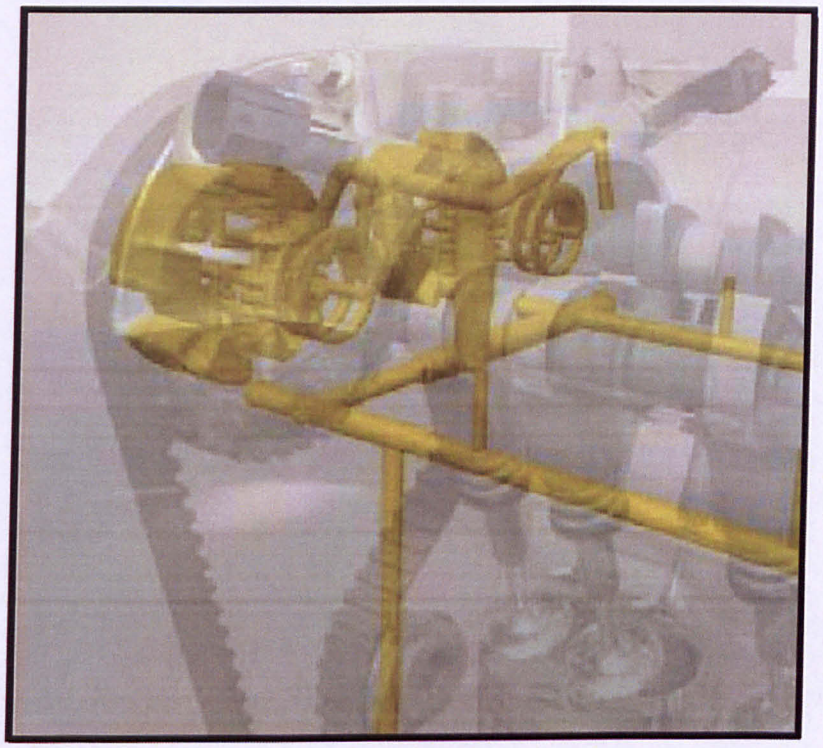

Figure 3.4 Oil Flow to VCT's [53]

3.3.3 Exhaust system

The exhaust system retains the original manifold and the two close couple catalysts, being connected directly to the test cell down pipe, without any muffler [Figure 3.5].

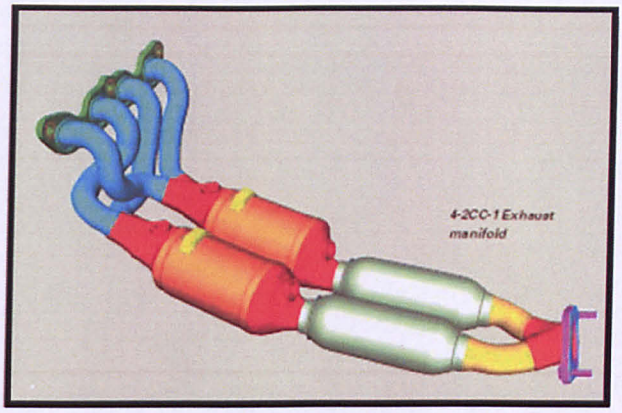

Figure 3.5 Exhaust Manifold [53]

3.3.4 Cooling System

The engine water cooling system that was used was the one belonging to the test cell and controlled by the dynamometer's control unit, allowing closed loop control over an adjustable target temperature, which was set to 90 °C throughout the whole test. Engine water cooling was achieved through a water/water heat exchanger, which comprised a 3-way valve to control the coolant water flow rate to the engine [Figure 3.6 and Figure 3.7].

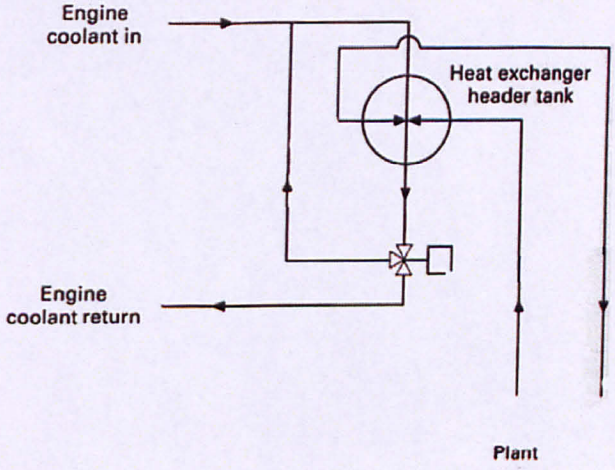

Figure 3.6 Cooling water schematic

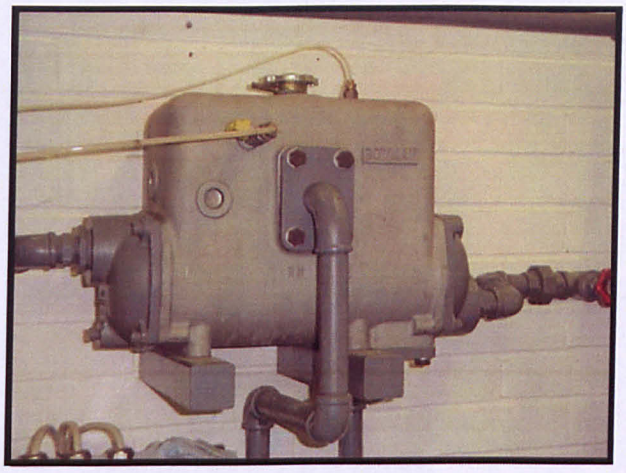

Figure 3.7 Cooling Water Heat Exchanger

3.3.5 Engine Lubrication

This system was kept the same as the production engine [Figure 3.8], which was fed with SAE 5W30 oil, as recommended by the manufacturer. Oil temperature was kept on safe levels via the original oil/water heat exchanger, which has the function of enhancing oil warm up, in order to ensure good lubrication at the engine's cold start/warm-up phase and to keep it cool enough at normal engine operation.

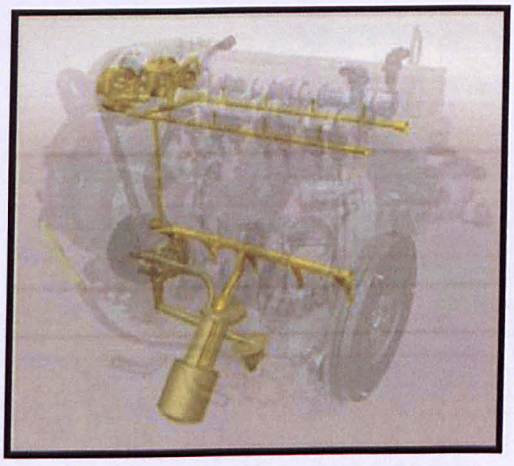

Figure 3.8 Engine Lubrication System [53]

3.3.6 Fuel System

The engine had a port fuel injection system, whose fuel was supplied by means of an electrical fuel pump, delivering fuel through a non-return system (Figure 3.9). Unlike the original system which had an immersion type fuel pump and regulator, a standalone dry fuel pump and regulator was used (Figure 3.10). Fuel pressure was set via an adjustable fuel regulator to the levels of the original engine (3.25bar).

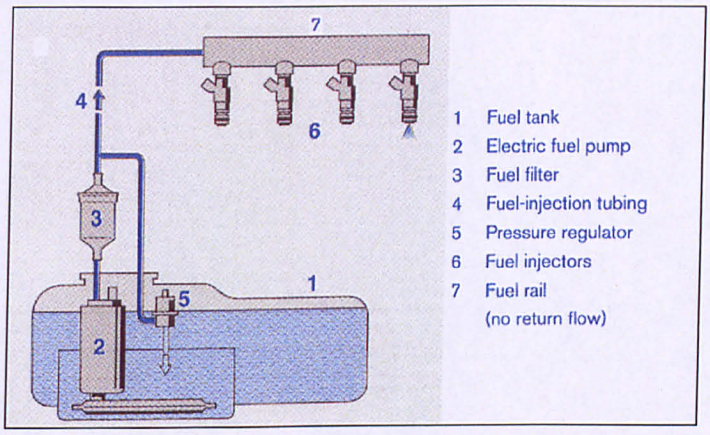

Figure 3.9 Standard non-return fuel pumping system schematic [54]

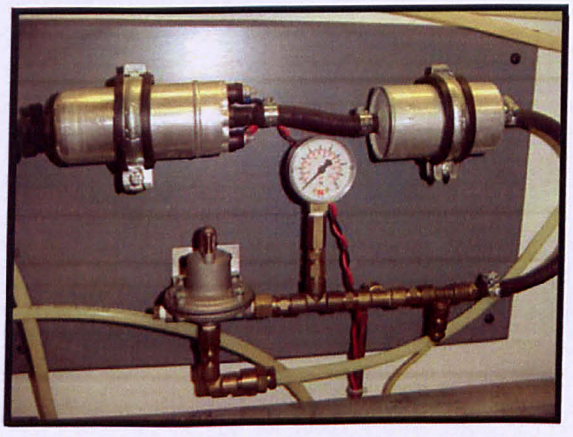

Figure 3.10 Modified dry-pump non-return fuel pumping system

3.3.7 Ignition System

The ignition system remained very similar to the original one. The original ignition coil remained the same and the only change was the addition of an external Bosch™ ignition amplifier (Part. Number 0 227 100 200)(Figure 3.11). This was necessary once Motec ECU does not come with an internal one, as in the original ECU.
This ignition amplifier as well as all the timing strategy is controlled by the Motec ECU.

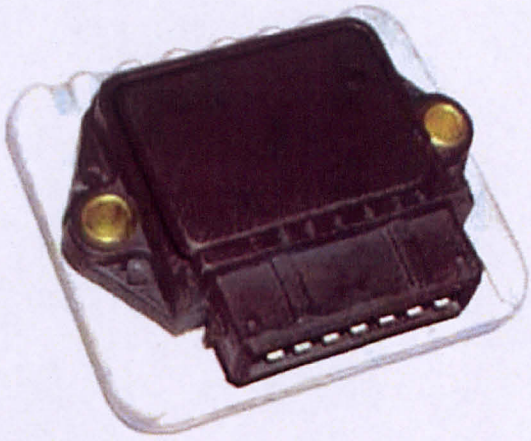

Figure 3.11 Bosch™ Ignition Amplifier

3.4 Turbocharged test set-up

For the boosted operation set-up (Figure 3.12), several items had to be modified on the previous set-up and will be discussed in this section. All the items not listed below remained the same as for naturally aspirated set-up.

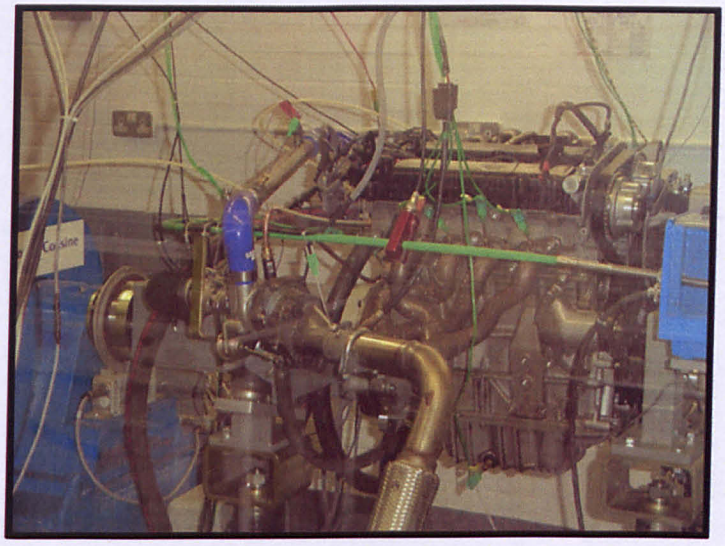

Figure 3.12 Turbocharged set-up

3.4.1 Intake System

The intake system had to be greatly modified for accommodating a turbocharger. The turbo unit was attached directly to the exhaust manifold, being located, therefore, on the left side of the engine, needing a long pipe to reach the intake manifold on the right. The intake sequence of devices was: air filter, compressor, compressor outlet pipe, throttle, and intake manifold (Figure 3.13).

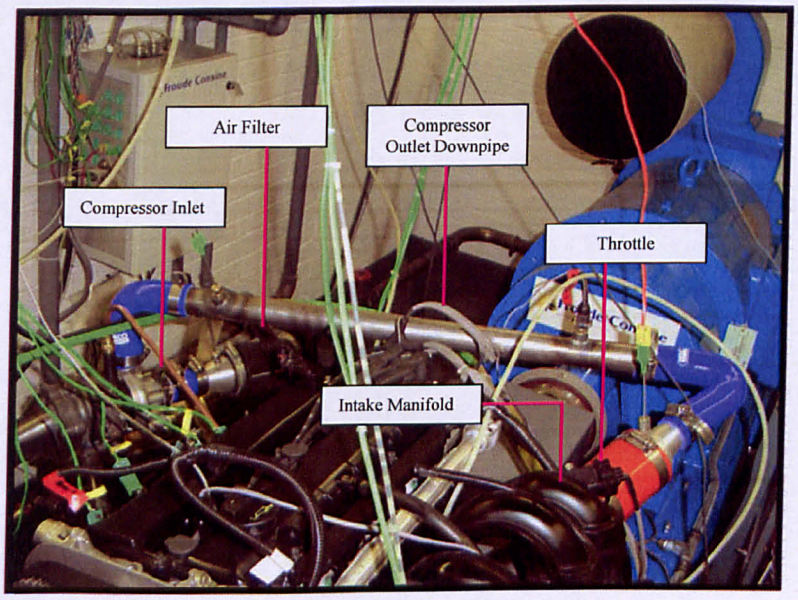

Figure 3.13 Turbocharged Intake System

3.4.2 Exhaust System

Since the turbocharger used was a very small unit, not normally used in such an engine, there was no aftermarket turbocharging kit suitable for this set-up. Therefore, the only choice was to fabricate another manifold by using some parts from the original unit.

3.4.3 Turbocharger

The turbocharger selected to best suit the engine was a MHI TDO2 with an integrated waste-gate. This was found to be one of the few turbochargers available in the market for the power range of the engine. The manufacturers of turbochargers hardly disclose detailed information about efficiency and operating points, i.e. turbine and compressor maps. Hence, the turbocharger selection was based purely on power range, given that this information was the only available from the manufacturers. The MHI TDO2 turbocharger is meant for engines ranging from 8-40bhp, which was the power range expected to be achieved in the turbocharged test. More details of MHI turbochargers can be found on Appendix B.

3.4.4 Compression Ratio

The compression ratio was reduced from the standard value of 11:1 to 8.8:1 through the use of a bespoke cylinder head spacer, consisting of a steel plate 1.6mm thick and one original cylinder head gasket on each side, yielding a total thickness of 2.4 mm.

3.4.5 Cooling System

The cooling system used in the naturally aspirated test showed some limitations when running the turbocharged test. The 3-way valve previously used was found to be too slow to react to the quick temperature rise that happens when the turbo is boosting, leading to either overheating or running the engine too cold. Therefore, based on experiment, it was found that the best way was to run with the 3-way valve fully open, to isolate it's by-pass flow and to put back an original thermostat on the engine's cooling circuit, which, in fact, provided coolant temperatures much more stable then before.

3.4.6 Engine Lubrication and Oil Cooling

The engine's lubrication system was kept almost the same as in the previous set-up. The only difference was the turbocharger oil feed, introduced to the engine's lubrication circuit. The oil flow for the turbocharger was supplied from the engine's main oil gallery, by means of a T-piece installed in the oil pressure sensor connection hole (Figure 3.14). The oil return from the turbocharger was achieved gravity to the sump, by means of a flexible hose and a connector to the sump as shown in Figure 3.15.

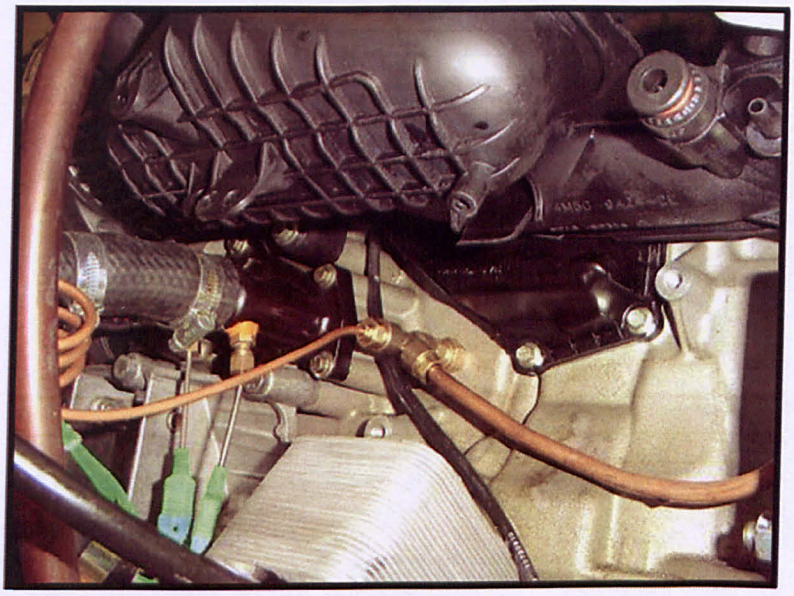

Figure 3.14 Oil feed to the turbocharger

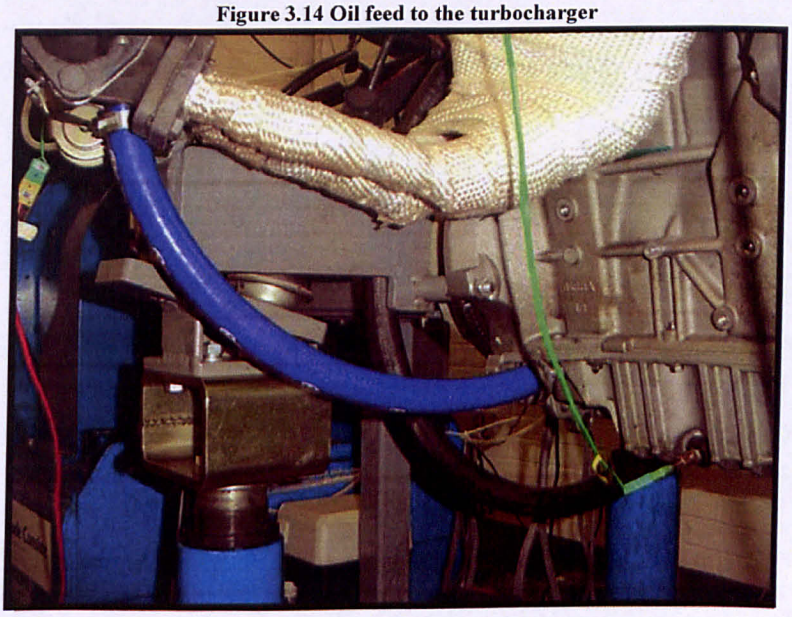

Figure 3.15 Oil return from turbocharger to engine

3.5 Engine Management System

In order to allow engine operation and to control all systems related to SI combustion and CAI operation, a fully programmable ECU (Electronic Control Unit) was needed.
Besides being able to manage engine basic operation, it was also necessary to have camshaft control capability, data logging and several inputs and outputs available for general use. Choice was made, therefore, for the Motec M880 Engine Management System as this would best suit the needs of the experiment. Appendix C provides further information about the Motec ECU.

The Motec^{TM} ECU can be accessed trough a PC running a Windows based tuning software (Motec ECU Manager) (Figure 3.16). The PC and ECU communicate to each other via a CAN (Controlled Area Network) cable, which allows real time data transfer between the two. Data can be displayed, read and written in real time, while the engine is operated.

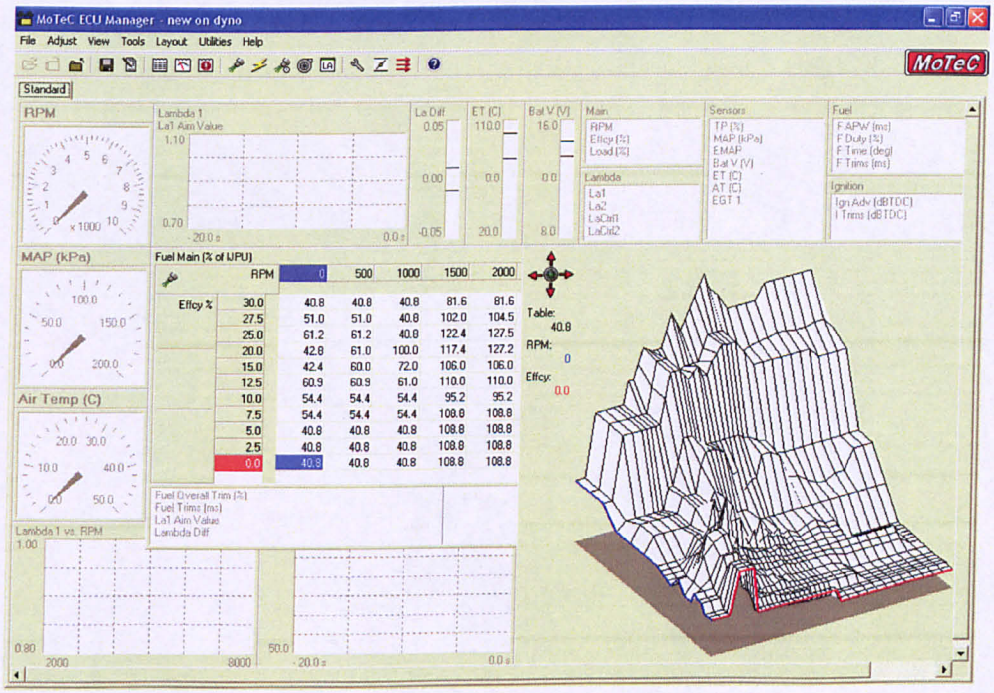

Figure 3.16 Motec^{TM} ECU Manager tuning software

3.5.1 Engine Sensors and Actuators

For the engine to be able to run, several sensors need to send signals to the ECU which then commands some actuators and enable engine operation.

To run the engine with the desired sequential fuelling strategy, at least three sensors are required: crankshaft sensor, camshaft sensor and throttle position sensor. Furthermore, it was decided to run the engine in closed loop lambda control, which then required also a lambda sensor to be permanently connected. All the other sensors (air temperature, map sensor, coolant temperature sensor, etc.) acted as auxiliaries to monitor engine operation and parameters and will not be described.

3.5.1.1 Crankshaft position sensor

Also known as *engine speed sensor*, the crankshaft position sensor provides a signal from which the ECU calculates two vital informations: crankshaft rotational speed and position.

The sensor is a Variable Reluctance (VR) Sensor, and is mounted directly opposite of a 60-2 (sixty minus two) teeth flywheel. Every time the flywheel rotates and a tooth passes by the sensor, it changes its permanent magnet's flux, generating, therefore a current (pulse), providing the movement information to the ECU. The flywheel has 2 deliberate missing teeth, which provide the information of crankshaft/piston position (TDC) to the ECU (Figure 3.17).

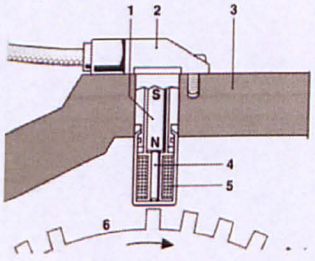

Figure 3.17 Crankshaft Position Sensor [54]

3.5.1.2 Camshaft Position Sensor

Also known as phase sensor, the camshaft position sensor provides the ECU with the information of camshaft position, therefore enabling the ECU to know at which stroke the engine is in, or, in other words, providing the phase information.

The sensor used was a Hall Effect rod sensor (Figure 3.18), consisting of a Hall element with a semiconductor wafer through which current flows. This ferromagnetic Hall element responds to activation by a trigger wheel rotating in unison with the camshaft by generating voltage at right angles to the direction of the current passing through it.

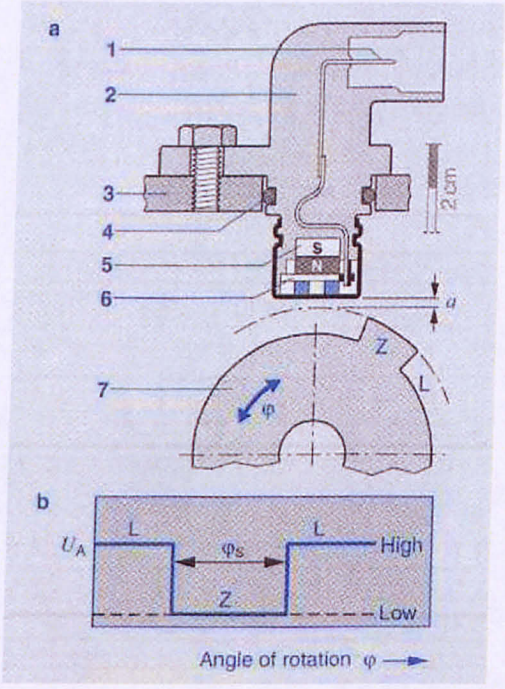

a Positioning of sensor and single track trigger wheel
b Output signal characteristic U_A

1 Electrical connection (plug)
2 Sensor Housing
3 Engine Block
4 Seal ring
5 Permanent Magnet
6 Hal IC
7 Trigger wheel with tooth/segment (Z) and gap (L)

A Air gap
φ Angle of rotation

Figure 3.18 Hall-effect Rod Sensor [54]

The trigger wheel (Figure 3.19) has one tooth only and is bolted on the end of the camshaft. Since the engine has two VCT (variable cam timing) devices, each camshaft needs to have a position sensor, which, in conjunction with the signal from the crankshaft position sensor, enables the ECU to know accurately each camshaft position.

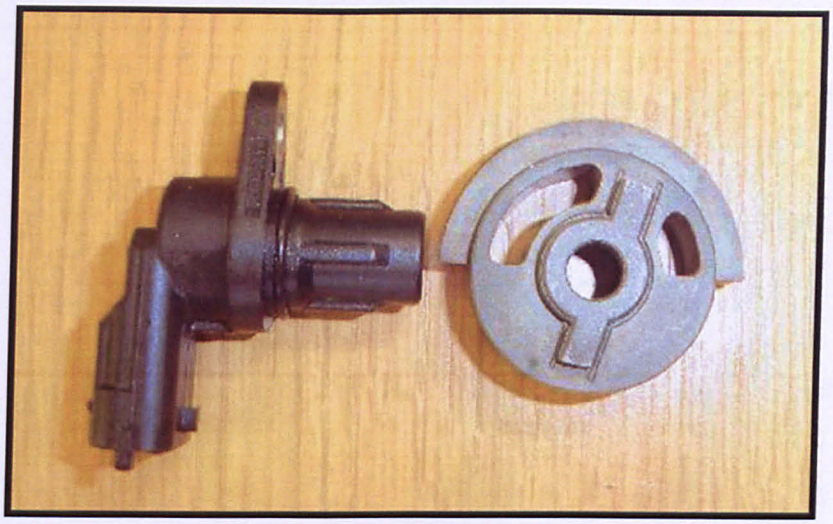

Figure 3.19 Camshaft Position Sensor and Trigger Wheel

3.5.1.3 Throttle-valve Position Sensor

The Throttle-valve Position Sensor (TPS) registers the angle of rotation of the throttle valve. It is necessary for the ECU to know accurately this information since it's the primary load signal required for fueling and ignition calculations.

This sensor (Figure 3.20) consists of a potentiometer wiper arm, fastened to the throttle-valve shaft. The potentiometer wiper arm has one or two resistance tracks depending on model. A 5V supply is distributed between the resistance tracks; the ratio of distributed voltage determined the throttle angle.

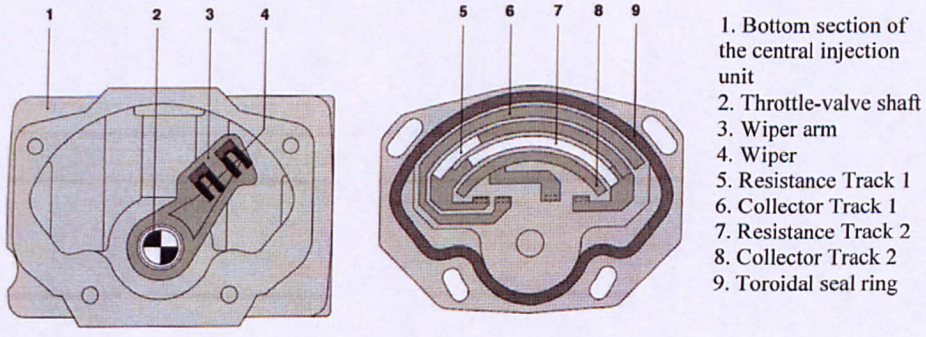

Figure 3.20 Throttle-valve Position Sensor [54]

3.5.1.4 Wide Band Lambda Oxygen Sensor

As the name implies, the wide-band oxygen sensor (also called Lambda sensor) is used to determine the oxygen concentration in the exhaust gas. It is capable to make precise measurements ranging from $0.7 < \lambda < \infty$ (= air with 21% O_2).

It was used during the experiment for measurement and to enable the ECU to perform air/fuel ratio closed loop control over the engine's operational range.

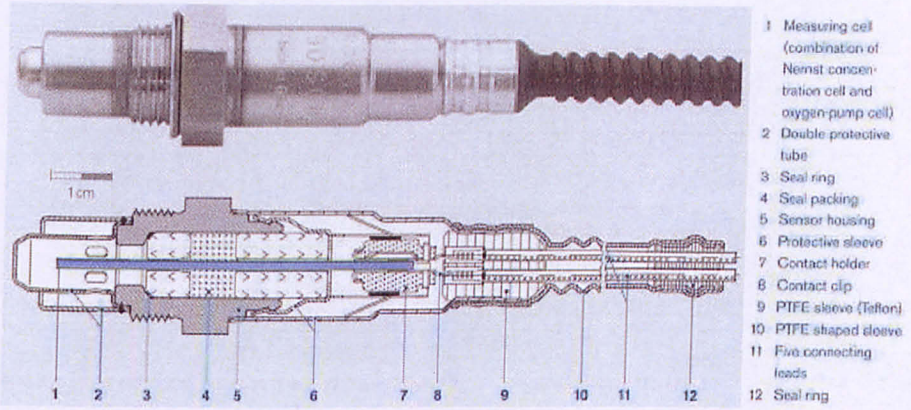

Figure 3.21 Wide-band Lambda Sensor [54]

3.6 Engine Instrumentation and Measurement

3.6.1 Dynamometer

In order to simulate load and measure engine power, the tests were done using a Froude Hoffmann AC Dynamometer (Figure 3.22), capable of absorbing 250 kW (335hp) at a maximum speed of 10,000 rpm and motoring up to 235 kW (315hp). The dynamometer's control system is capable of doing either manual or fully automatic test cycles. Due to its low inertia AC motor, it provides exceptional performance in control and torque measurement, being designed for steady state, transient and dynamic testing applications. When in power absorbing mode, the dynamometer acts as a generator, feeding the energy needed to load the engine back to the mains. When in motoring mode, however, the energy is consumed from the mains.

The dynamometer operation and data-logging is performed on a PC based control and data acquisition system Froude Hoffmann Texcel V8^{TM} (Figure 3.22).

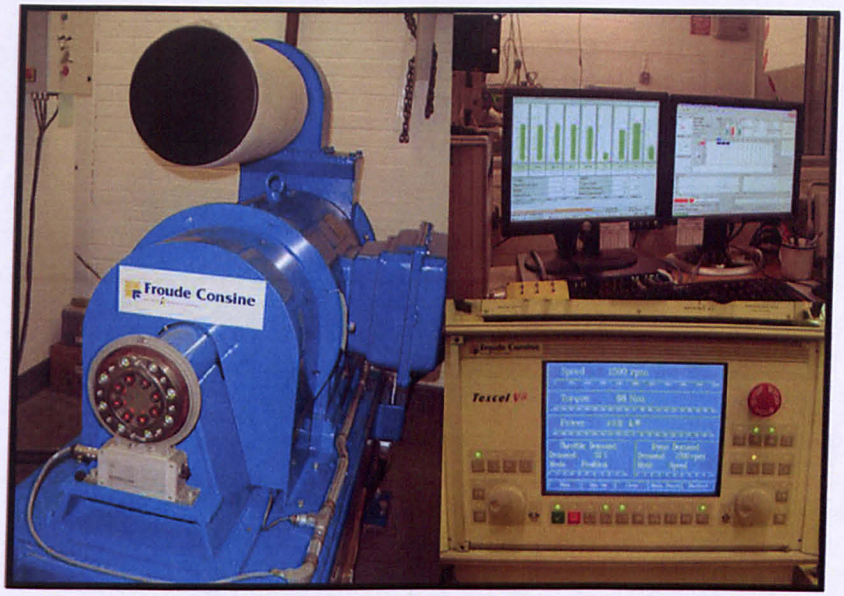

Figure 3.22 Dynamometer and control system

3.6.2 Fuel Flow Measurement

Fuel mass flow rate was measured by means of an AVL 7030 gravimetric flow meter. It consists of a vessel attached to a load cell, forming a balance that indicates the weight of its contents. There is a set of solenoid valves that control the filling and emptying of the vessel. An electronic control computes the mass variation over a user defined time thus indicating the mass flow rate. The result can be displayed either in kg/h or g/s and is also delivered to an analog output for connection to external data acquisition systems.

3.6.3 Temperature Measurements

All temperature measurements were done using a standard RS K type thermocouple. Thermocouples consist of two wires of dissimilar metals joined near the measurement point. The output is a small voltage measured between the two wires (Figure 3.23). This

voltage can be converted to a calibrated temperature and displayed on a digital display or to be read by a Data Acquisition System.

In the current tests all thermocouples were connected to the dynamometer's transducer box (Figure 3.24), which conditioned the signals sent to the computer for monitoring and data acquisition purposes.

Figure 3.23 Schematic diagram of a standard bimetal thermocouple

Temperature was measured at many different points depending on the test, as shown in the table below.

Table 3.2 Temperature measurement points

THERMOCOUPLE LOCATION	TYPE OF TEST	
	NATURALLY ASPIRATED	TURBOCHARGED
Intake Manifold	X	X
Exhaust Manifold (at each port)	X	X
Compressor Inlet		X
Compressor Outlet		X
Turbine Outlet		X
Coolant Inlet	X	X
Coolant Outlet	X	X
Coolant By-pass inlet	X	X
Oil Temperature	X	X

3.6.4 Pressure Measurement

3.6.4.1 General Pressure Measurements

Several pressure values needed to be monitored to ensure that the engine was running safe and at the required test condition. All of these were measured by Piezoresistive Pressure Transducers, which were part of the dynamometer's transducer box (Figure 3.24).

This kind of sensor consists of an internal diaphragm and a silicon chip that changes its resistivity as the diaphragm deforms with pressure. The pickup points had hoses connecting them to the respective pressure sensors at the transducer box.

Figure 3.24 Transducer Box

3.6.4.2 In-cylinder Pressure Measurement

A Kistler 6121 (Figure 3.25) piezoelectric transducer was installed in cylinder no. 4 to measure in-cylinder pressure. A piezoelectric pressure transducer consists of a pressure-sensing diaphragm that transmits the force to a stack of disks made of piezoelectric ceramics or crystalline quartz. Electrical charges are picked up from the faces of the stack and are proportional to the pressure. As the sensor is of high impedance, it requires a charge amplifier (Kistler type 501) for charge-to-voltage conversion. The measurement range was 0-100bar gauge with a sensitivity of -15PC/bar with in an operating temperature of -50 to 350°.

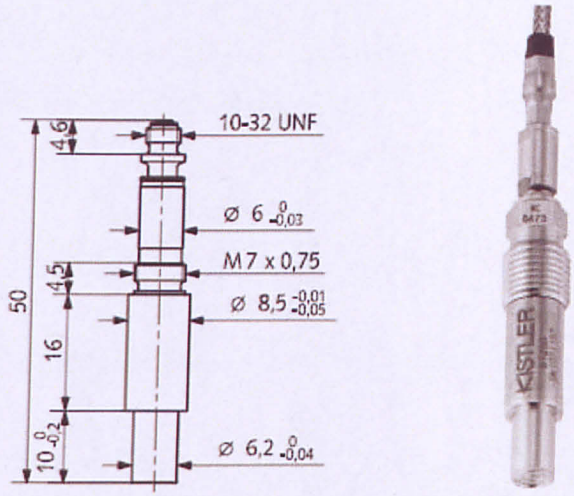

Figure 3.25 Kistler 6121 Pressure Transducer

3.6.5 Trigger Wheel

In order to perform cycle related measurements, a bespoke toothed wheel was used to measure rotational speed and crankshaft position (therefore indicating TDC).The wheel had 360 teeth evenly spaced and one concentric extra tooth to indicate TDC related position, to serve as a reference for the Data Acquisition System. Both signals from the wheel were picked up by a Variable Reluctance (VR) sensor and the two correspondent sine waves were converted in to square waves by a custom-built circuit. The converting circuit also had a frequency divider applied to the reference (TDC) signal, in order to provide only one reference signal per engine cycle.

After the converting circuit, two treated signals are available: the first (clock) is a train of pulses and the second (reference) is a single pulse per every 2 revolutions of the crankshaft.

3.7 Exhaust Measurement

Exhaust measurements were carried out by means of Horiba MEXA-7000 series analyzers. Emissions of Carbon Monoxide (CO), Carbon Dioxide (CO_2), Oxygen (O_2), Unburned Hydrocarbons (uHC) and Oxides of Nitrogen (NO_x) could be shown onscreen.

The analyzers employ a variety of techniques that exploit particular properties of the exhaust gas components. CO and CO_2 are measured using nondispersive infra-red absorption (NDIR), O_2 is measured via paramagnetism, uHC are measured via flame ionization (FID) and NO_x by chemiluminescence (CLD).

The following sections will discuss the individual setup and emissions measuring principles.

3.7.1 Horiba AIA-72X Series: CO and CO_2 measurement

The AIA-72 analyzer is designed to measure the concentration of CO, CO_2 and other gases using Non-Dispersive Infrared (NDIR). It is based on the fact that a molecule, consisting of different atoms, absorbs infrared energy at specific wavelengths and that the degree of absorption is proportional to the concentration at constant pressure.

A typical NDIR analyzer configuration is shown in (Figure 3.26), consisting of a light source, sample cell, detector, and electrical system. The infrared beam from the light source passes through both the sample and comparison cells. The sample cell has the gas to be measured (sample gas) introduced continuously via the inlet port, whereas the comparison cell contains a gas that does not absorb infrared radiation (such as nitrogen).

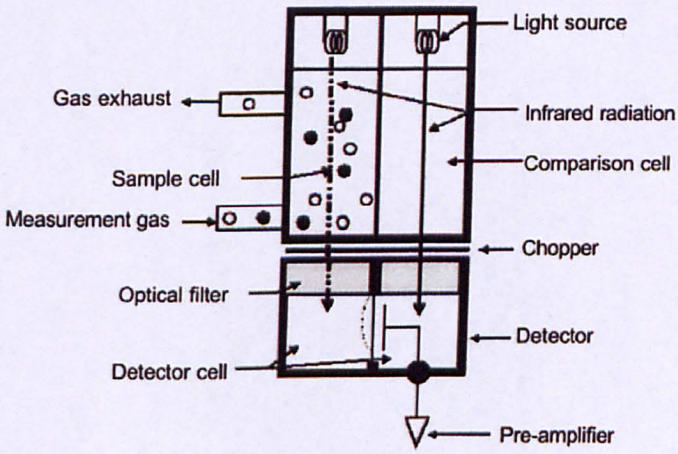

Figure 3.26 Example of NDIR configuration

The detector consists of two cells, either side of a movable membrane, in which the gas to be measured is sealed. The gas enclosed in each cell absorbs infrared radiation as heat and expands; the degree of expansion depends on the quantity of radiation received. As a result of the expansion, a differential pressure is generated between the two detector cells and the position of the movable membrane changes. The infrared radiation is transmitted intermittently by a light chopper, so the change of gas concentration in the sample cell can be detected as electrical output by the displacement of the movable membrane.

3.7.2 Horiba MPA-720: O_2 measurement

Magneto-pneumatic detection (MPD) is the method used by the MPA-720 to measure the concentration of oxygen (O_2) in the sample gas. Magneto-pneumatic detection relies on the fact that oxygen has a much greater response to a magnetic field than other gases.

The principle of a magneto-pneumatic oxygen analyzer is shown in Figure 3.27. AC current flows in the electromagnet so an alternating field appears between the poles of the electromagnet. When the sample gas flows into the magnetic field, the pressure around the poles changes according to the concentration of oxygen. This is because oxygen whose susceptibility is high is attracted by the magnetic poles. This pressure change is detected by a condenser microphone as an alternating signal as electric capacity changes.

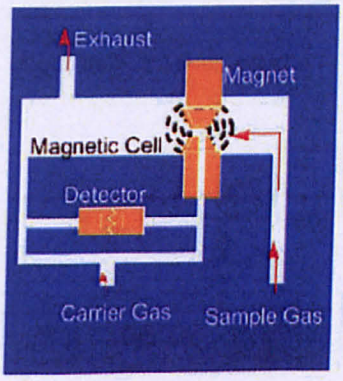

Figure 3.27 Schematic configuration of magneto-pneumatic oxygen analyzer

3.7.3 Horiba FIA-720: Unburnt Hydrocarbon measurement

The Horiba FIA-720 analyser is designed to measure the concentration of total hydrocarbon (uHC) using hydrogen flame ionisation detection (FID). Hydrogen flame ionisation uses the phenomenon in which ions, generated by the heat energy when hydrocarbons are introduced into a hydrogen flame, are proportional to the number of carbon atoms in the sample. It is widely used for the measurement of exhaust gases from engines because it is sensitive to almost all HC compounds.

The configuration of the FID is shown in Figure 3.28. H_2 and air are supplied to the burner nozzle and a hydrogen flame is formed. Two electrodes are fitted on either side of the flame, and a DC voltage is applied. The sample gas is mixed with the fuel H_2 and introduced to the hydrogen flame. It is thermally dissociated and generates ions in the high-temperature area. The ions generated migrate to the electrodes and are detected as current. The characteristic of this method is that the detector output is nearly in proportion to the number of carbon atoms and so is used for measurement of total hydrocarbons (uHC).

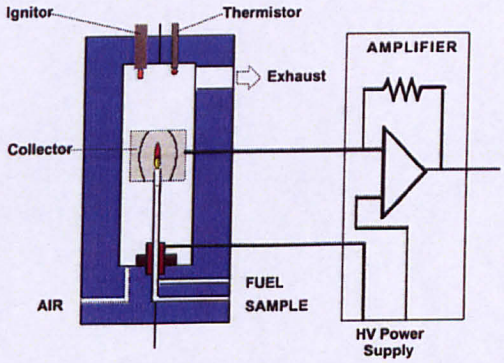

Figure 3.28 Schematic of a Flame Ionization Detector (FID)

3.7.4 Horiba CLA-720A: NO and NOx measurement

The Horiba CLA-720A Analyser is designed to measure the concentration of NO and NOx using chemiluminescence detection (CLD). It is widely used as the measurement method of NO and NOx in exhaust gases from engines because it is highly sensitive to NO and is not interfered by other components easily.

When sample gas with NO and ozone gas (0_3) gas is mixed in a reactor, NO is oxidized and is transformed to $N0_2$.

$NO + 0_3 \rightarrow N0 + 0_2$

A part of $N0_2$ that is generated here is in excited state, which means its energy is higher than normal. Excited $N0_2$ molecules release excited energy as light when returning to the ground state.

$NO + 0_3 \rightarrow N0_2^* + 0_2$ $N0_2^*$: $N0_2$ molecules in excited state

$NO_2^* \rightarrow N0 + hv$ hv: photon's energy

This phenomenon is called chemiluminescence and the degree of light is directly proportional to the quantity of NO molecules before the reaction. Thus, NO concentration in the sample can be acquired by measuring the amount of light emission.

3.8 Summary

This chapter presented the details of the engine and equipment used during all the experimental tests. It described the particularities of the naturally aspirated setup as well as the turbocharger setup. The operating principle of the variable valve timing mechanism and all the main sensors was explained.
Operational details concerning the measurement and/or control systems such as dynamometer, ECU and gas analyzers were also explained.

4. Data Processing and Analysis

After naturally aspirated and turbocharged operation described in chapter 3 were made operational, a large amount of data could to be collected. The data was acquired with the engine running at constant speed. For each test point, 3 groups of data were generated. The first group, consisted of pressure data collected using Brunel's Data Acquisition System based on Labview ™ 6.0 software. Another group was acquired using the dynamometer's own data acquisition software (Froude Texcel ™ V8) and consisted of the engine's main parameters (power, torque, temperatures and pressures). The third group consisted of manually recorded data, referring to the ECU parameters and Gas Analyser results.

In addition, the manually recorded data also held information needed to synchronize the three groups for processing on in a MS Excel ™ spreadsheet. This spreadsheet has a MS Visual Basic for Applications (VBA) ™ macro which collects and synchronizes all the data and generates an output table with all the results needed, for every engine test point. The calculations performed in this spreadsheet are described in the following sections and they were used to analyse heat release, engine emissions and performance. All plots were made using MS Excel ™ and, when isoline plots were needed, Uniplot for Windows V4.1.5 (using linear interpolation) was applied.

4.1 Data Acquisition Software

The pressure data is the core of the heat release analysis. Thus, it is essential that this data is properly obtained in order to ensure reliable results.

Pressure data was acquired through a National Instruments™ PCIMIO16-1 data acquisition board, installed in a dedicated Pentium III™ desktop computer, running a Labview™ program (Figure 4.1) specially written for the task by a former Brunel PhD student, John Williams.

To provide useful information, the pressure data has to be referenced to the crankshaft position. Hence, a toothed wheel is installed on the crankshaft (section 3.6.5) and

provides a clock signal per every 1° CA and a TDC signal (reference tooth) per every crankshaft revolution. Since for a four-stroke cycle the relevant events only happen once every two revolutions, only one TDC event is required for referencing the pressure data and this is realized by a signal conditioner that incorporates an electronic divider (Figure 4.2).

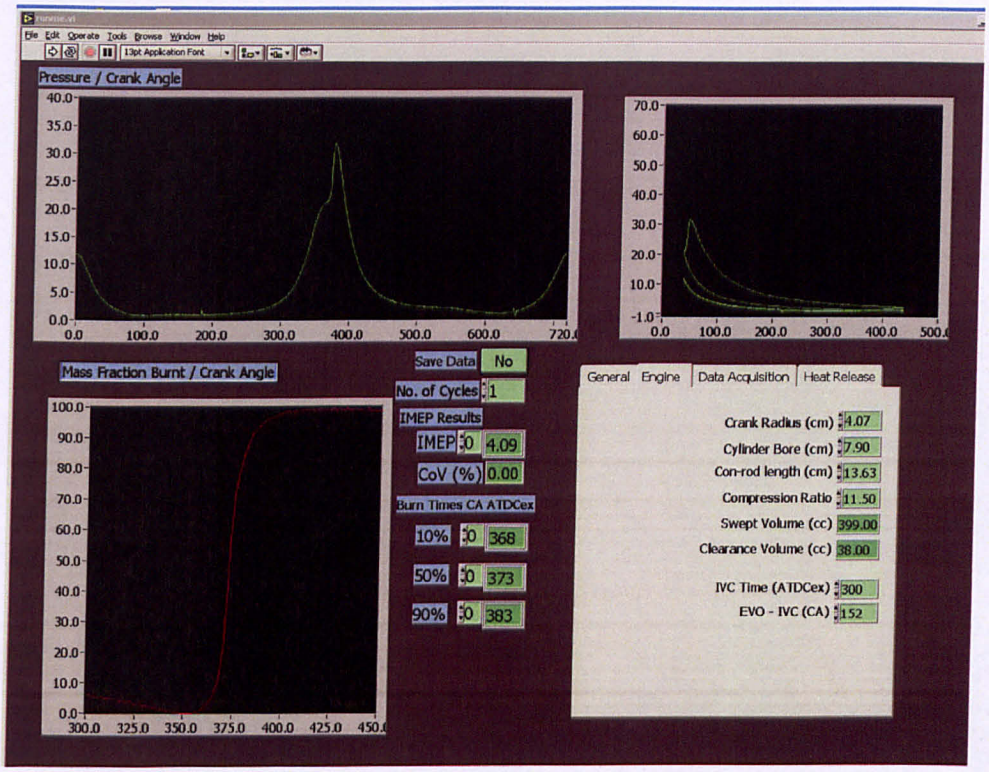

Figure 4.1 Front Panel of the custom built Labview™ Program

The TDC signal sent to the DAQ board should be the one at the beginning of the intake stroke. If by any chance the TDC signal is out of phase, a toggle switch on the box would shift the signal by 360 ° CA.

When installing on the engine, the reference tooth can be placed at any angle in relation to TDC, so long as this angle is typed in the Labview program for correct referencing. However, it should be avoided to place the TDC reference tooth at the engine's TDC, since this is the range in which the crankshaft accelerates the most, increasing the chances of inaccurate readings. Thus, the reference tooth is placed at 89°CA before TDC and this value is input in the "trigger position" field, in the Labview program.

The signals generated by the toothed wheel are picked up by a Variable Reluctance (VR) sensor, which provides a sine-wave as a result. The two resultant sine-waves have their frequency divided and are converted into square-waves by the "Signal Conditioner Box" (Figure 4.2) and then fed into the "I/O Connector Block" box. The latter collects all the signals from the coaxial cables and supplies them to the PC's DAQ Card (NI 6070E) through a 68-pin connector cable.

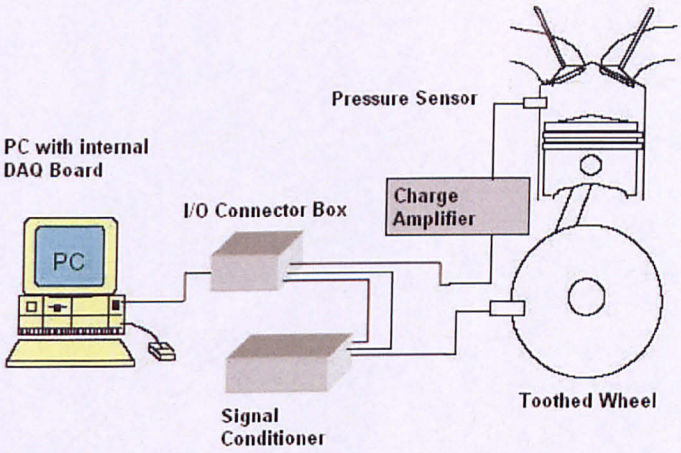

Figure 4.2 Pressure data acquisition set-up

To obtain sufficiently accurate results, it is necessary that piston position and crank angle are phased correctly, i.e. the pressure data is properly phased with the TDC reference provided by the toothed wheel. Hence, it is of paramount importance that TDC is determined correctly. According to Zhao [55], peak cylinder pressures occur near 1°CA BTDC. Using the data acquisition program, the pressure trace is then checked and, if necessary, the phase can be fine-tuned for having the peak pressures at this point. The phasing can be further checked in the program by pressing a toggle button which switches from the p-V diagram to a log p-V diagram.

Following the above procedure, the Labview program is able to calculate and display online pressure trace, P-V diagram and values of IMEP, 10%, 50% and 90% MFB.

4.2 Calculation of Engine performance Parameters

This section describes the calculation procedure for gross and net IMEP, BMEP pumping and frictional losses.

Figure 4.3 shows an example of a four stroke engine p-V diagram which will be used to explain the following calculation.

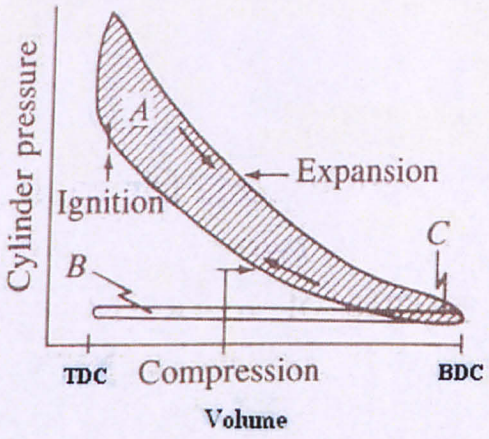

Figure 4.3 Example of a p-V diagram for a four-stroke engine [33]

Area A + area C is the Gross Indicated Work per Cycle; work delivered to the piston over the compression and expansion strokes only. Area B + area C is the pumping work, work transfer between the piston and the cylinder gases during inlet and exhaust strokes.

The work delivered to the piston over the entire four-stroke cycle is defined as Net Indicated Work per cycle and is (area A + area C) – (area B + area C), which equals to (area A – area B).

Hence, pumping work is given by

$$Wp = \oint_{B+C} pdV \tag{4.1}$$

The Gross Indicated Work per cycle can be calculated by

$$w_{i,g} = \oint_{A+C} pdV \tag{4.2}$$

In a similar fashion, one finds the Net Indicated Work per cycle:

$$W_{i,n} = \int_{A-B} pdV \tag{4.3}$$

Net IMEP is found by dividing the Net Indicated Work per cycle by the displaced volume, V_d:

$$\text{Net IMEP} = \frac{W_{i,n}}{V_d} \tag{4.4}$$

Likewise, Gross Indicated Mean Effective Pressure is calculated by dividing the Gross Indicated Work by the displaced volume:

$$\text{Gross IMEP} = \frac{W_{i,g}}{V_d} \tag{4.5}$$

After having found these two results, one can then calculate the Pumping Mean Effective Pressure (PMEP):

$$\text{Gross IMEP} = \text{Net IMEP} + \text{PMEP} \tag{4.6}$$

Brake Mean Effective Pressure is calculated from the power output measured by the dynamometer:

$$BMEP\ (\text{kPa}) = \frac{\text{P (kW)} \times 10^3 \times n_r}{V_d(dm^3)N(rev/s)} \tag{4.7}$$

Where:

n_r = 2 crank revolutions for each power stroke per cylinder

V_d = displaced volume = 1596 cc

P = Power (kW) delivered by the engine and absorbed by the dynamometer

$$P = 2\pi NT \tag{4.8}$$

Substituting for P:

$$BMEP\ (\text{bar}) = \frac{4\pi \mathrm{T} \times 10^5}{0.001596} \tag{4.9}$$

where

T = torque exerted by the engine

4.3 Specific Fuel Consumption

In order to ease the comparison amongst engines, values for fuel consumption are more useful when converted onto specific values, such as BSFC and ISFC.

Brake Specific Fuel Consumption is the fuel flow rate per unit power output and is given by:

$$BSFC = \frac{\dot{m}_f (g/s)}{P(kW)} \tag{4.10}$$

Substituting for P

$$BSFC = \frac{\dot{m}_f(g/s)}{2\pi N(rev/s)T(Nm)} \tag{4.11}$$

where

N = engine speed

m_f = fuel mass flow rate

P = Power

T = Torque produced by the engine

Based on values of IMEP, BMEP and BSFC, Indicated Specific Fuel Consumption is readily calculated:

$$ISFC = \frac{BSFC * BMEP}{IMEP} \tag{4.12}$$

4.4 Emissions Calculations

Similar to the previous data, emissions data are more useful when converted to specific values, allowing easy comparison amongst different engines. This section describes how the emissions values are converted from "raw" values (ppm or vol. %) to brake and indicated specific values.

The Horiba Mexa 7000 series gas analyser (section 3.7) was used to collect the data for CO, CO_2, O_2, uHC and NO_x.

Brake Specific Emissions and Indicated Specific Emissions are calculated using the formula below [56], respectively:

$$BS(X) = (1 + AFR_S) * BSFC * \frac{X(Vol.\%)}{100} * \frac{M_X}{M_{EXH}} \tag{4.13}$$

$$IS(X) = (1 + AFR_S) * ISFC * \frac{X(Vol.\%)}{100} * \frac{M_X}{M_{EXH}} \quad (4.14)$$

Where:

BS(X)	= brake specific value for the emission of interest
IS(X)	= indicated specific value for the emission of interest
AFRS	= stoichiometric air/fuel ratio
BSFC	= brake specific fuel consumption
ISFC	= indicated specific fuel consumption
X	= concentration of the emission of interest
M_X	= molecular mass of the emission of interest
M_{EXH}	= average molecular mass of exhaust products

It should be noted that when the raw value of the emission of interest is given in ppm, it should be converted to Vol. % to enter it in the equations above. The average molecular mass of exhaust products for the air/fuel ratios in use is 29g, according to Heywood [33].

4.5 Trapped residuals, In-Cylinder Temperature and Heat Release Calculations

During this research, CAI combustion is achieved by trapping residual gas in the cylinder by means of advanced exhaust valve closure. It is of vital importance `to know the amount of trapped residuals at EVC. The mass of trapped residuals in the cylinder can be calculated through equation (4.15). The in-cylinder pressure is measured with the pressure transducer installed in the combustion chamber. Based on engine geometry, and with the information of piston position provided by the tooted wheel, the cylinder volume at EVC can be calculated. The burnt gas temperature was assumed to be the exhaust temperature at EVC, measured by the thermocouples placed in the exhaust ports. The amount of residuals at EVC was assumed to be the total amount for the whole cycle.

$$PV = m_r RT \quad (4.15)$$

Where,

P = in-cylinder pressure
V = cylinder volume
m_r = mass of trapped residuals
R = specific gas constant
T = burnt gas temperature

This procedure proved to be reasonably accurate despite of the differences between the exhaust gas temperature and the actual burnt gas temperatures.
The amount of fresh charge in the cylinder is calculated from lambda and fuel flow rate data. Hence, one can calculate the ratio of Trapped Residuals to Total In-Cylinder Charge. In addition, since pressure and volume are known, In-Cylinder Temperature values can be estimated.

4.6 Heat Release Analysis

Heat Release Analysis is a useful tool for studying the combustion process in the engine. The amount of heat necessary to produce an observed pressure variation can be calculated based on the first law of thermodynamics applied to the cylinder contents (equation (4.16)). The cylinder contents are treated as being a single zone and therefore reactants and products are fully mixed. Likewise, it is assumed that there is no difference between reactants and products properties.

$$\delta Q_{hr} = dU + \delta W + \delta Q_{ht} \tag{4.16}$$

Where:

δQ_{hr} = Heat released by combustion
δQ_{ht} = Heat transfer to the chamber walls

$$\delta W = pdV \tag{4.17}$$

$$dU = mc_v dT \tag{4.18}$$

$$mdT = \frac{[pdV + Vdp]}{R} \tag{4.19}$$

Combining equations (4.17) and (4.18), substituting terms into equation (4.19) and writing on an angle incremental basis gives:

$$\frac{dQ_n}{d\theta} = \frac{dQ_{hr}}{d\theta} - \frac{dQ_{ht}}{d\theta} = \frac{\gamma}{\gamma - 1} p \frac{dV}{d\theta} + \frac{\gamma}{\gamma - 1} V \frac{dp}{d\theta} \qquad (4.20)$$

The ratio of specific heats γ is equal to c_p/c_v, and is assumed to have a constant value of 1.35.

Thus, the net heat release rate $dQn/d\Theta$ is obtained from the measured pressure array, the calculated volume array, an estimation of average ratio of specific heat values during compression and expansion, and arrays that define the rate of change of pressure and volume with respect to crank angle.

Integrating equation (4.20) with respect to crank angle gives a cumulative heat release function, from which the normalized mass fraction burned (MFB) curve can be obtained and the CA at 10%, 50% and 90% MFB can be calculated. MFB curves are useful to quantify ignition timing and combustion duration [57].

4.7 Summary

The present chapter explains the method used for data acquisition and the devices involved in such a task. The main features of the data acquisition program are discussed. It also explains the importance of synchronizing the different sets of data and the post processing operation using the macro program. All the main equations and mathematical operations contained in the program are described.

5. Naturally Aspirated CAI

5.1 Introduction

As previously discussed in Chapter 2, there are several ways to achieve CAI combustion. The method chosen in this study is to trap large amounts of exhaust residuals inside the cylinder. The large amount of retained residuals provides sufficient energy to promote auto-ignition of the charge and also controls the heat release rate due to the dilution imposed. This is all made possible through the negative valve overlap (NVO) approach, further described in this chapter.

This chapter also describes the methodology used in this research and investigates the effects of CAI combustion on a naturally aspirated engine. Performance and emissions parameters are presented and discussed, for various conditions. Effects of varying valve timing and lambda are likewise assessed.

5.2 CAI Combustion via Negative Valve Overlap Approach

To retain a large amount of exhaust residuals inside the cylinder without having to use external EGR, one strategy is to close the exhaust valve before TDC, trapping the residuals inside the cylinder. Furthermore, if one has a situation in which EVC occurs before TDC on the exhaust stroke and IVO after TDC on the intake stroke, intake and exhaust valves are never opened simultaneously, and the duration in °CA between EVC and IVO is defined as the negative valve overlap (NVO) period.

In order not to loose the energy accumulated by the recompression of the exhaust gases, the intake valve has to open around a symmetrical position in relation to TDC. In other words, EVC and IVO need to occur at similar crank angle intervals, relative to TDC. If IVO occurs too early, the energy accumulated by the recompression event will be dissipated in backflow to the intake manifold, rather than being used to push down the piston.

However, with standard camshafts with fixed profiles and, therefore, valve durations, to achieve NVO is not just a matter of advancing EVC and retarding IVO. Standard

camshafts generally have durations of more than 220°CA for both intake and exhaust cams. If EVC is too advanced, there is an impact on the power stroke, by having a too early EVO. In addition, if IVO is too retarded, there is a negative effect on the compression stroke, limiting the compression ratio and pumping the intake charge back in the intake manifold. Consequently, for CAI operation, shorter duration cams are needed.

In previous research [23][24], camshafts having durations (at 0.1mm valve lift) of 110°CA for exhaust and 120°CA for intake and lifts of 2 and 2.5 mm for intake and exhaust, respectively, were used successfully.

The CAI camshafts are bespoke, re-profiled units, based on standard production items. Re-profiling the cams for the desired duration, however, has a penalty on lift. This happens because, in order to keep an optimum cam profile with good dynamic behavior, the lift has to be reduced from the original values of around 9mm to 2 mm for the exhaust and 2.5 mm for the intake.

The company designated to re-profile the cams received, therefore, a file containing these specs for the desired camshafts. However, the actual finished unit has a slightly smaller lift for both cams: 1.85 mm for exhaust and 2.33 mm for intake. The durations, however, are according to the requested values: 120°CA for intake and 110°CA for exhaust.

Intake and exhaust valve timings are selected to be similar to previous experiment [23][24], with EVC ranging from 57°CA to 104°CA BTDC and IVO ranging from 72°CA to 124°CA ATDC. As mentioned on section 3.3.2, the shifting range for the VCT unit is 47°CA for the exhaust and 52°CA for the intake respectively.

In order to minimize experimental variables and to stay in the most efficient range, with minimum back flow and energy losses, IVO was chosen to always open on a symmetrical position, compared to EVC, in relation to TDC, in this part of the experiment. However, the recompression stroke after EVC and the subsequent expansion between TDC and IVO has some heat losses, creating the small pumping loop presented on Figure 5.1.

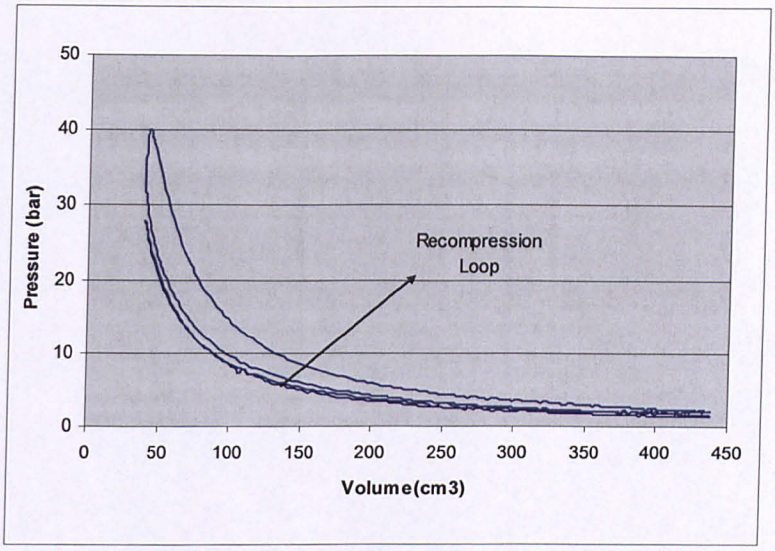

Figure 5.1 Experimental P-V diagram at 1500 rpm

The ECU controls the solenoid valves which supply the oil to the VCT units, allowing the camshafts to be shifted. This camshaft control has a precision of 1°CA. As described in section 3.3.2, the default (start-up) camshaft position is fully advanced exhaust and fully retarded intake. In general, the shift increments were of 5°CA until the end of the VCT range is reached. Figure 5.2 shows the possible valve timing range as well as valve lift profiles for both intake and exhaust. It should be noted that although all the "mechanical" VCT range was available, it was not used completely, since the operation was limited by either misfire or knock.

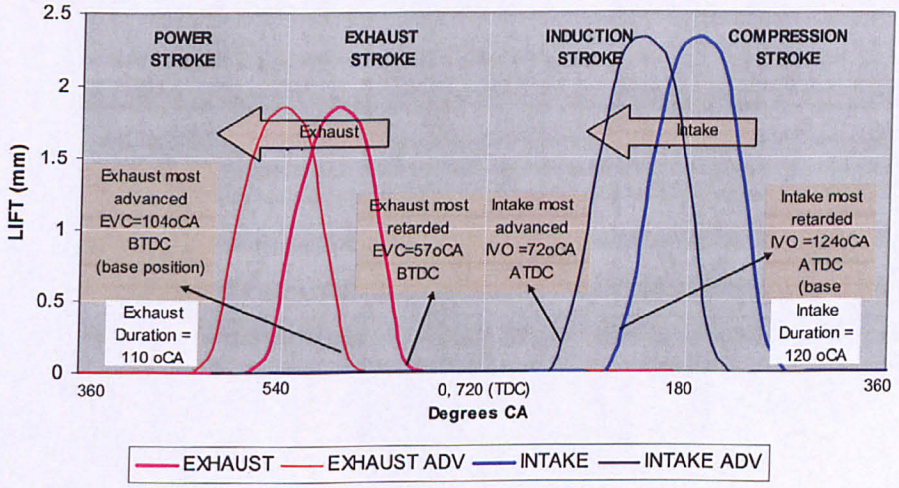

Figure 5.2 Intake and Exhaust cam profile and VCT range for the short duration camshafts

5.3 Naturally Aspirated CAI Engine Operation and Test Procedure

Table 5.1 shows a summary of engine operating conditions for the naturally aspirated CAI testing.

Table 5.1 NA CAI Engine Test Conditions

Coolant temperature	90 °C
Fuel	Gasoline 95 RON
Fuel line pressure	3.5 bar
IVO	75°-104° ATDC
EVC	75°-104° BTDC
Engine Speed	1000-3500rpm
Throttle Opening	100%

For engine start up SI operation was required. Since CAI needs hot residuals to start, the engine had to first generate the hot residuals by running in SI operation and then, progressively, switch to CAI operation.

The procedure was to set the throttle opening to around 30% and to crank the engine. As soon as the engine started, the oil pressure rose and released the cams from the base position, after which they were controlled by the ECU, following a valve timing table, with preset values for each condition.

For easier starting, a richer mixture of lower λ value was set, being controlled by the ECU via closed loop with a λ sensor.

The engine was then left to warm up at a constant speed, still at part throttle. When the coolant temperature reaches 80°C, the throttle was fully opened, and CAI started to take place, depending on the valve timing combination. If EVC was too late, knocking took place, as it could be confirmed from the pressure trace, with a rate of pressure rise higher than 10bar/°CA. Conversely, if it was too early, the engine tended to misfire, showing a coefficient of variation in IMEP (COV_{imep}) higher than 10, as it will be explained in the following sections. As the temperature rose further and stabilized at around of 90°C, the engine started to be less sensitive to manual changes in ignition timing and ignition could be actually shut off.

However, during each engine test the spark was left on, since it ensured that CAI would occur, avoiding occasional cylinder stall due to misfire, specially when the engine was still in the warm up phase. Moreover, it could broaden the CAI range by allowing a spark-assisted CAI zone, normally found on the boundaries of the normal, sparkless, CAI, as shown by Kalian [57].

Testing was carried out with the dynamometer set for constant engine speed. In order to determine the CAI operating range, constant speed test points of 1000, 1250, 1500, 2000, 2500, 3000 and 3500 rpm were used. For each test point, load was varied mainly through valve timing change. For example, increasing NVO with advanced EVC traps more exhaust residuals and hence reduces the volume of fresh air/fuel mixture inducted in the following cycle. When the minimum load for stable operation at λ=1.00 was achieved, λ was then progressively increased up to the lean limit. For speeds of 3000 and 3500 rpm, stable operation could only be achieved with mixtures leaner than λ=1.05 and λ=1.10, respectively. Load was varied and lambda progressively increased until misfire took place. Figure 5.3 shows the CAI operational range that was possible to achieve.

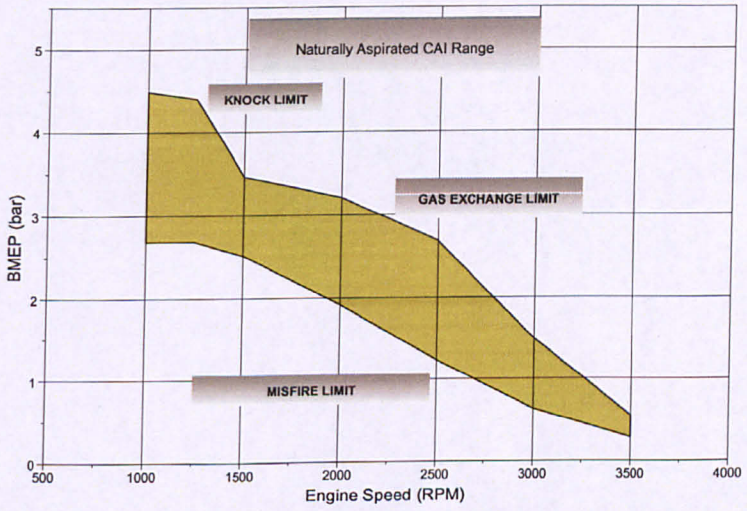

Figure 5.3 NA CAI Combustion Operational Range

The higher load range was limited by knock at speeds up to 2000 rpm. For higher speeds, knock was not observed and load limitation was caused only by the gas exchange restriction imposed by the short duration/low lift camshafts. For the same reason, for speeds higher then 3500 rpm the engine could not achieve stable operation anymore.

At every speed, there was a lower load limit (lowest BMEP). At this situation, a high amount of exhaust residuals (Figure 5.4) was trapped in the cylinder and the exhaust temperature was already very low as shown in Figure 5.5.

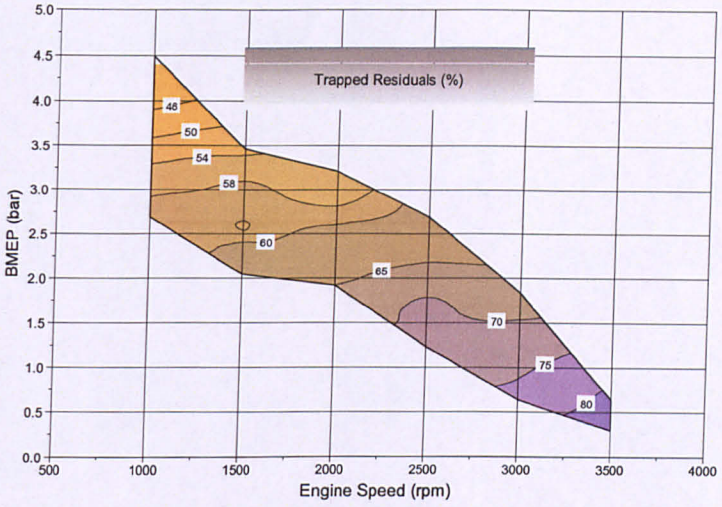

Figure 5.4 NA CAI Exhaust Residuals (%)

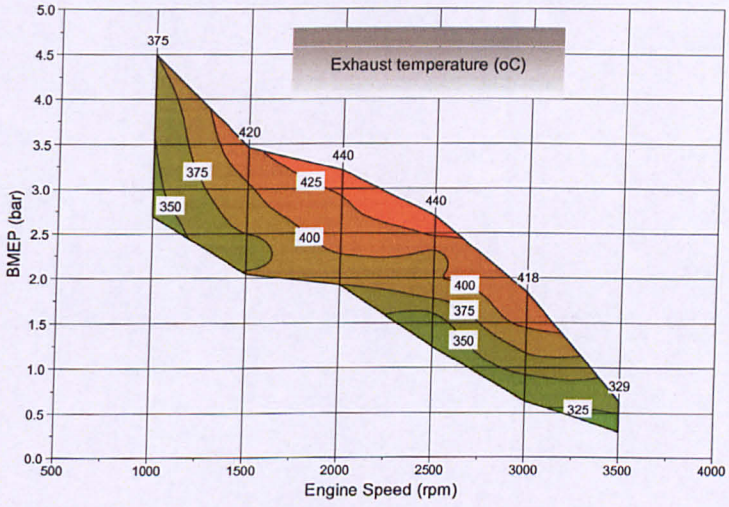

Figure 5.5 NA CAI Exhaust Temperature

For each valve timing combination at each test point, the lambda target value was always set to λ=1.00 and progressively increased, in steps of 0.05 until the engine starts to misfire. For speeds more than 2500rpm, however, the engine did not achieve stable operation with lambda values less than 1.05. The mixture was progressively leaned until the maximum achievable lambda value.

At every test point, for every combination of valve timing and lambda value, the engine was left to stabilize for few seconds and then data was acquired according to the

procedure described in chapter 4. In addition, the combustion characteristics were monitored real-time on the screen, using the Labview program, where pressure vs. crank angle, pressure vs. volume and mass fraction burn diagrams were displayed (Figure 4.1).

5.4 Performance and Emissions Overview

The results presented in this section were taken mostly at λ=1.00, with some lean boundaries at low load, as described in section 5.3. To minimize testing time and to replicate conditions from a road car, emissions were sampled only downstream from the catalyst, which means, no raw emissions measurements were taken.

Figure 5.6 shows BSFC over the CAI range. It can be noticed that fuel consumption tends to be more sensitive to load than speed, with BSFC reducing as load increases, for the same speed.

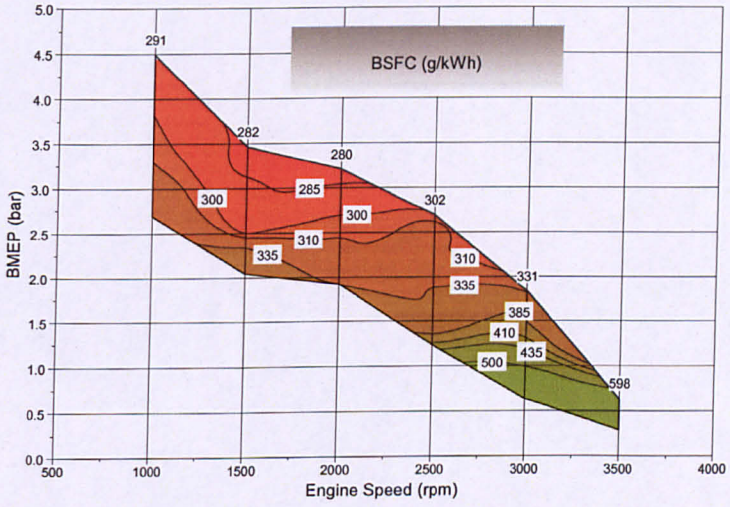

Figure 5.6 CAI fuel consumption

Figure 5.8 to Figure 5.10 present NO_x, CO and HC emissions of the CAI combustion range. Emissions of NO_x are extremely low compared to spark ignition combustion as to be shown later. The level of NO_x emissions increase as the load increases. This is expected due to the lower amount of residuals (Figure 5.4) and increased cylinder temperatures at this condition, as shown in Figure 5.7. As speed goes up and load goes down, NO_x emissions are further reduced.

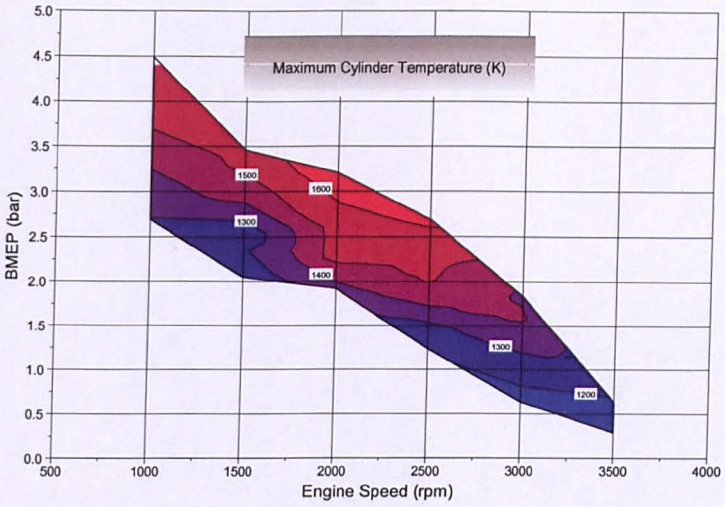

Figure 5.7 Maximum In-Cylinder Temperature for the NA CAI range

In Figure 5.9, CO shows very high values at 1000rpm. The reasons for this are still under investigation, but possible causes could be the formation of a fuel rich zone in the cylinder or the occurrence of bulk quenching. As the speed goes up, CO emissions fall drastically and increase again around 2500rpm, when the engine operation becomes less stable at λ=1. Above this speed, the engine could not run anymore with λ<1.05, which explains the very low values of CO at the higher speeds. At the top speed of 3500rpm, CO emissions increase once more, especially at the low load region. This is expected since the engine was approaching the misfire range. At any given speed it is observed that CO decreases with increased load.

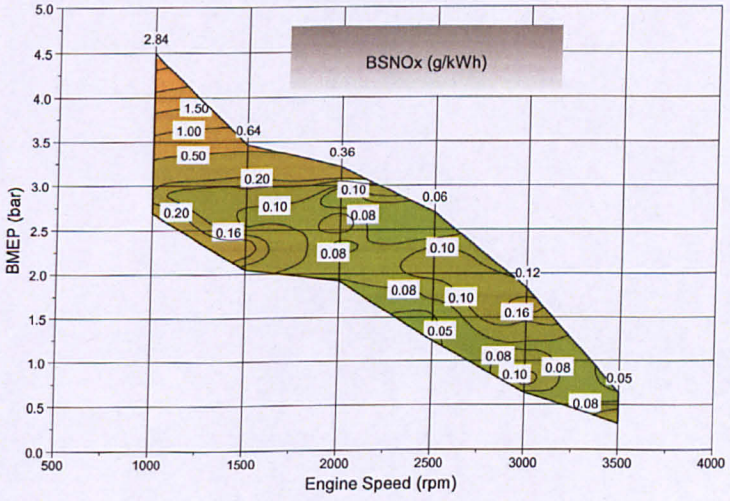

Figure 5.8 CAI brake specific NOx emissions

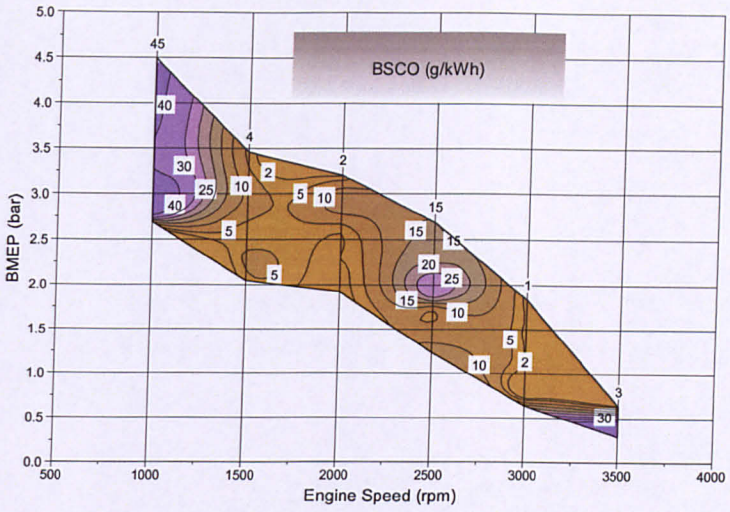

Figure 5.9 CAI brake specific CO emissions

Figure 5.10 shows that HC emissions decrease with increased load, for each speed point. Keeping the load constant and increasing speed also helps to reduce HC emissions, suggesting that for these two conditions combustion tends to be more complete.

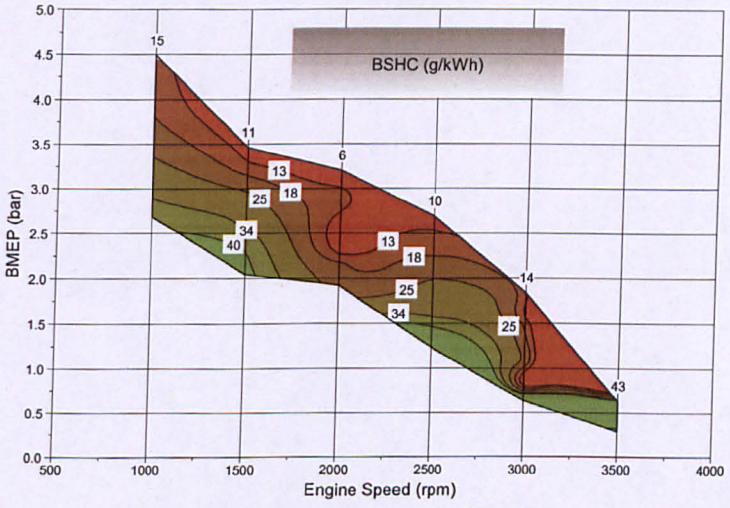

Figure 5.10 CAI brake specific HC emissions

Figure 5.11 to Figure 5.14 shown a comparison between the brake specific results of CAI combustion operation in this engine and SI combustion operation from a 1.8 litre standard production gasoline engine (Ford Zetec^{TM}), tested at stoichiometric mixtures, supplied by the manufacturer. It can be seen in Figure 5.11 that BSFC is reduced over the whole CAI operation and tends to improve with increased speed and reduced load. The improvements in BSFC are mainly due to the almost absence of pumping losses at part

load because, as the load approaches the lower limit, the SI engine has to operate with more throttling, impairing BSFC in comparison to the CAI engine. Moreover, the fact that CAI combustion is very fast, with constant volume heat addition, also leads to improvements in fuel consumption.

Figure 5.12 shows the advantages of CAI combustion in NOx reduction. Over the whole speed range, NOx emissions are dramatically reduced to up to 99%. The combustion analysis carried out in the next section will explain that this is due to the low CAI combustion temperature.

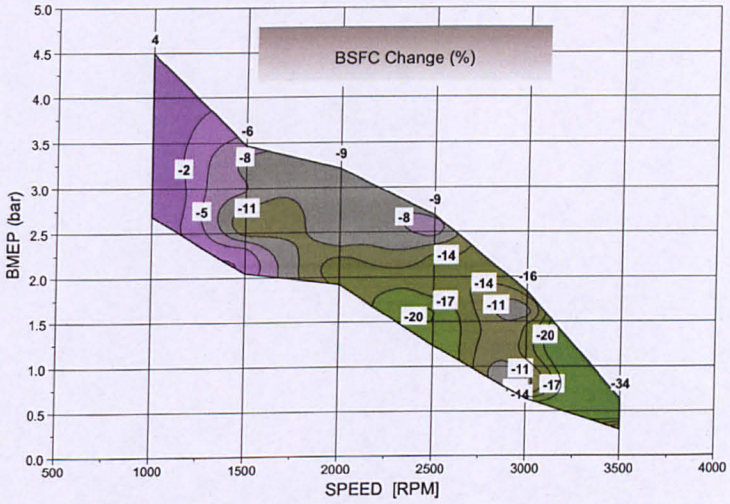

Figure 5.11 Change in BSFC (%) with CAI combustion

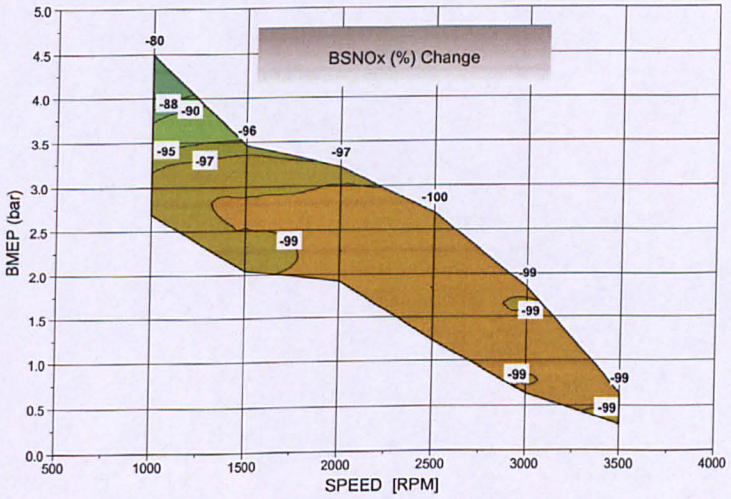

Figure 5.12 Change in BSNOx (%) with CAI combustion

Figure 5.13 Change in BSCO (%) with CAI combustion demonstrates that, apart from the 1000 rpm region, CO is greatly reduced over the remaining CAI range. It has a little increase at 2500 rpm, when the engine starts to be less tolerant to λ=1 and then falls again thereafter.

Figure 5.14 shows, however, that unlike the other emissions, BSHC is much higher with CAI than with SI combustion. A possible reason for that is the low combustion temperature achieved with CAI.

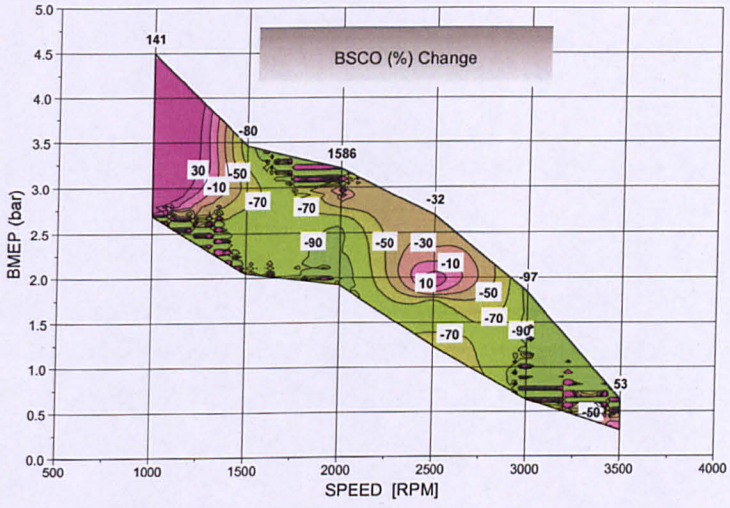

Figure 5.13 Change in BSCO (%) with CAI combustion

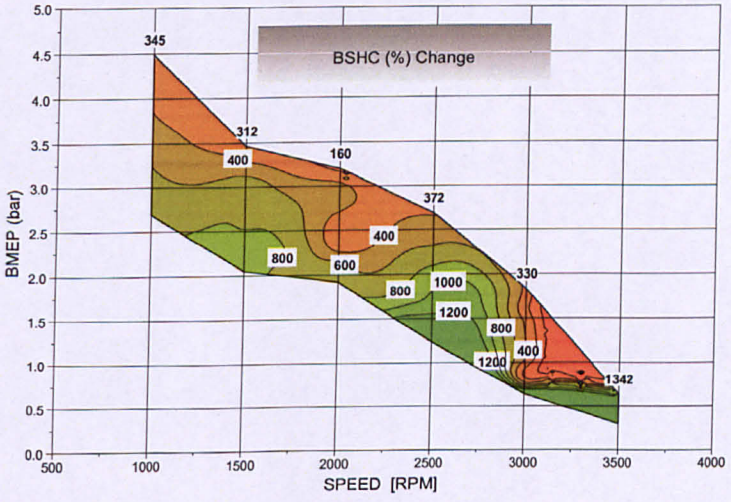

Figure 5.14 Change in BSHC (%) with CAI combustion

5.5 Analysis of In-Cylinder Conditions

To draw conclusions on how to improve the usable range of CAI (Figure 5.3) and to understand its limiting factors, the analysis of the in-cylinder conditions was carried out. This section presents data taken at λ=1 for speeds up to 2500 rpm. Values for 3000 and 3500 rpm were taken at λ=1.05 and λ=1.15 respectively, since the engine could not run stable with stoichiometric mixture at such speeds.

5.5.1 Effects of Trapped Residuals on Engine Performance

Figure 5.15 describes the effects of exhaust residuals throughout the whole CAI range. It can be seen that there is a linear correlation between the amount of residuals and engine performance. As the quantity of residuals increase, torque output decreases. For a given speed, bearing in mind that the engine was operated at WOT, as the mass of exhaust increased, less fresh charge could be drawn into the engine, resulting in lower torque. This confirms that changing the residual fraction via valve time adjustment is an effective way of controlling load, resulting in throttleless operation and, therefore, reduced pumping losses.

Together with Figure 5.3, Figure 5.15 also describes the upper and lower limits of the CAI operation, for every speed. The upper limit, at low speed, was due to knocking combustion and, at high speed, due to restrictions in the gas exchange process imposed by the low lift camshafts. The lower limit was caused by misfire, since there was not enough energy for the charge to ignite. At lower speed, the volumetric efficiency of the engine was improved, yielding a higher maximum torque. Conversely, as the speed increased, the volumetric efficiency fell, limiting the maximum torque obtainable. To expand the maximum limit at high speed, the gas exchange process has to be improved. Some possible ways to do that could be forced induction and to use a more flexible valve train.

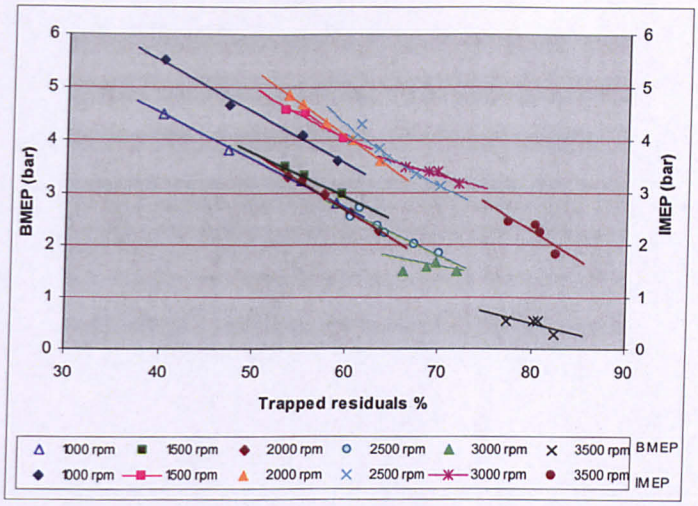

Figure 5.15 Effect of residual fraction on MEP values for the whole CAI range

Frictional losses are indicated in Figure 5.15 by the difference between IMEP and BMEP. It shows that the friction increases from about 1 bar at 1000rpm to 1.5bar at 3500rpm.

5.5.2 Effect of Exhaust Gas Temperature

Trapped residuals were used to obtain CAI. Therefore, exhaust gas (or burnt gas) temperature would have a major effect on auto-ignition and hence on engine operation. Figure 5.16 demonstrates that exhaust temperature decreases with increasing residuals, for the same speed. This is logical since with increased residuals, less air/fuel mixture will be burnt in the cylinder. For the same residual fractions, exhaust temperature increases with the engine speed. This is mostly due to the reduced heat losses at higher engine speeds.

It is noticeable that at the maximum residual rate the exhaust temperature was always between 600 and 700 K. Below this misfire took place, limiting the BMEP range. This shows that any means to increase residual gas temperature would help to extend the lower load limit.

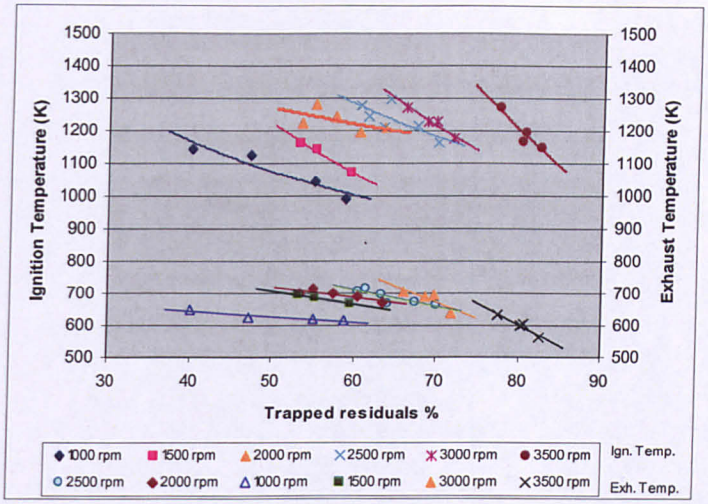

Figure 5.16 Effect of Residual fractions on exhaust and ignition temperature

5.5.3 Combustion Analysis

Figure 5.16 also shows the average charge temperatures at the time of autoignition (T_{ig}). The autoignition time was defined as the crank angle at which 10% of the charge had been burnt. The charge temperature was calculated by assuming that the fresh charge and residuals were homogeneously mixed and that combustion took place simultaneously across the combustion chamber. Although these assumptions might differ from the real case, they yield useful information about the in-cylinder conditions.

As shown in Figure 5.16, T_{ig} for gasoline was between 1000 and 1300K and it could vary up to 20% with the residual fractions. It can clearly be seen that, for a given speed, as the residual rate increases, T_{ig} becomes lower. This is the opposite of what should be expected and the reasons for this unusual behaviour are under investigation, although a plausible reason could be the larger amount of more reactive species present.

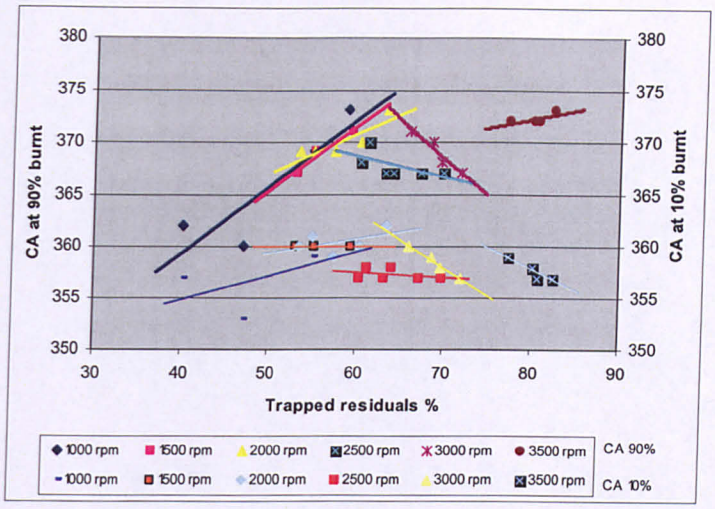

Figure 5.17 Effect of residual fractions on 10% and 90% burn angle

Figure 5.17 shows the crank angles for 10% and 90% mass fraction burnt. Autoignition (10%MFB) started between 355 and 365°CA depending on speed and load. At low speed and high loads, autoignition showed a tendency to start early, since exhaust residuals are at high temperature. As speed increases, first it tends to happen slightly later and then advances again, coming back to around 355°CA, once more due to the high temperature of the exhaust gases. At high speed, although the amount of residuals is higher, their temperature still remains high, due to the lower heat losses.

Figure 5.18 shows the combustion duration, which is the interval between 10 and 90% mass fraction burnt. The trend lines in the graph indicate that the combustion duration in crank angles increases with speed and decreases with load but they are of similar values in absolute time. Other than 2500rpm and 3000rpm, combustion gets faster as the residual fraction decreases. The engine had points of instability at 2500rpm and slightly less at 3000rpm, where it could only run with lean mixtures of λ=1.05 and above. This led to the scattered data shown in Figure 5.18.

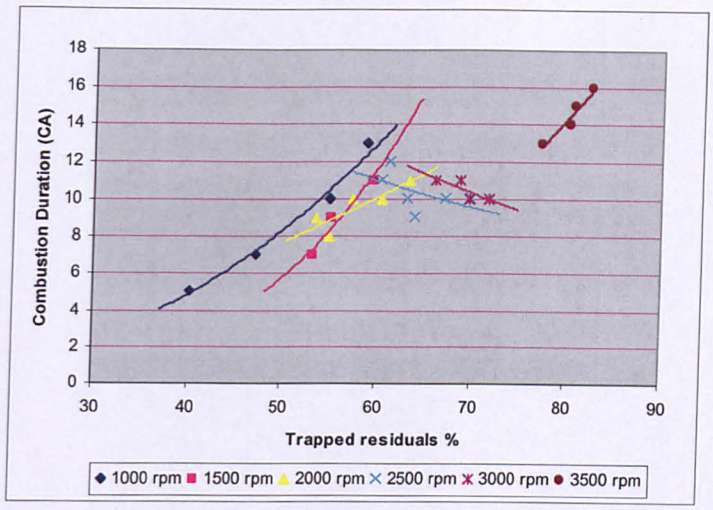

Figure 5.18 Effect of residual fraction on combustion duration

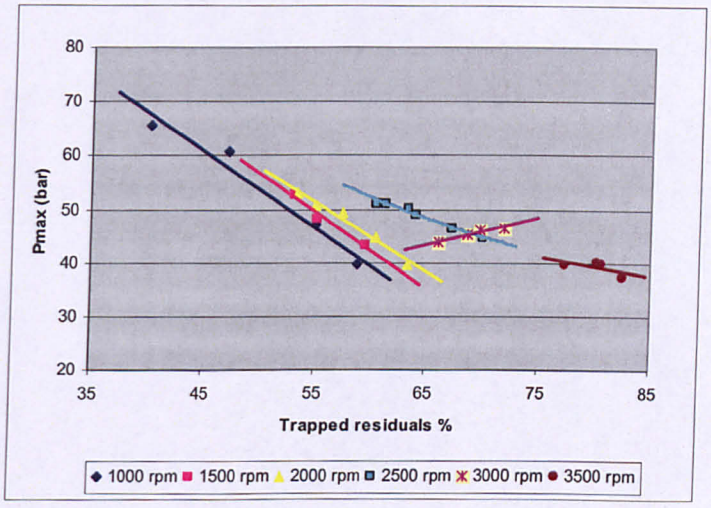

Figure 5.19 Effect of residual fractions on peak cylinder pressure

Figure 5.19 shows the peak cylinder pressures for the CAI range. Peak pressure increases with load (less residuals), given the same speed. For the same load, peak pressure increases with speed except for the lean conditions above 2500 rpm.

The maximum rate of pressure rise for constant values of λ=1.00 (1000-2500 rpm) and λ=1.05 (3000 rpm) as mentioned before, can be seen in Figure 5.20, which shows that it reduces as load decreases (the amount of residuals increase). For the same load, it tends to increase with speed. Again, the behaviour changes slightly for the leaner conditions at high speed.

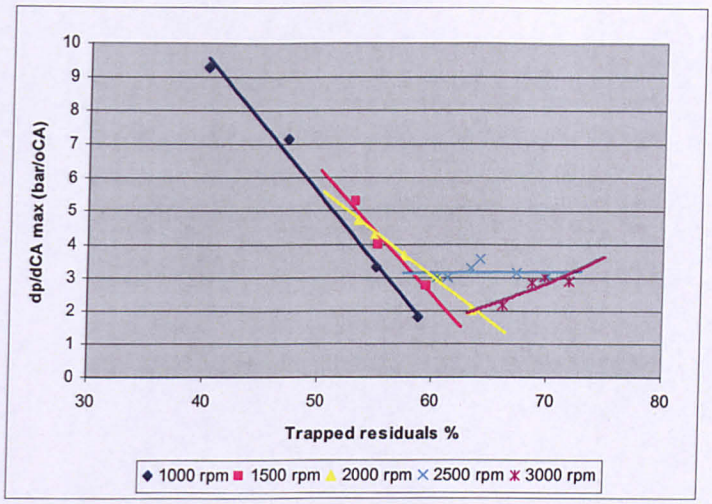

Figure 5.20 Effect of residual fractions on maximum rate of pressure rise

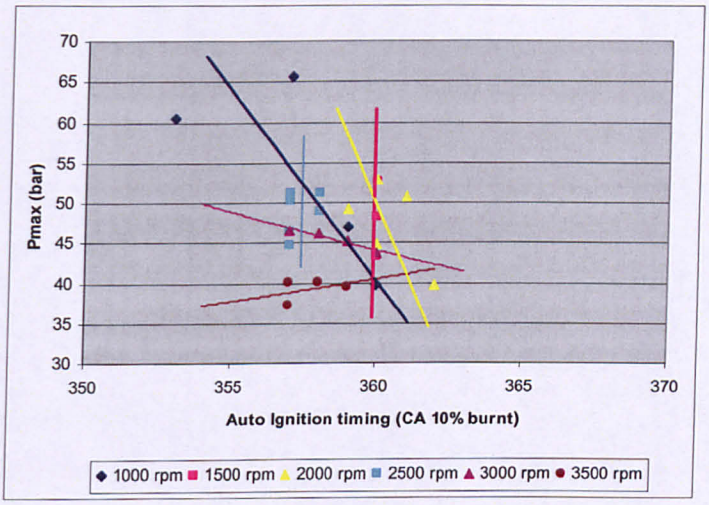

Figure 5.21 Effect of combustion phasing on peak cylinder pressure

From Figure 5.21 it can be seen that combustion phasing advances as speed reduces, and, therefore, load increases, since the highest loads were achieved at low speed. Conversely, combustion phasing retards as the residual fraction increases (load decrease). In addition, the maximum cylinder pressure decreases with increased speed and residual fraction. The same behaviour also applies to the maximum rate of pressure rise, as Figure 5.22 demonstrates. It should be pointed out that although the rate of pressure rise was approaching 10bar/^{o}CA, the engine wasn't actually knocking. There was combustion noise, but not at the same level that could be deemed as knocking.

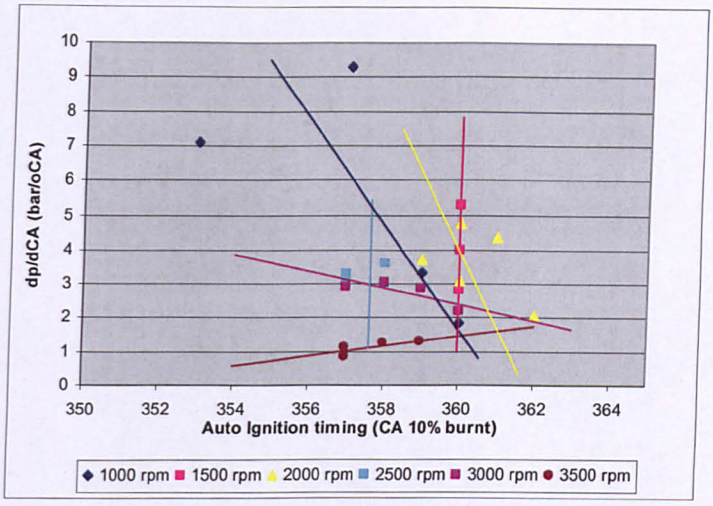

Figure 5.22 Effect of combustion phasing on the maximum rate of pressure rise

To summarize, load has a strong effect on CAI combustion. At high loads, CAI combustion starts earlier and burns faster. Ignition temperature, exhaust temperature, peak pressure and maximum pressure rise were higher. Speed has an effect on load, caused mainly by the flow limitation imposed by the low lift camshafts. At high speeds, heat losses are lower, thus temperatures are higher and ignition happens earlier.

5.5.4 Analysis of Emissions

Figure 5.23 demonstrates that NOx emissions are strongly affected by load. As load increases, NOx emissions rise steeply. Conversely, as load decreases (i.e. the residual fraction increases) NOx emissions fall down and remain very low for the majority of the test points. In addition, for a fixed load point, NOx emissions tend to increase with speed. To better understand the NOx results, a calculation was made to determine the in-cylinder temperature (Figure 5.24), assuming the mixture was perfectly homogeneous. Figure 5.24 shows temperature profiles for two different load conditions at 1000 rpm. Until ignition takes place the temperature exhibits no significant difference between the two conditions. After ignition, the temperature at 5.5bar BMEP was considerably higher, rising steeply up to 2500K, while at the 3.6bar BMEP it reached only up to 1800K.

The substantially higher in-cylinder temperature at 5.5bar BMEP explains the difference in NOx emissions, as shown in Figure 5.25. It presents the effects of peak cylinder temperature on NOx emissions for different speeds. It can be seen that negligible NOx emissions are present before 1800K, after which they increase exponentially with temperature.

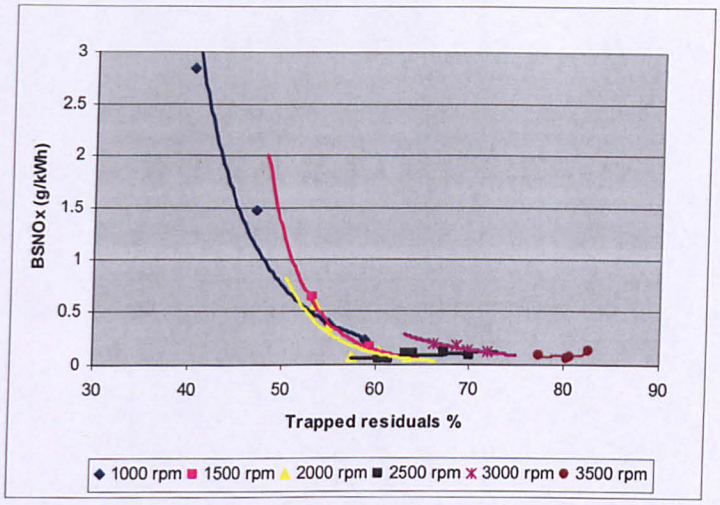

Figure 5.23 Effects of load and speed on NOx emissions

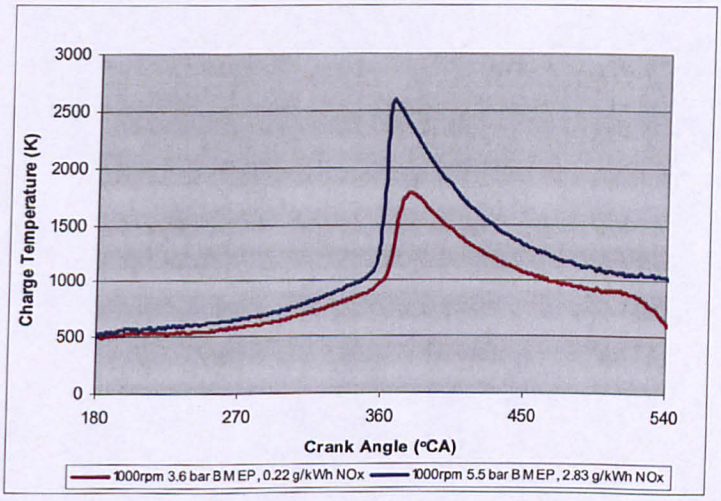

Figure 5.24 In-cylinder gas temperature histories

The results shown in Figure 5.25 demonstrate that CAI combustion does not always yield ultra-low NOx emissions. In fact, when the cylinder temperatures were high enough the NOx emissions were comparable to those from a SI combustion engine. Hence, it's clear

that cylinder temperatures need to be kept down to minimize NOx emissions. That can be achieved by maintaining enough dilution rate as the load is increased. This all suggests that forced induction could be a good alternative if it could operate with a higher residual fraction or a leaner air/fuel mixture.

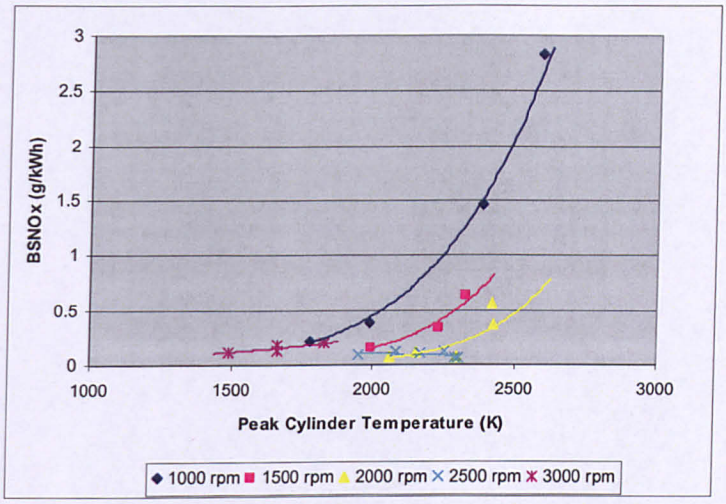

Figure 5.25 Effects of peak cylinder temperature on NOx

Figure 5.26 presents brake specific values of CO versus residual rates. At the speed of 1000 rpm CO emissions are very high, possibly due to poor mixing and cylinder filing, as mentioned previously. They also show no significant variation as load goes up. As the speed increases, CO emissions have a tendency to decrease. There is a point of unstable operation at 2500 rpm, with an increase in CO emissions. At this speed it was difficult to achieve stable operation, possibly due to some manifold tuning effect. For higher speeds, combustion becomes stable again and CO emissions fall significantly and increase again when the speed reaches 3500 rpm, where flow restrictions are at the maximum, leading to unstable combustion. Hence, except for the speed points of 2500 and 3500 rpm, CO emissions are not greatly affected by load.

Figure 5.27 shows brake specific HC emissions against the residual fraction. For the same speed, HC emissions decrease with load. For a constant load, HC emissions decrease with increased speed, possibly due to the higher in-cylinder temperatures achieved.

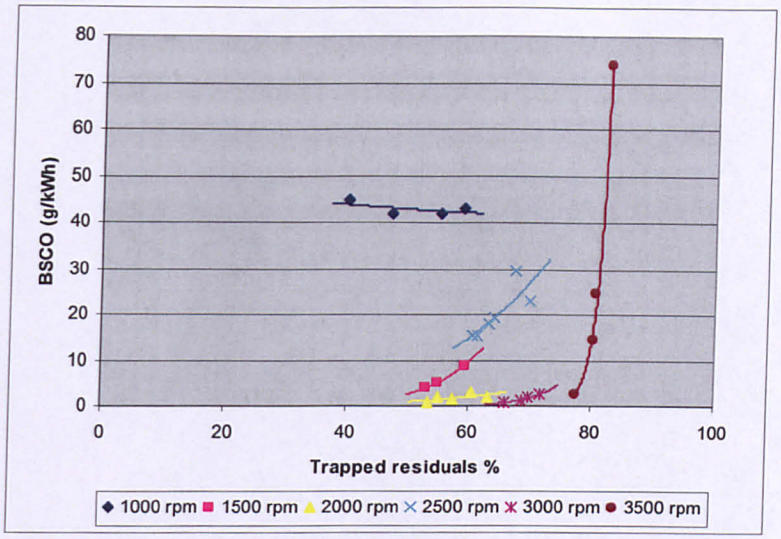

Figure 5.26 Effect of load and speed on CO emissions

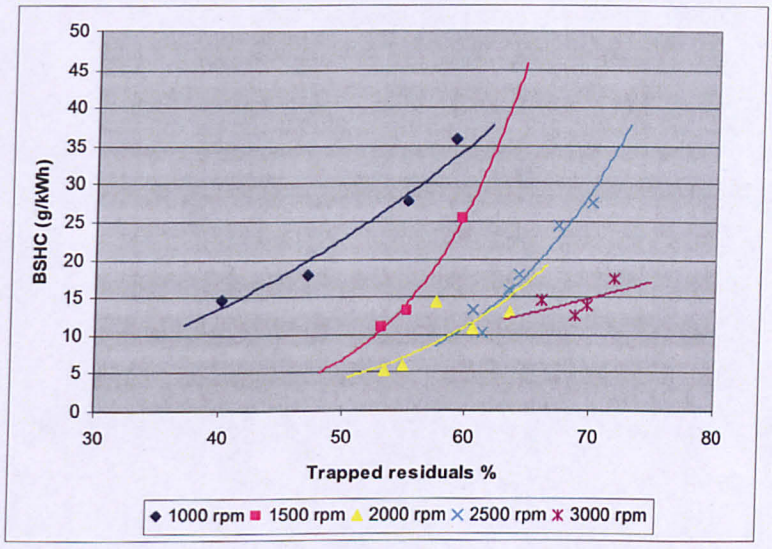

Figure 5.27 Effects of load and speed on HC emissions

5.5.5 Analysis of Specific Fuel Consumption

Figure 5.28 shows how BSFC varies with load and speed. For speeds up to 2500 rpm, BSFC decreases with load. From 1500rpm up to 2500 rpm, speed seems to have no great effect on BSFC. For the speeds of 3000 rpm and especially 3500 rpm, BSFC increases dramatically with speed and load. The variation with load will be better explained later.

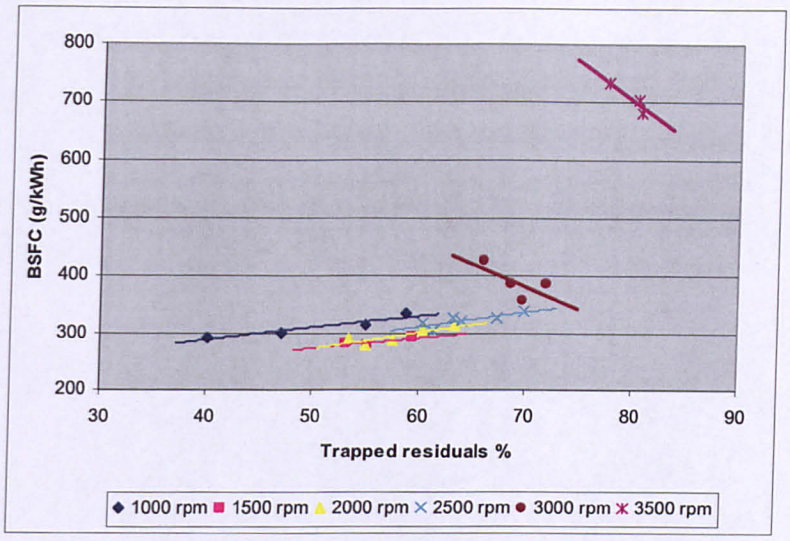

Figure 5.28 Effects of load and speed on BSFC

A good way to analyze the effects of speed and load on CAI combustion is to plot net ISFC (Figure 5.29) and to compare it with BSFC (Figure 5.28). The ISFC results are very different from the BSFC ones. Unlike the BSFC values, ISFC decreases with engine speed. The difference between ISFC and BSFC can only be caused by frictional losses. This explains, therefore, high BSFC values at high speeds because of the increased frictional losses.

5.5.6 Effects of Pumping Losses

As previously explained, the necessary high amount of residuals to obtain CAI was achieved by early exhaust valve closure and late inlet valve opening, running on negative valve overlap. During this stage, exhaust gases were recompressed and expanded again during the piston movement downwards, at the beginning of the intake stroke. Obviously there are some heat losses in this process, which generate the small pumping loop (Figure 5.1) as explained previously. According to Figure 5.30, one can see that the average pumping losses have a tendency to decrease with speed.

For 1000 rpm only, it tends to increase with increased residuals (less load). As the speed from 1500 rpm and above, this behaviour changes and, for a constant speed, pumping losses increase dramatically as the residuals decrease (higher load). This can be explained by the fact that at high speeds, during the exhaust stroke, the piston has to overcome a

large flow restriction caused by the low lift camshafts, generating considerable energy losses. If the exhaust valve is closed early and the intake valve opens late enough, the piston does not need to pump exhaust out and dissipates less energy. The piston has then to recompress the exhaust gases, but, since the speed is high, there is not much time for heat losses to occur and the gases still retain much of their potential energy, which will be delivered back to the piston during the intake stroke.

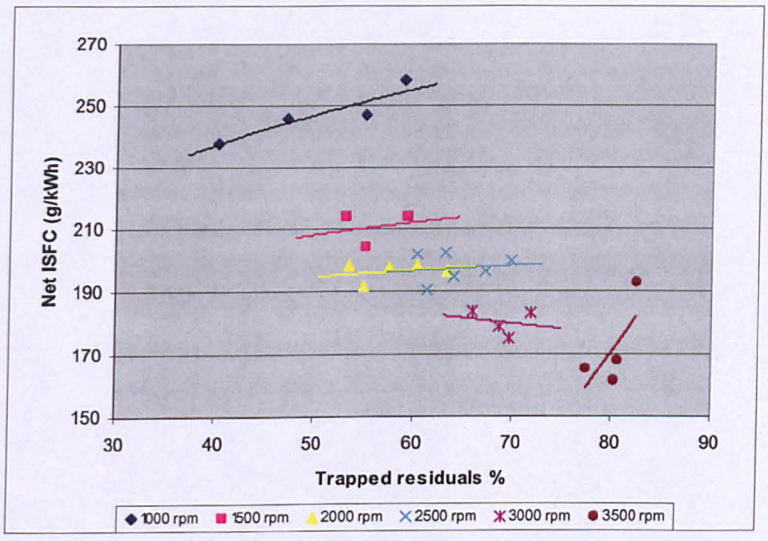

Figure 5.29 Load and speed effects on Net ISFC

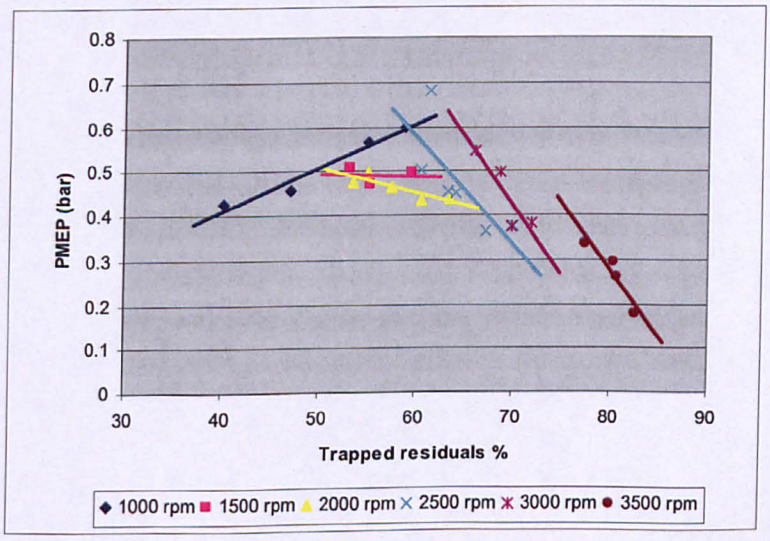

Figure 5.30 Load and speed effects on PMEP

Figure 5.31 shows the effects of pumping losses on ISFC. It can be seen that the recompression and expansion loops account for an average of 12% losses on ISFC, increasing slightly with speed and then remaining at a constant threshold. This leads to the conclusion that the main cause for the high BSFC value at high speed is really the friction, rather than pumping losses.

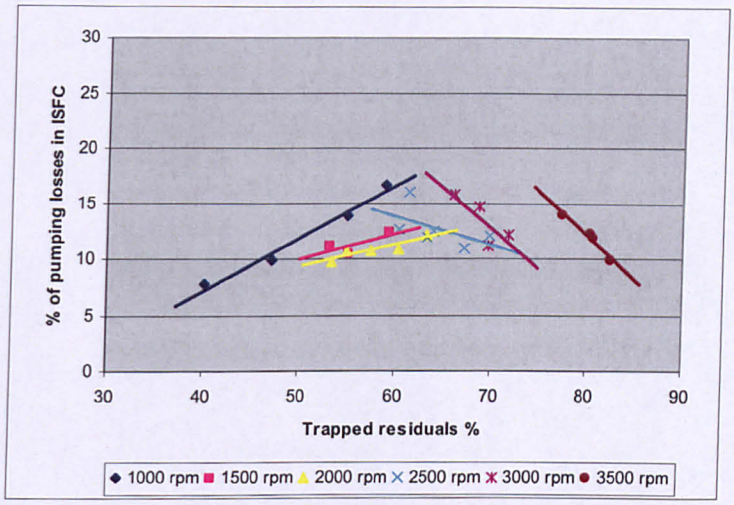

Figure 5.31 Effect of pumping losses on ISFC

5.6 Summary

This section presented the results obtained during the Naturally Aspirated CAI test. The engine performance and emissions characteristics for the CAI operation were analysed. In-cylinder conditions were assessed, from which several parameters were studied. It was found that load has a determinant effect on CAI combustion, as well as on emissions. For the majority of the CAI range values for NO_x emissions were ultra-low and brake specific fuel consumption was lower than the standard SI engine.

6. Spark Assisted Turbocharged CAI Engine

6.1 Introduction

This chapter looks into the potential of turbocharging for enlarging the CAI range. The method for obtaining CAI is similar to the one used in the NA CAI test, with the particularity of having a turbocharger installed. Together with intake boosting, the NVO approach was used during the test and the amount of residuals will be directly affected by the boost pressure as well as valve timing..

Performance and emissions parameters are presented and discussed, for various conditions. The effects of varying spark, valve timing and lambda are assessed, together with their consequences on boost, trapped residuals and overall engine performance. It should be noted that all the values for boost pressure are given as gauge.

6.2 Turbocharged operation with Negative Valve Overlap

Similarly to the previous NA engine test, NVO was used in order to enable CAI operation. The base engine was the naturally aspired one used for NA CAI operation, as discussed in Chapter 5. A turbocharger was installed as described in section 3.4.

During the initial tests with the same camshafts as the NA CAI set-up, it was found that the turbocharger would not generate enough boost, with maximum values limited to 0.2bar. As a result, it was decided to use another bespoke intake camshaft (Figure 6.1), with higher lift and duration than that used for the NA CAI operation.

With the use of the higher lift intake cam (4mm), it was possible to produce substantially higher boost levels, which would put the engine straight into the knocking zone. Even with increased residuals, knock would take place, narrowing the available operating range. In order to reduce the engine's knock sensitivity, it was decided to reduce its compression ratio.

After having the compression ratio lowered from 11:1 to 8.8:1 via a bespoke cylinder head spacer (section 3.4), further tests started. This time, it was found out that the operating range was largely improved, and it was decided that the actual experiment could start.

The profile for the new intake camshaft was determined from previous experiments, as well as the valve timing to start with. This information is plotted on Figure 6.1. EVC had a range from 44 to 64°CA BTDC and IVO had a range from 25 to 75°CA ATDC. The VCT units were unchanged and had the same shifting range as before, 47°CA for the intake and 52°CA for the exhaust.

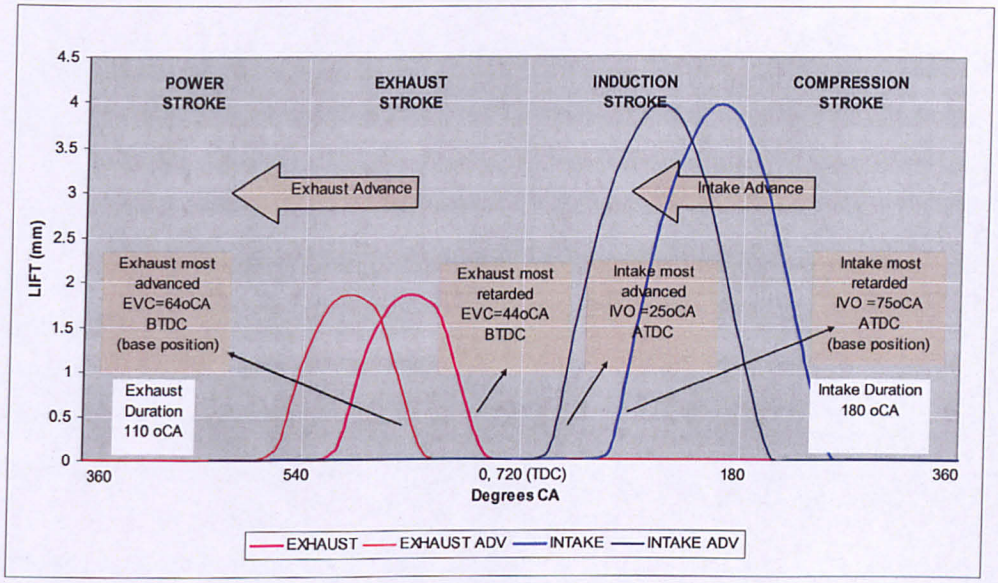

Figure 6.1 Intake and Exhaust cam profiles and VCT range for the turbocharged operation

6.3 Turbocharged Engine Operation and Test Procedure

The operation of the turbocharged engine was essentially the same as the NA CAI engine. The same starting procedure was needed, with all the other controls being the same as explained in Section 5.3. Table 6.1 shows a summary of the test conditions for the turbocharged engine.

Table 6.1 Turbocharged CAI engine test conditions

Coolant temperature	90 °C
Fuel	Gasoline 95 RON
Fuel line pressure	3.5 bar
IVO	25°-75° ATDC
EVC	44°-64° BTDC
Boost Pressure (gauge)	0.14 - 0.64bar
Engine Speed	1250-4500rpm
Throttle Opening	100%

The only substantial difference in operation was the fact that the engine was, at low speed, much more sensitive to the spark timing variation.

6.4 Operational Range of the Turbocharged Engine with Negative Valve Overlap

The achievable operational range with the turbocharged operation and NVO is shown in Figure 6.2, where for each torque value it was selected the combination of λ values, valve and spark timing that yielded the lowest BSFC. As it can be noticed in comparison with the NA CAI range (Figure 6.3), the minimum speed in which stable operation can be accomplished is a little higher: 1250rpm. Below this speed, large cycle-to-cycle variation and too low turbo boost was achieved, making the operation rather unstable.

Similarly to what happens with the NA CAI operation in the low speed range, the higher load range is limited by knock at speeds up to 3000rpm. Between 3000rpm and 4500rpm, the limits are the restricted gas exchange process, imposed by the low lift cams, and the increased combustion noise. Speeds above 4500rpm could not be achieved, since there was not enough fresh charge being drawn into the cylinder anymore.

At every speed, there is a lower load limit, determined primarily by the amount of residuals (Figure 6.5) that was trapped inside the cylinder. After this condition is achieved, further decrease in load can be achieved by increasing λ up to the lean limit and by moving ignition timing away from MBT.

A region of strong instability is found at 2500rpm, narrowing the operating range at this point. However, as soon as the engine passes this point and goes up on speed, combustion becomes more stable and the operating region widens once again. This phenomenon could be due to the manifold geometry causing some adverse tuning.

As it can be noticed from Figure 6.3, much higher load figures can be obtained with the turbocharged operation. The lower load limit, in its majority, tends to be higher than the higher load limit obtained in the NA CAI operation.

Even having higher exhaust temperatures than shown by the NA experiment (Figure 6.6), the lower load limit is still much higher than the NA counterpart. As it will be shown later in this section, this is due to the presence of forced induction and associated pumping losses. Therefore one of the ways to achieve a lower load limit could be to reduce boost.

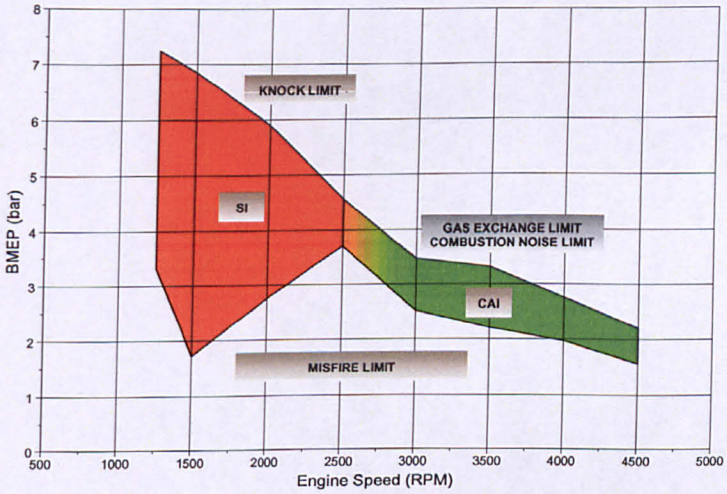

Figure 6.2 Operational Range of the Turbocharged Engine

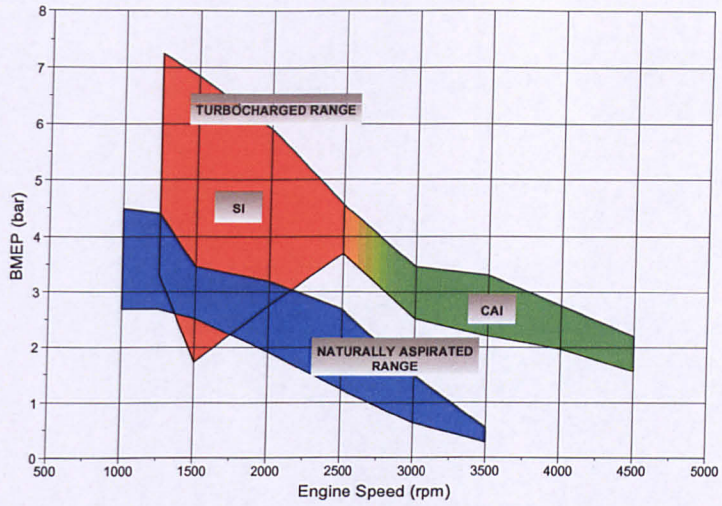

Figure 6.3 Comparison between NA and turbocharged range

It is interesting to notice that the turbocharged full load curve when in CAI operation, i.e. for speeds of 3000rpm and above, resembles the NA CAI full load curve from 1000 rpm to 3500rpm. The increased air flow caused by the combination of a higher lift intake cam and forced induction seem to have shifted the original NA CAI range to a higher speed region (Figure 6.4). The maximum load achieved in the CAI range of the turbocharged operation is similar to the one achieved during the NA CAI test, with the difference that it happens at a higher speed.

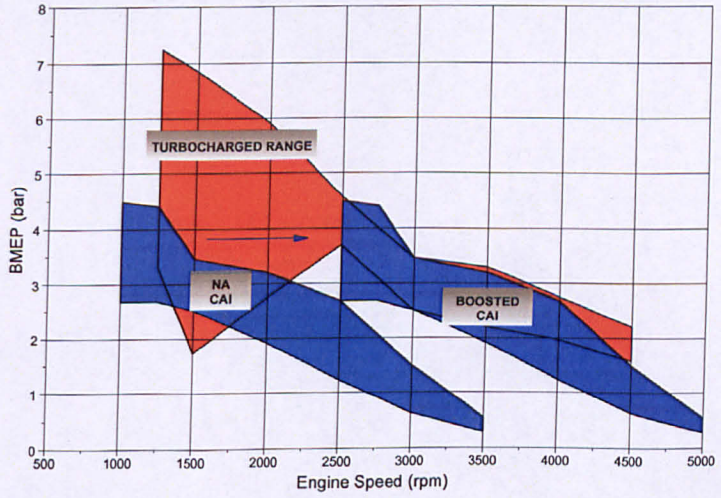

Figure 6.4 Shifting in CAI range between NA and boosted operation

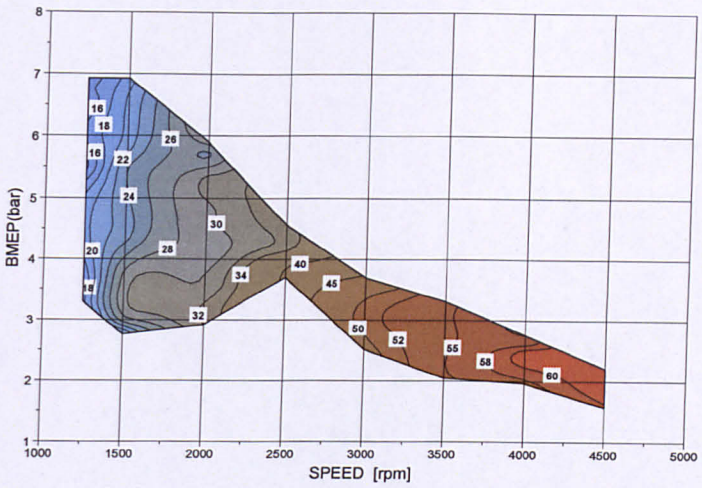

Figure 6.5 Residual concentration as a function of speed and load (%)

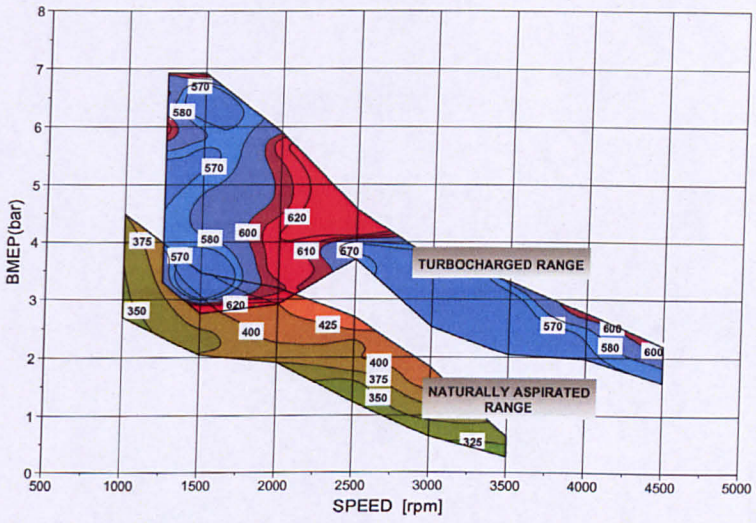

Figure 6.6 NA vs. Turbocharged exhaust temperature (°C) comparison

6.5 Performance and Emissions Overview

This section presents and discusses the performance and emissions results for the whole turbocharged range. In order to minimize data points and to get more comprehensible plots, only data for best BSFC figures was used in this section. For every speed, the load range was swiped in increments of 0.5 bar BMEP from minimum to maximum load, and,

at every step, the combination of IVO, EVC, λ and spark timing that would yield the lowest BSFC value was selected. Figure 6.7 shows an example of a minimum BSFC contour plot at 1500rpm with optimized λ and spark timing. It is noted that the minimum BSFC region is obtained around symmetrical EVC/IVO timings.

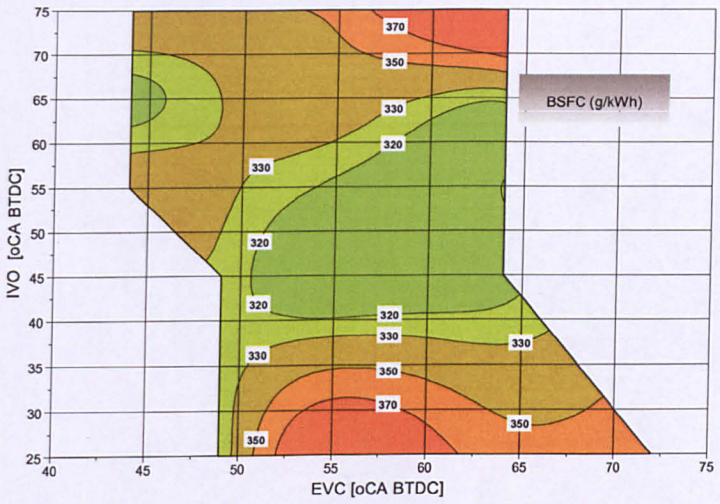

Figure 6.7 BSFC as a function of IVO vs. EVC for 1500rpm

Figure 6.8 shows the boost pressure used for minimum BSFC through the operational range. As expected, the boost pressure increases with both engine speed and load as more exhaust energy becomes available.

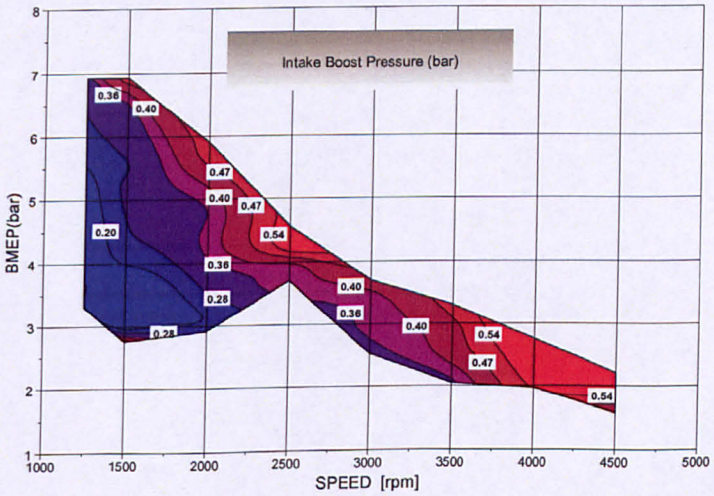

Figure 6.8 Intake boost pressure (bar) for the turbocharged operation

Figure 6.9 shows the λ range for minimum BSFC. It is noted that leaner mixtures are required and that the leanest mixture occurs at high speed.

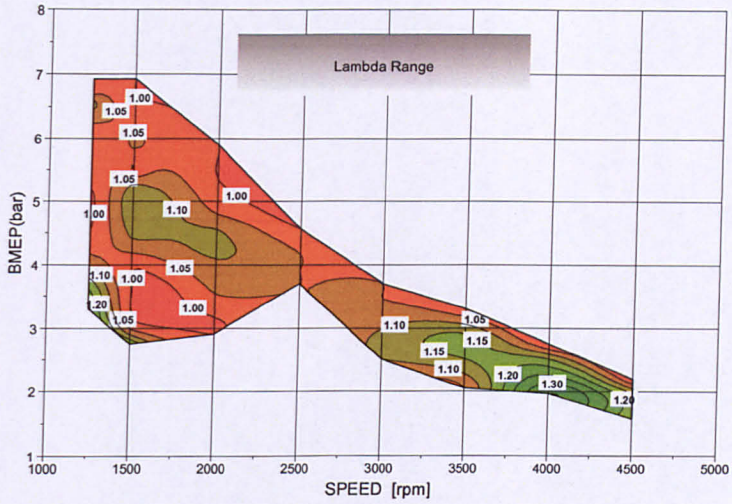

Figure 6.9 Lambda range for the turbocharged operation

Figure 6.10 shows the BSCO emissions throughout the turbocharged range. As one can expect, there is a strong correlation between CO emissions and λ. Where λ is the minimum, CO is the maximum, and vice-versa. On the full load line, where the figures for best BSFC demanded λ=1.00, CO increases substantially and reaches its maximum value.

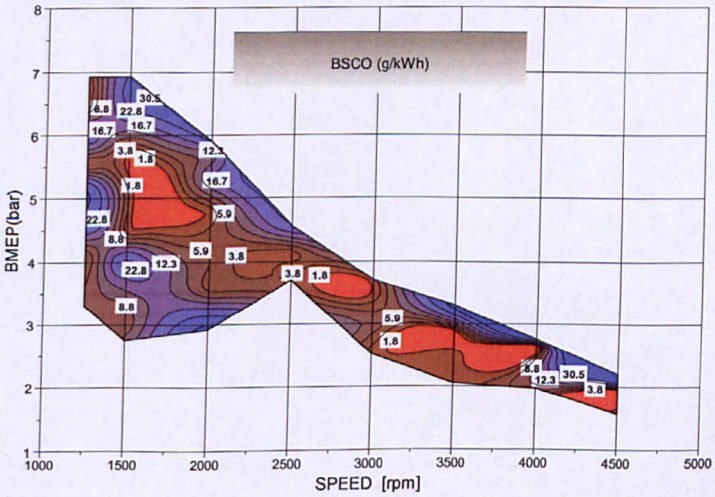

Figure 6.10 BSCO for the turbocharged range

Figure 6.11 shows the corresponding BSHC emissions for the turbocharged operation. As it will be shown later, the values are substantially higher than the ones of the standard engine. The peak values happen towards the lower load limit, where the boost pressure is lower, mixtures are leaner, in-cylinder and exhaust temperatures are lower. Conversely, when the load approaches the higher limit, in-cylinder temperatures tend to be higher and uHC emissions tend to decrease, especially where λ approaches 1.05, and burned gas temperatures are higher.

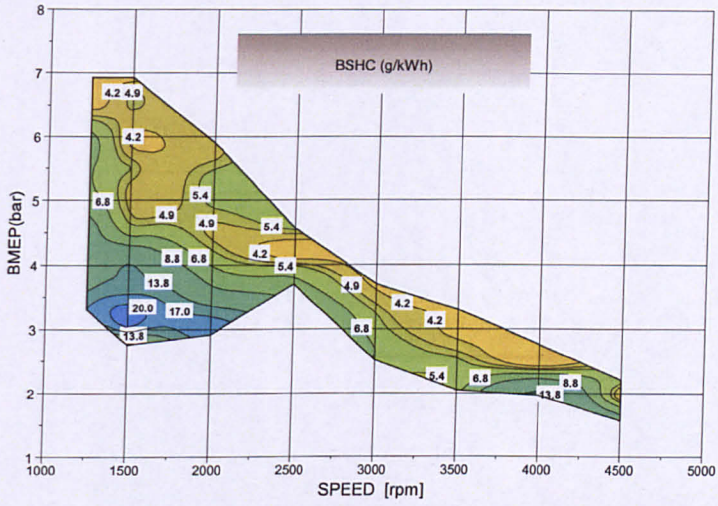

Figure 6.11 BSHC emissions for the turbocharged range

Figure 6.12 shows the NOx emissions values for the whole turbocharged operational range. It can be readily seen that the lowest values happen near the lower load curve. From BMEP of 4bar and below NOx values tend to stabilize below 2 g/kWh. On the other hand, as expected, the maximum values happen near the highest load point, where exhaust residuals tend to be the minimum (Figure 6.5) and cylinder temperatures reach the maximum (Figure 6.13). For a constant load line, NOx values decrease as speed increases. This is caused, again, by the increase in residual fraction as speed goes up. Calculations show that maximum cylinder charge temperatures are always above 1800K, which explains the relatively high NOx levels.

It is not a coincidence, however, that the lowest NOx values happen exactly inside the CAI zone (Figure 6.2), reaffirming, thus, the advantages of CAI combustion in reducing NOx emissions.

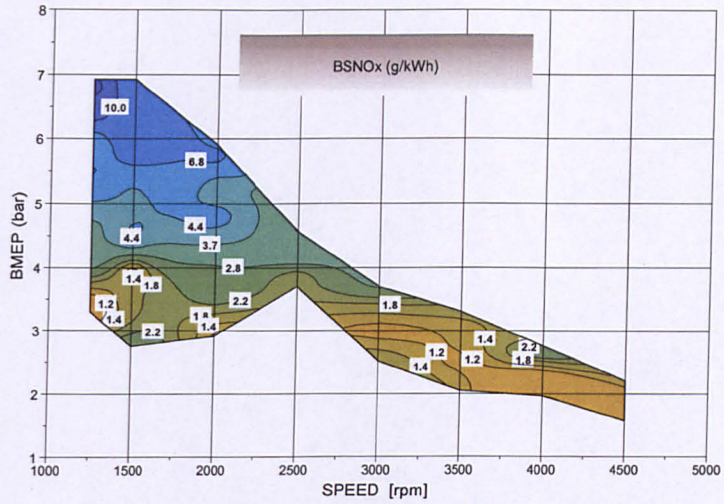

Figure 6.12 BSNOx emissions for the turbocharged range

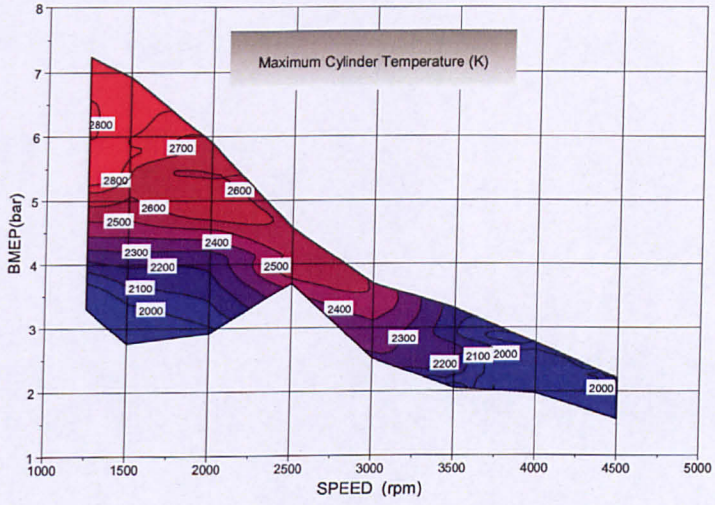

Figure 6.13 Maximum in-cylinder temperatures for the turbocharged range

Figure 6.14 shows the BSFC values for the turbocharged operation. It can be noticed that BSFC has a stronger correlation with load than with speed. The lowest BSFC values are found next to the highest load points at low speed. At a constant speed, if load goes down, BSFC increases. For a constant load, as speed increases, so does BSFC, although this tendency is less pronounced at low loads.

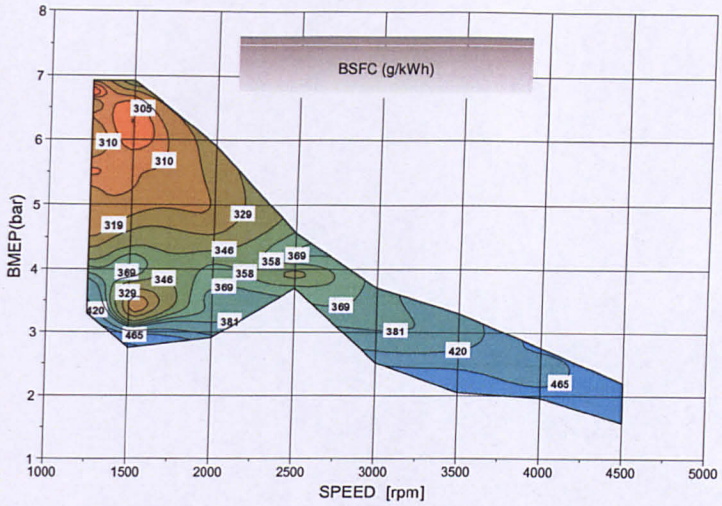

Figure 6.14 BSFC values for the Turbocharged range

6.6 Performance and Emissions: Comparative Analysis

This section presents a comparative analysis between the emissions and fuel consumption results obtained with the turbocharged operation in comparison to the standard, spark ignited Ford Zetec 1.8L Naturally Aspirated engine and to the naturally aspirated CAI operation.

A CO emissions comparison between the standard engine and the turbocharged CAI operation is shown in Figure 6.15. It can be noticed that CO emissions are reduced for the vast majority of the operating range. This is mainly due to the lean mixtures used, and this fact can be confirmed when one looks at Figure 6.9, where it is possible to conclude that CO emissions follow the λ pattern very closely. If the mixture is lean (lower loads), BSCO emissions are lower than the standard engine. Conversely, whenever the mixture approaches λ=1.00 (higher loads), BSCO values become higher than the ones from the standard SI engine.

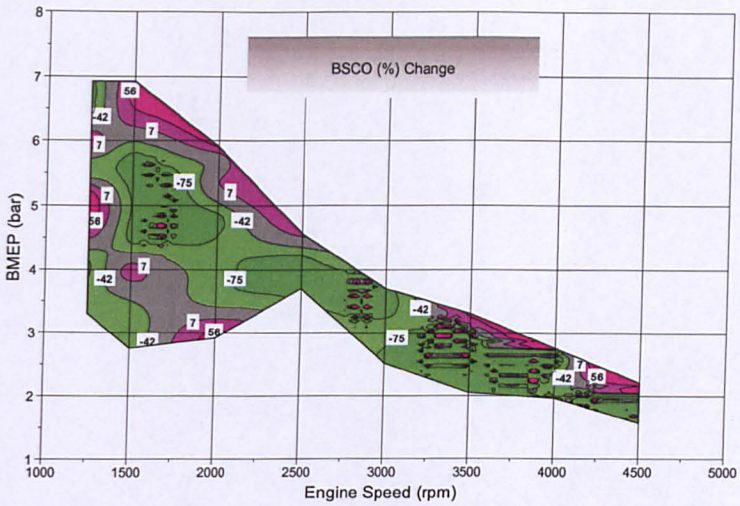

Figure 6.15 Change in BSCO (%) with Turbocharged Operation

Figure 6.16 shows the HC emissions changes in comparison to the standard SI engine. Similar to what happens during the NA CAI operation, HC emissions are much higher in the Turbocharged CAI engine than in the standard SI one. The main reason for that is the presence of a large amount of exhaust residuals in the cylinder, in comparison to the standard SI counterpart.

However, the percentage of HC increase is much less in the turbocharged operation than in the NA CAI operation (Figure 5.14). This is because the in-cylinder temperatures (Figure 6.13) in the turbocharged engine are much higher than the NA CAI ones (Figure 5.7) and the turbocharged engine could operate at considerably higher loads with leaner mixtures, leading to a reduction in HC emissions. Moreover, the presence of the turbocharger increases the exhaust temperatures and pressures, improving the oxidation for hydrocarbons that flow out of the cylinder.

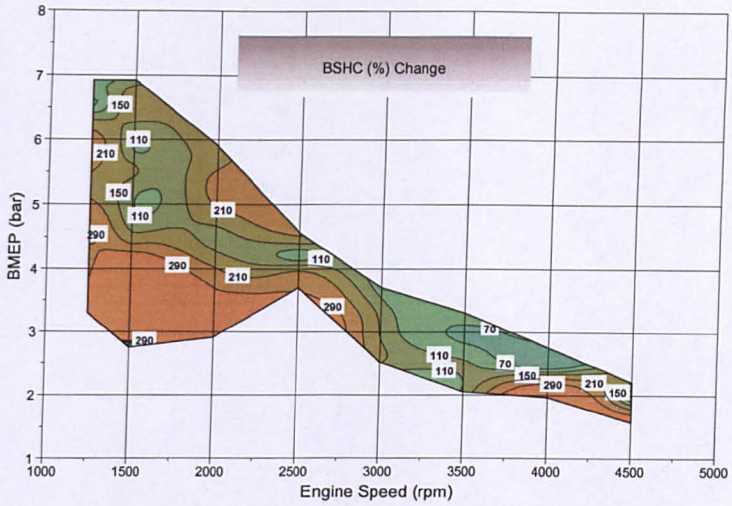

Figure 6.16 Change in BSHC (%) with Turbocharged Operation

Figure 6.17 shows that NO_x emissions are much lower than the standard SI engine. As expected, when the turbocharged engine reaches the CAI range, i.e., above 3000rpm, the reduction in NOx emissions becomes similar to the one showed by the NA CAI engine (Figure 5.12). This is caused mainly by the high residuals rate existent in the turbocharged CAI range.

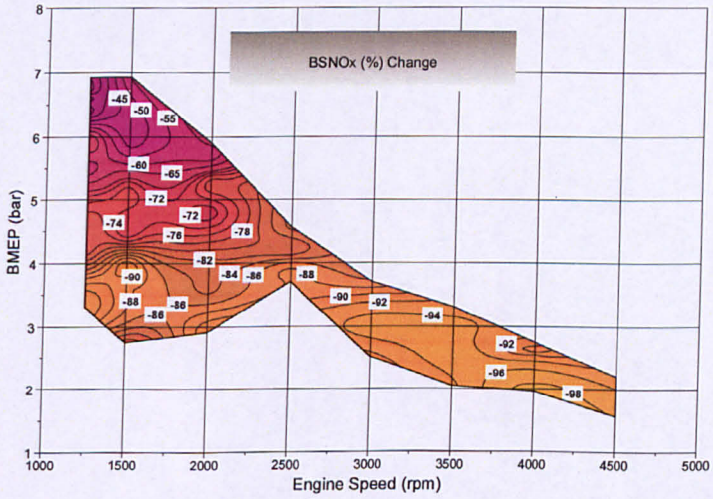

Figure 6.17 Change in BSNOx (%) with Turbocharged Operation

Figure 6.18 shows the changes in BSFC in comparison to the SI standard engine. BSFC is higher over the whole range by an average of 20%. The main reason for that, as will be shown later, is the increase in pumping losses caused by the turbocharger and the very restrictive camshaft profiles. It can be noticed, however, that the difference becomes smaller at the lowest load points, at high engine speeds, where the standard SI engine operates with more throttling and becomes less efficient.

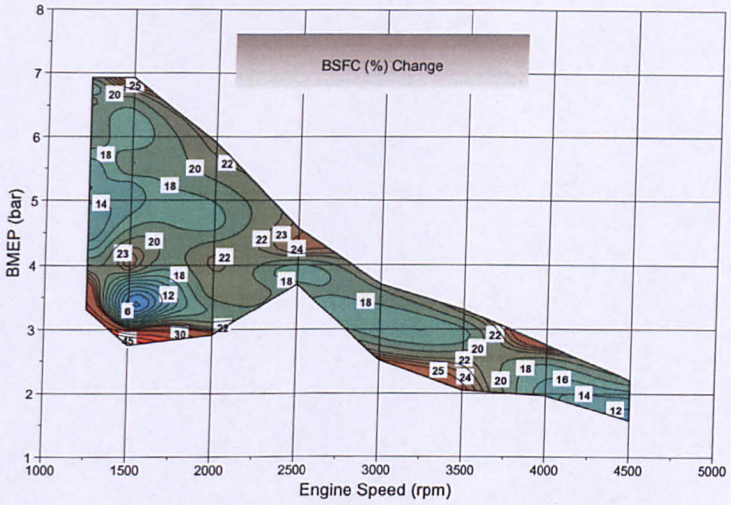

Figure 6.18 Change in BSFC (%) with Turbocharged Operation

The thermal efficiencies of the NA CAI engine, the Turbocharged CAI and the SI standard engine can be seen in Figure 6.19. As it is shown, the NA CAI engine operates always at higher efficiencies than the SI standard engine, whereas the Turbocharged CAI engine doesn't. Apart from the pumping losses, there is also a small drop in indicated fuel conversion efficiency, in the turbocharged CAI engine, due to its smaller compression ratio (section 3.4.4).

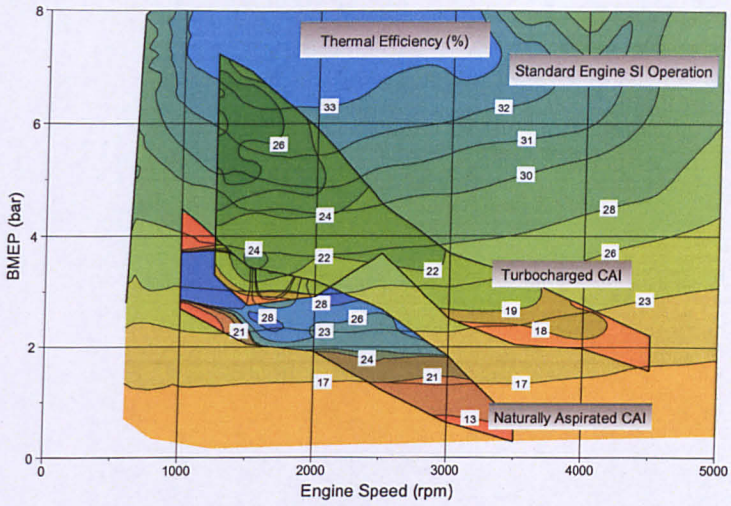

Figure 6.19 Thermal Efficiency comparison

Figure 6.20 shows the pumping losses for the Turbocharged CAI engine. It is easy to notice that PMEP is higher at high loads and high speeds, exactly where air flow and intake boost pressure reach the maximum values (Figure 6.8). For speeds above 4000rpm, pumping losses start to fall, despite the increased boost and air flow. This is an indication that the compressor was reaching its best efficiency point.

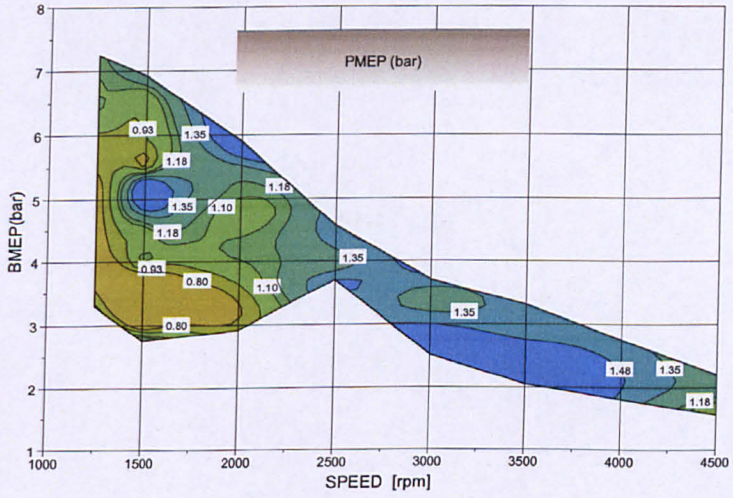

Figure 6.20 Pumping Losses for the Turbocharged CAI engine

6.7 Effects of boost and trapped residuals on engine performance

In the current turbocharged CAI engine set-up, boost pressure is highly dependent on trapped residuals, therefore these two quantities can not be analyzed separately, as it will become evident in this section.

The turbine chosen for the turbocharged CAI engine set-up was the best match available at the time. However, it is still a little oversized for the current CAI set-up. Thus, in order to have good levels of boost throughout the whole operational range, the waste-gate is always kept closed, and the turbine receives all the exhaust gases produced by the engine. There is no direct boost control and the turbine speed is, therefore, solely dependent on the enthalpy of the exhaust gases produced by the engine and on the restrictions imposed by the low lift camshafts.

By changing EVC, the exhaust flow rate can be changed, causing the speed of the turbine and, consequently, the boost pressure to change. With early EVC timings, less exhaust gases are delivered to the turbine and hence lower boost is produced. Conversely, for late EVC timings, higher levels of exhaust are delivered and higher levels of boost are generated.

Intake manifold pressure (boost pressure), therefore, has a direct correlation with exhaust residuals, which in turn, affects directly the engine's output. The higher the amount of exhaust residuals, the lower is boost and load. As shown in Figure 6.21, it becomes apparent that there is an almost linear relationship between load and residuals rate.

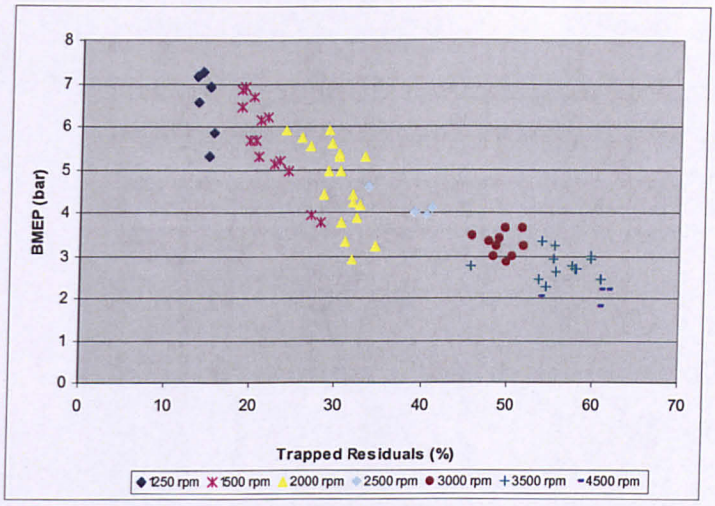

Figure 6.21 Effect of trapped residuals on load

Since the engine has no direct, independent boost control, intake manifold pressure is always determined and inversely proportional to the exhaust residual rate, as it can be seen in Figure 6.22.

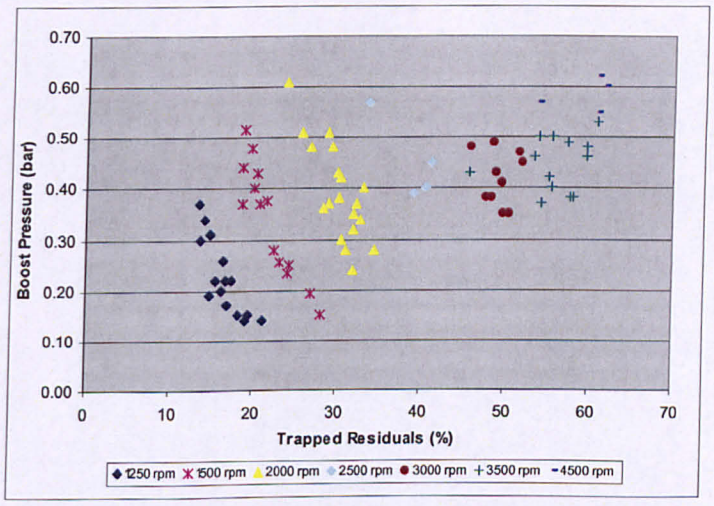

Figure 6.22 Effect of trapped residuals on boost for λ=1.00 at MBT

At low speeds, it can be seen that a slight variation in trapped residuals cause a strong effect on boost. However, this variation, achieved by means of changing the valve timing, has less effect at high speeds. The reason is that, at high speeds, the gas exchange

process is more limited by the small camshaft profiles than by the valve timing itself. The operational range becomes very short and the amount of trapped residuals reaches its highest levels, which, in turn, despite of the higher boost, end up limiting the achievable load, as it can be seen in Figure 6.23.

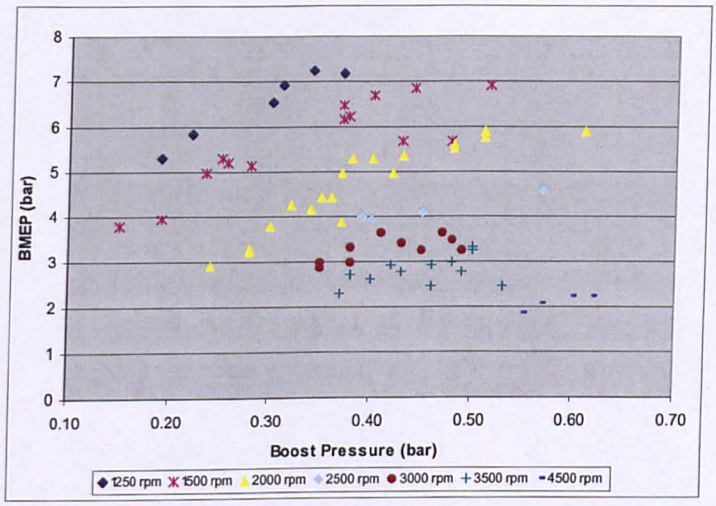

Figure 6.23 Effect of boost on load

Boost also has an effect on intake air temperature, since the compressor work adds heat to the intake charge, increasing its temperature, as it can be seen in Figure 6.24 and is subject to analysis in the next section.

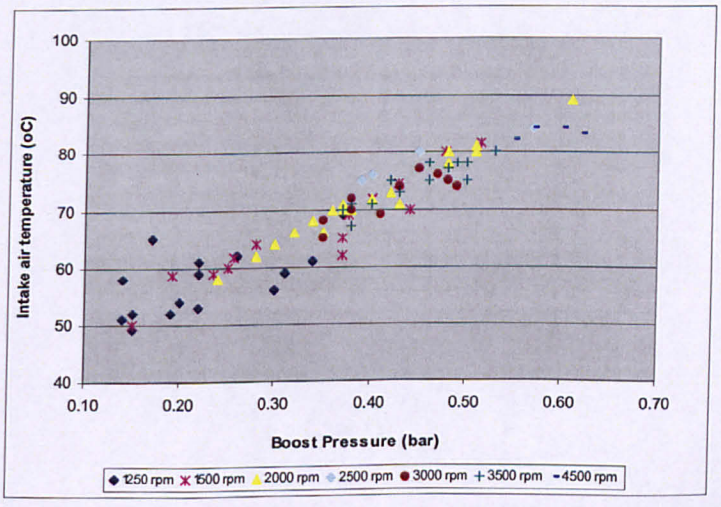

Figure 6.24 Effect of boost on intake air temperature

6.8 Effect of Intake Air Temperature

One immediate adverse effect of increasing intake air temperature on the Turbocharger CAI engine is that whenever the temperature approaches 90 °C, knock takes place if the residuals quantity is not high enough. That is observed at low speeds, particularly below 2500 rpm. If the intake charge could be cooled down by adding a standard intercooler or any other cooling device, it could probably extend the higher load limit at low speeds and decrease combustion noise at high speeds.

Intake air temperature also affects BSFC, as it can be observed in Figure 6.25. It is important to stress, however, that intake air temperature is more an indicator of changes in BSFC than the actual cause of them, since its variations are the result of changes in the turbocharger compression work.

It is noticeable that the points for lowest BSFC are always in general in the middle of the temperature range, at each engine speed. For low temperatures, the graph shows increased BSFC. However, this is more due to the reduced boost (which would produce lower temperatures in the intake charge) than to the low temperature itself. As the temperature goes up, as a result of an increase in boost (Figure 6.24), BSFC starts to rise again because of the associated pumping losses (Figure 6.20).

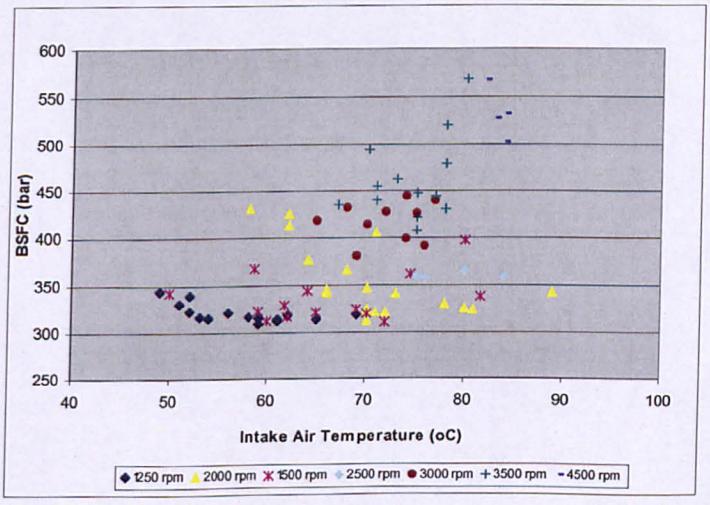

Figure 6.25 Effect of intake air temperature on BSFC

Another negative effect of a high intake air temperature is to lower the charge's density, which impairs the volumetric efficiency and decreases the achievable load range. Also, by lowering the charge's density, the turbocharger will have less exhaust flow to drive it, generating, in turn, lower boost.

6.9 Effects of Spark Timing on Engine Performance

When the engine is running in SI mode, i.e., in speeds below 3000 rpm, spark timing has a strong effect engine performance. Only above 3000rpm, when the engine goes onto CAI combustion, it has less or no effect at all. The effects of spark timing over combustion on the turbocharged CAI set-up are directly related to the boost levels.

If ignition is retarded, exhaust temperatures increase and the turbocharger spins faster, generating higher levels of boost. On the other hand, if ignition is advanced, exhaust temperatures decrease and lower levels of boost are produced. These facts can be better observed when looking at Figure 6.26.

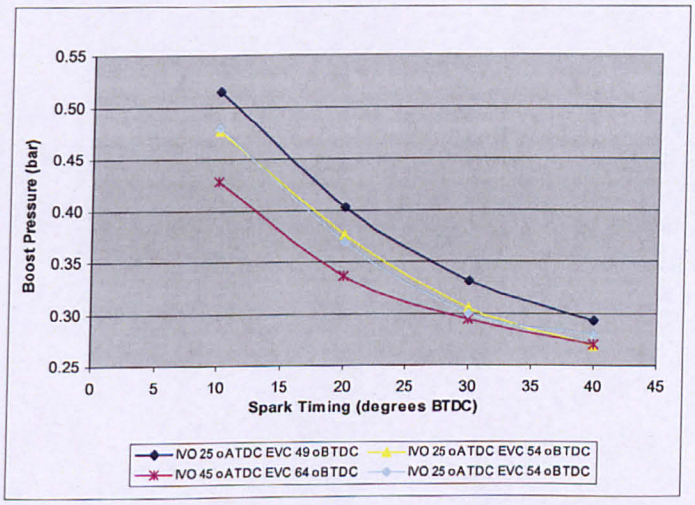

Figure 6.26 Effect of spark timing on boost, for 1500rpm at λ=1.00

As it was already mentioned in section 6.7 changes in boost affect load. Thus, the effects of spark timing on boost and, therefore, load are shown in Figure 6.27. As it can be noticed, for one of the valve timing combinations, load could, theoretically, further increase if spark timing could be later than 10 °BTDC. However, that was not possible, since more retared spark timings put the engine into very unstable operation.

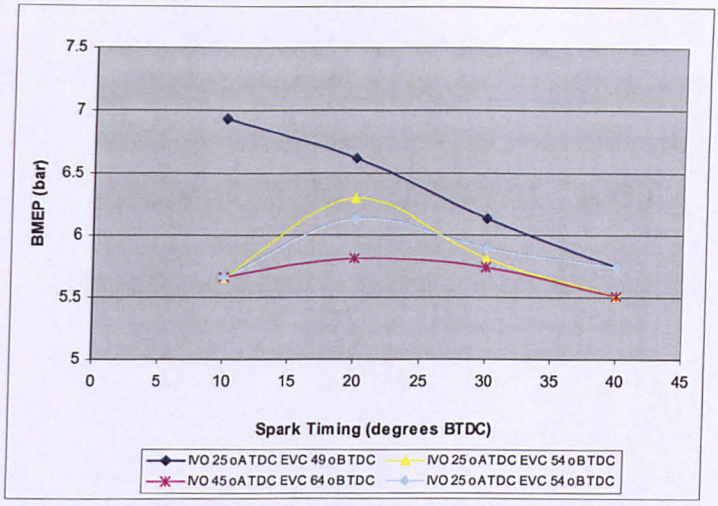

Figure 6.27 Effect of spark timing on load, for 1500rpm at λ=1.00

As it can be expected, there is also a strong impact of spark timing on BSFC, as Figure 6.28 shows. For each valve timing combination, there is optimum spark timing for lowest BSFC that is, in general, earlier than 20°BTDC. Different from NA engines, the spark timing for best BSFC is not always the same as the MBT timing.

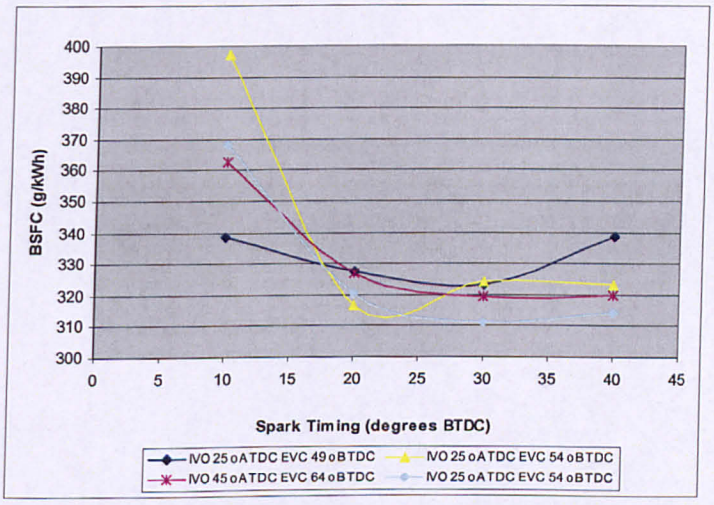

Figure 6.28 Effect of spark timing on BSFC, for 1500rpm at λ=1.00

Spark timing also has an effect on the residuals rate. For every engine operating condition, there is an average range of trapped residuals that is mostly dependant on the valve timing combination, in particular EVC timing. However, the residuals rate can be further varied by varying the spark timing. This is because the spark timing affects boost, and hence the amount of fresh charge in the cylinder. This is illustrated by Figure 6.29.

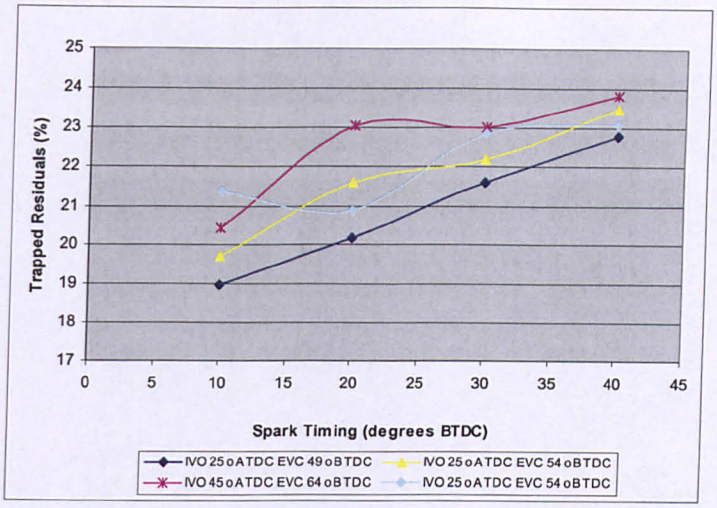

Figure 6.29 Effect of spark timing on residuals rate, for 1500 rpm at λ =1.00

6.10 Effects of λ on Engine Performance

This section analyses the effects of the relative air/fuel ratio λ for the engine speeds of 1500 and 3000rpm during the Turbocharged CAI engine operation.

For each speed and λ value, a particular valve timing combination and ignition timing which would yield the best BSFC were chosen. For 1500rpm the valve timing combination was IVO at 45° ATDC and EVC at 54° BTDC; for 3000rpm it was IVO at 25° ATDC and EVC at 49° BTDC.

Figure 6.30 shows the effects of λ on trapped residuals. It can be noticed that the residual rate is almost constant for each speed. This is expected since what really determines the amount of trapped residuals is the valve timing, which is constant and different for each case. Obviously, the residuals rate is much higher at 3000rpm than at 1500rpm due to the gas exchange restrictions at that speed. At 3000rpm, there is a trend showing a decrease in residuals as the mixture becomes leaner.

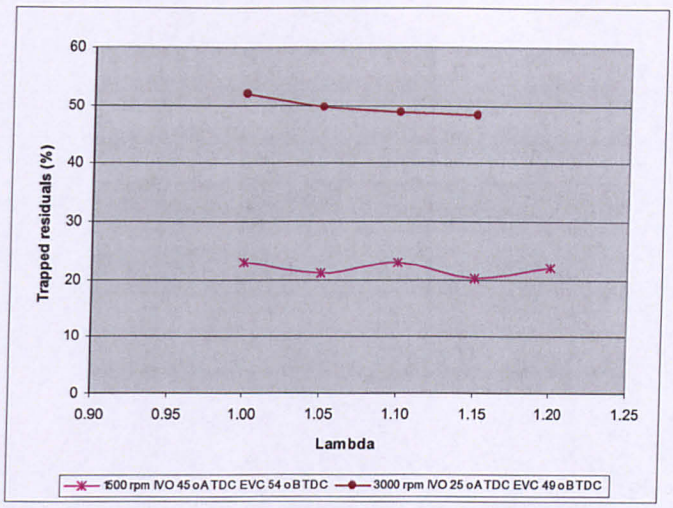

Figure 6.30 Effect of λ on Trapped Residuals

Together with the trapped residuals, changes in λ also contribute to the change in the maximum cylinder temperature, as shown by Figure 6.31. It is readily noticeable that temperatures are higher for 1500 rpm, which is expected since the residual fraction at this speed is smaller.

Increasing λ seems to have little effect for 3000rpm when compared to those at 1500rpm. For both speeds, the temperature drop becomes higher for mixtures leaner than λ=1.10, since on one hand there is an increase in residuals rate and on the other there is less fuel being burnt, generating, therefore, less heat.

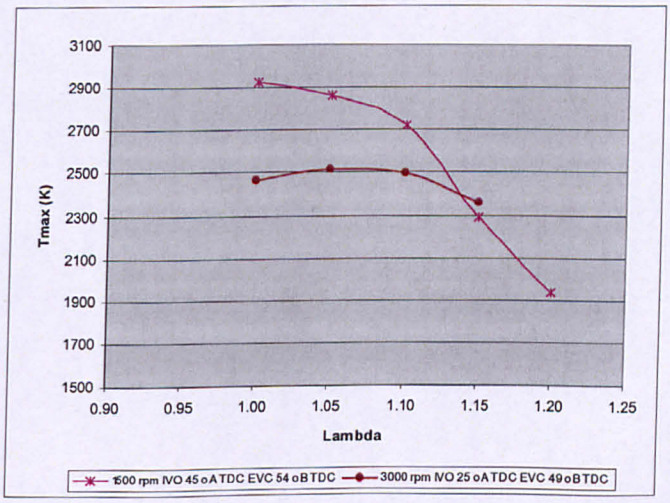

Figure 6.31 Effect of λ on Maximum Cylinder Temperature

Figure 6.32 shows the effects of λ on BMEP. It can be noticed that as lambda increases, load decreases, as expected. However, for 1500rpm, the difference between λ=1.00 and λ=1.05 is negligible. For 3000rpm there is no such behavior, since load decreases linearly with the increase in λ. Nevertheless, the variations in load with changing λ for 3000rpm are minor, when compared to the ones of 1500rpm. In fact, load at 3000rpm could be considered almost constant, in comparison with the magnitude of the changes at 1500rpm.

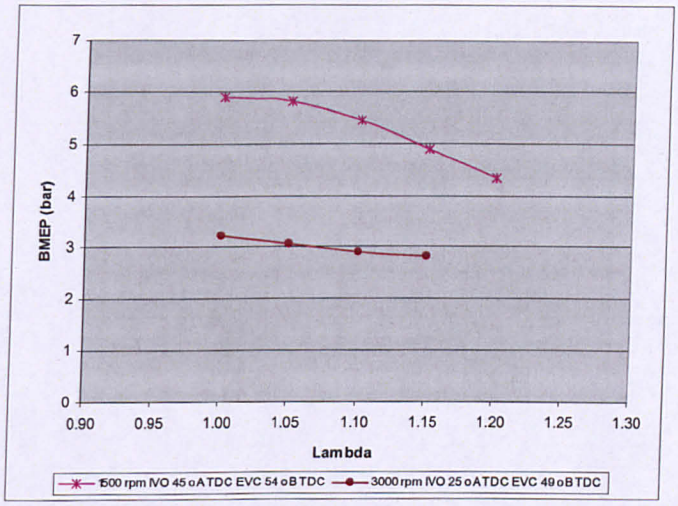

Figure 6.32 Effect of λ on BMEP

Figure 6.33 shows the effects of λ variation on BSFC. It is possible to notice the lower figures for BSFC at λ=1.05 for both engine speeds. For 1500 rpm, however, the reduction in BSFC at λ=1.05 is less pronounced. With λ higher than 1.05, there is an increase in fuel consumption for both speeds, which is minor for 3000rpm and exponential for 1500rpm. As a matter of fact, looking at the larger picture one could say that fuel consumption is constant with λ at 3000rpm and varies significantly at 1500rpm.

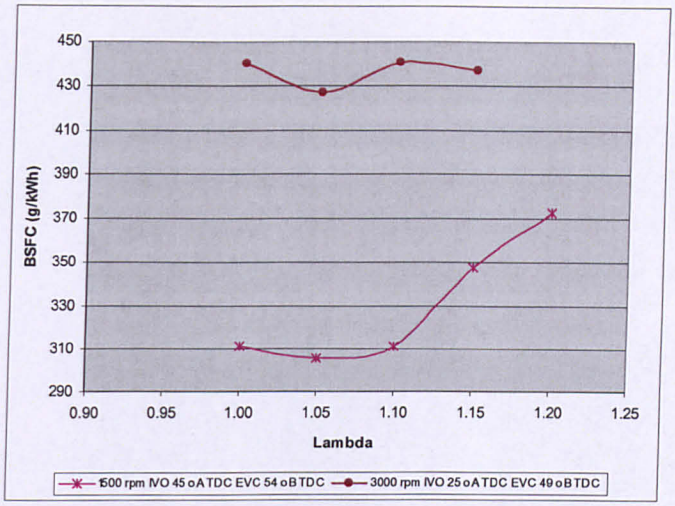

Figure 6.33 Effects of λ on BSFC

Figure 6.34 shows the effect of λ on NO_x emissions. As one could expect, NO_x emissions have a strong correlation with cylinder temperature. It is noticeable that values for 1500rpm are much higher than the ones of 3000rpm, which can be explained by the high cylinder temperatures at 1500rpm. For 1500rpm, as the mixture goes lean, NO_x emissions increase until a maximum at around λ=1.10 and then fall again for leaner mixtures due to the falling cylinder temperatures. This is typical of SI combustion. In comparison, NO_x emissions are much less affected by the λ value due to the presence of high amount of residuals and hence low temperature CAI combustion.

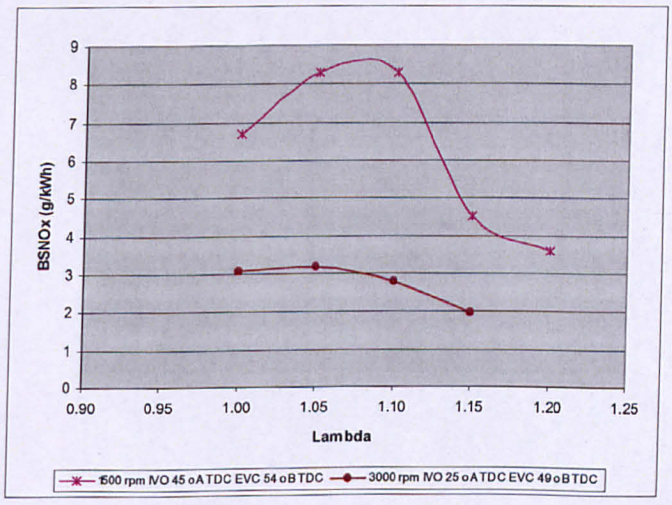

Figure 6.34 Effect of λ on BSNOx

Figure 6.35 shows the CO emissions as a function of λ. The trend for CO emissions seem to be much more affected by λ than by speed itself, since for both speeds the behavior is very similar, with minimum levels happening between λ=1.05 and λ=1.10. Therefore, it can be concluded that the dependency of CO emissions is the same for both SI and CAI combustion processes.

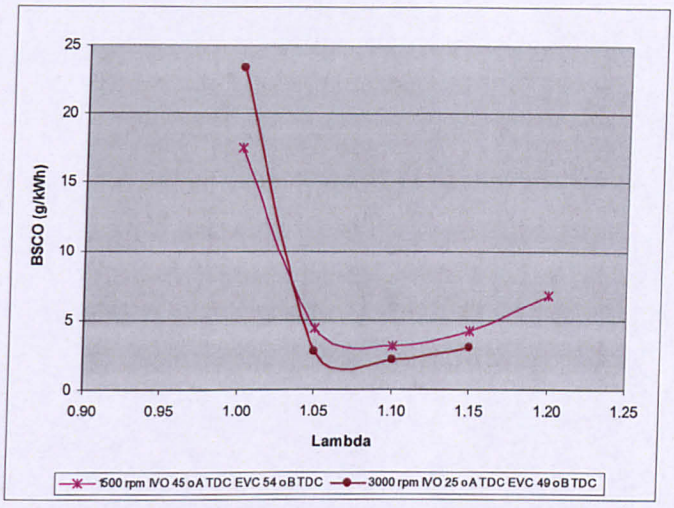

Figure 6.35 Effect of λ on BSCO

Figure 6.36 shows the effects of λ on BSHC. As the mixture goes from λ=1.00 until λ=1.10 there is a substantial emissions reduction, since there is excess air and still high cylinder temperatures to oxidize the unburned hydrocarbons. As mixture goes even leaner, cylinder temperatures fall substantially, impairing the HC oxidation process.

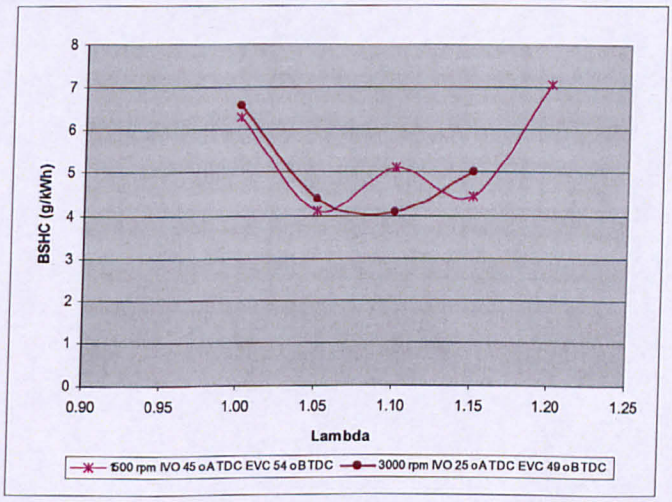

Figure 6.36 Effect of λ on BSHC

When running the engine in the CAI range, i.e. from 3000rpm to above, from the figures in this section, it becomes clear the advantage of operating with λ around 1.05, since this does not affect NOx emissions to a great extent, produces lower levels of HC and CO emissions and gives the lowest values for BSFC.

This also shows the ability of CAI to handle lean mixtures without great impact on NOx emissions, which is desirable from the fuel consumption point of view.

6.11 Operational Parameters for Minimum and Maximum Values of BMEP and BSFC

As it was found during the tests, several combinations of parameters can lead to similar engine outputs but with different fuel consumption results. For each speed, combinations of λ, ignition timing, EVC and IVO would generate a particular load range. However, many of the achievable load points would present high cycle-to-cycle variation, expressed in terms of the coefficient of variation in IMEP (COV_{imep}). According to Heywood [33], whenever COV_{imep} exceeds about 10%, vehicle drivability problems arise. Thus, in order to have more realistic figures, data was filtered and only combinations showing COV_{imep} values smaller than 10% were chosen.

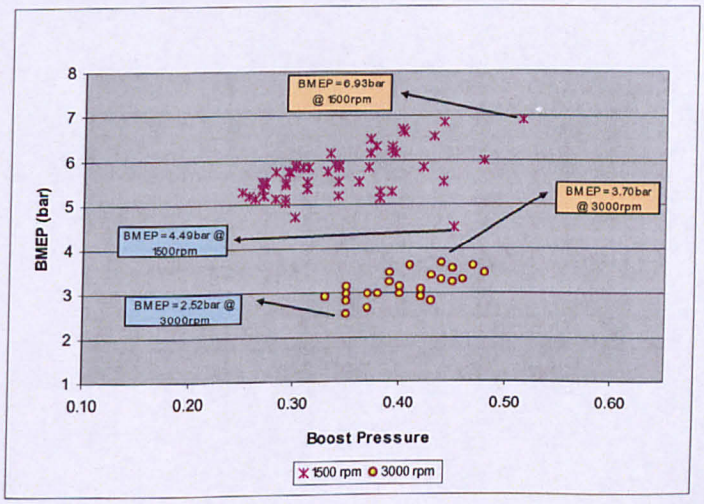

Figure 6.37 Load range vs. boost varying spark, valve timing and λ

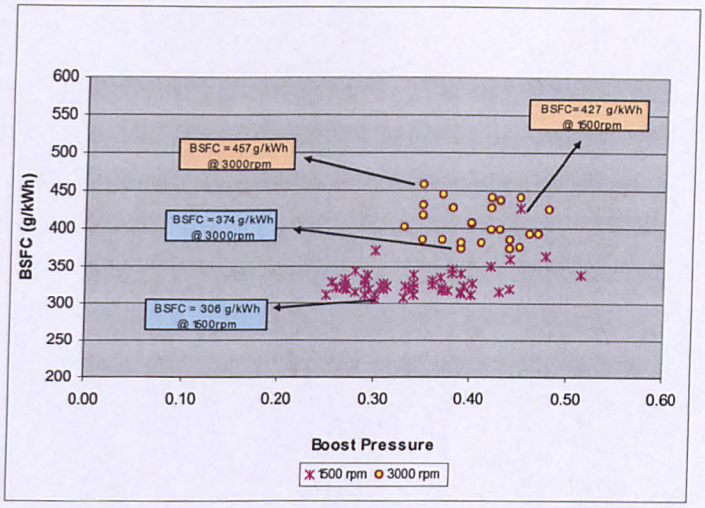

Figure 6.38 BSFC range vs. boost varying spark, valve timing and λ

Values for maximum and minimum load at each speed were selected (Figure 6.37) and can be found in Table 6.2. A similar procedure was done for the fuel consumption data, which covers the range shown in Figure 6.38.

Table 6.2 Operation parameters for Maximum and Minimum values of BSFC and BMEP at 1500 and 3000rpm

	SPEED	Torque	Boost	INT. Air Temp.	EXH. T	IGN. ADV.	λ	IVO	EVC		PUMPING LOSSES	FRICTION LOSSES							Thermal Efficiency
								oCA	oCA	netIMEP	PMEP	FMEP	BMEP	cov	BSFC	BSNOx	BSHC	BSCO	η
	rpm	Nm	bar	oC	oC	oBTDC		ATDC	BTDC	bar	bar	bar	bar	%	g/Kw-h	g/Kw-h	g/Kw-h	g/Kw-h	%
MAXIMUM AND MINIMUM VALUES OF BMEP																			
MIN	1500	57	0.45	77	541	10	1.10	45	54	6.04	0.82	1.55	4.48	2.62	427.49	4.94	2.68	6.38	19
MAX	1500	88	0.51	82	632	10	1.00	25	49	8.09	1.26	1.16	6.93	1.84	338.57	7.74	3.87	24.64	24
MIN	3000	32	0.35	70	558	45	1.10	25	54	3.56	1.84	1.04	2.52	3.36	456.93	1.74	6.62	3.03	18
MAX	3000	47	0.44	75	560	45	1.05	65	54	4.76	1.44	1.08	3.70	6.24	373.84	2.88	3.93	2.97	22
MAXIMUM AND MINIMUM VALUES OF BSFC																			
MIN	1500	74	0.30	60	582	35	1.05	45	54	7.06	0.89	1.24	5.82	2.01	305.37	8.31	4.12	4.36	27
MAX	1500	57	0.45	77	541	10	1.10	45	54	6.04	0.82	1.55	4.48	2.62	427.49	4.94	2.68	6.38	19
MIN	3000	44	0.39	70	549	45	1.05	55	54	4.78	1.26	1.31	3.46	3.65	373.84	1.94	4.66	2.37	22
MAX	3000	32	0.35	70	558	45	1.10	25	54	3.56	1.84	1.04	2.52	3.36	456.93	1.74	6.62	3.03	18

Both maximum load points, i.e. for 1500 and 3000rpm happen at the richest λ of their ranges, which was λ=1.00 for 1500rpm and λ=1.05 for 3000rpm. At these conditions, boost is at the maximum and pumping losses are higher. However, in proportion to the respective IMEP values, pumping losses are lower at high load than at low load, which means the engine is on a higher efficiency zone at high load. The points for best BSFC tend to happen at the maximum load point or very near to it, as shown in Table 6.2.

6.12 Combustion and In-Cylinder Conditions Analysis

In order to get more appropriate comparisons, this section analyzes the results obtained at λ=1.00 at MBT for the SI and spark assisted operation and at λ=1.00 for the CAI combustion operational region. Figure 6.39 shows the charge temperatures at the point of ignition, whether by spark or through autoignition, as well as exhaust temperatures. It is important to notice the clear difference in values between the SI and the CAI combustion ranges. For speeds less than 2500rpm, only SI combustion was present. At 2500rpm, spark-assisted CAI was taking place and from 3000rpm and above pure CAI was present. The occurrence of pure CAI could checked by turning off the spark and by the appearance of the pressure trace.

As shown by Figure 6.39, similar to what happened with the NA CAI engine, for the same amount of residuals, exhaust temperature increases as speed gets higher and heat losses become lower. This behavior is more pronounced in the SI combustion range, where larger variations in exhaust temperature were present. During the CAI operation, exhaust temperatures were lower.

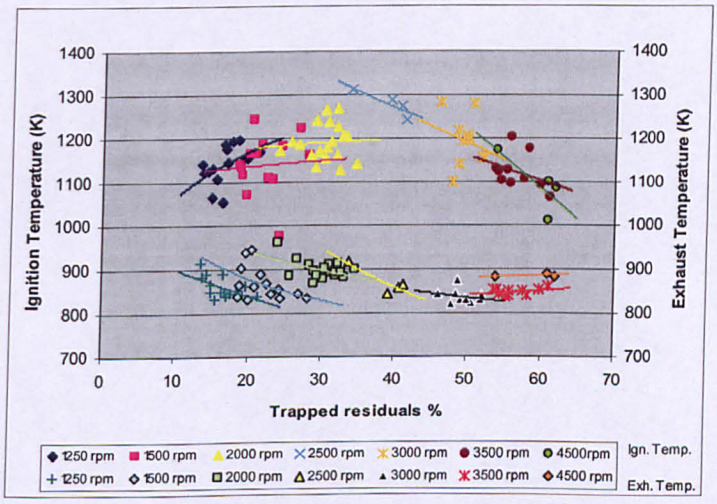

Figure 6.39 Effect of trapped residuals on ignition and exhaust temperature for λ=1.00 at MBT

It is also noticeable that CAI starts to happen only with a residual fraction higher than 35-40%, becoming fully stabilized from 40% onwards. This goes in accordance to the results obtained in the NA CAI set-up, where CAI would take place at the same residual fraction and above. Figure 6.39 also shows that as the residual fraction goes up, the ignition temperature, in the SI range, gets higher, which leads to the conclusion that ignition

needs more heat (from compression) to happen. However, the opposite occurs with CAI operation. There seem to be a threshold of 40% of trapped residuals after which autoignition starts to happen earlier and with less heat needed. The increased residuals seem to accelerate the autoignition process. This could be a result of more active species in the exhaust residuals.

Figure 6.40 further illustrates this phenomena by showing that as the residual rate increases, ignition starts later for the SI range and earlier for the CAI range. The end of combustion duration also has a tendency to happen earlier as residual fraction and speed increase, which means combustion gets faster, as it can be seen from Figure 6.41.

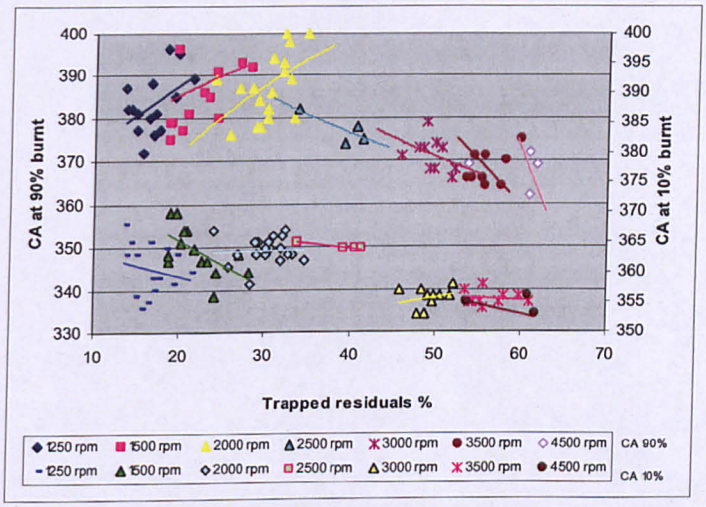

Figure 6.40 Effects of residual fraction on 10% and 90% burn angles

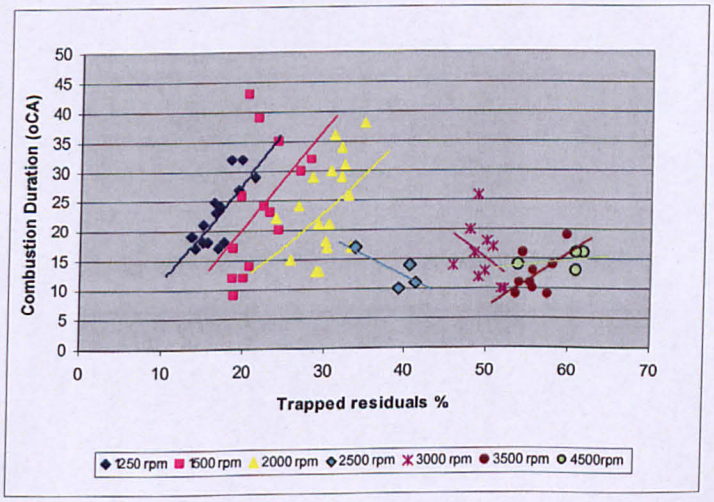

Figure 6.41 Effect of residual fraction on combustion duration

It is noticeable as well, in Figure 6.41 that combustion becomes much faster and more or less at a constant rate as the speed goes above 2500rpm, which is where CAI takes place.

Figure 6.42 shows the effects of the residual fraction on peak cylinder pressure. It can be seen that at higher speeds, in the CAI range, cylinder pressures are higher and tend to decrease with the residual rate, as expected. The peak pressures are similar to those of the NA CAI test (Figure 5.19).

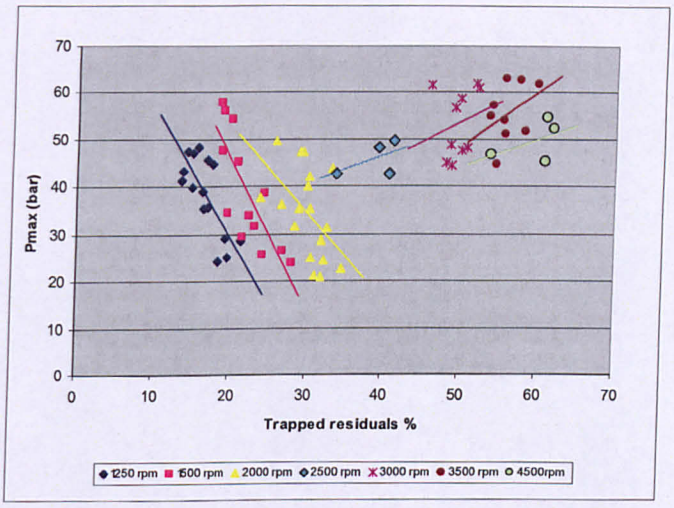

Figure 6.42 Effect of residual fraction on peak cylinder pressure

In relation to load, the maximum cylinder pressure shows a different behavior, as can be seen in Figure 6.43. The CAI region, which produces less load, has the highest pressures. The peak pressures do not happen, therefore, at the highest loads, but, as Figure 6.44 demonstrates, at the highest boost regions. Hence, one can conclude that what determines the peak cylinder pressures is boost rather than load or trapped residuals. It should be pointed out, though, that this is a particularity of the current set-up, in which there was no independent boost control. If independent boost control was applied, the residual fraction would have a larger effect on peak cylinder pressures since it could be possible to lower the boost at that condition, if necessary.

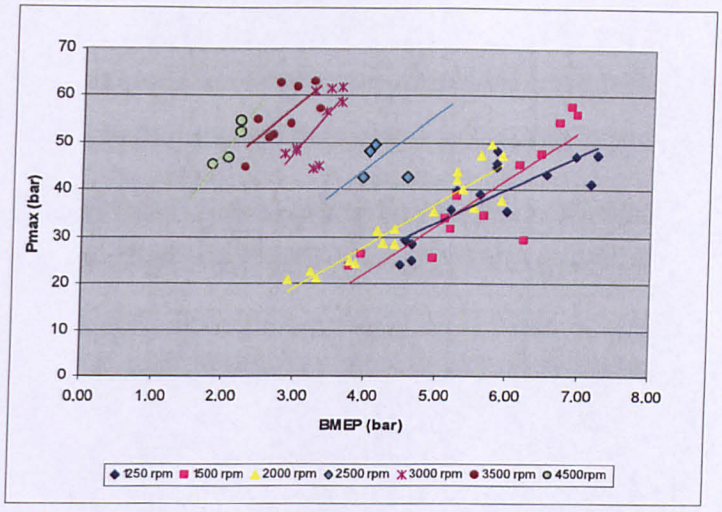

Figure 6.43 Effect of BMEP on maximum cylinder pressure

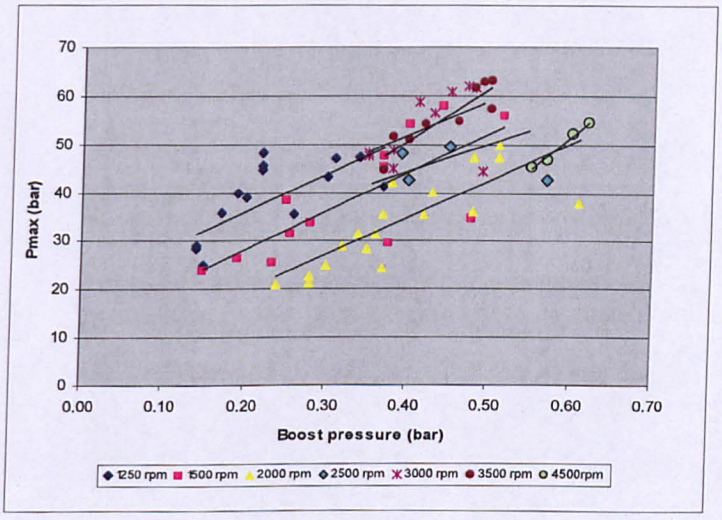

Figure 6.44 Effect of boost on peak cylinder pressure

The effect of residual rate on the maximum rate of pressure rise is plotted on Figure 6.45. There is a clear difference between data from the SI and from the CAI range. In the SI range, i.e. below 2500rpm, it decreases with the residual fraction. However, for the CAI range, on speeds starting from 2500rpm, the maximum rate of pressure rise increases as the residual fraction goes up. This is more due to the higher boost generated at high speeds than to the residual fraction itself, as Figure 6.46 can confirm. There is only one exception, at the speed of 4500rpm, where the maximum rate of pressure rise decreased with higher residual fraction. At this point, the gas exchange process was very restricted, limiting the effect of boost. In addition, the residual fraction was also very high, making the maximum rate of pressure rise fall again, for values around 3bar/^{o}CA.

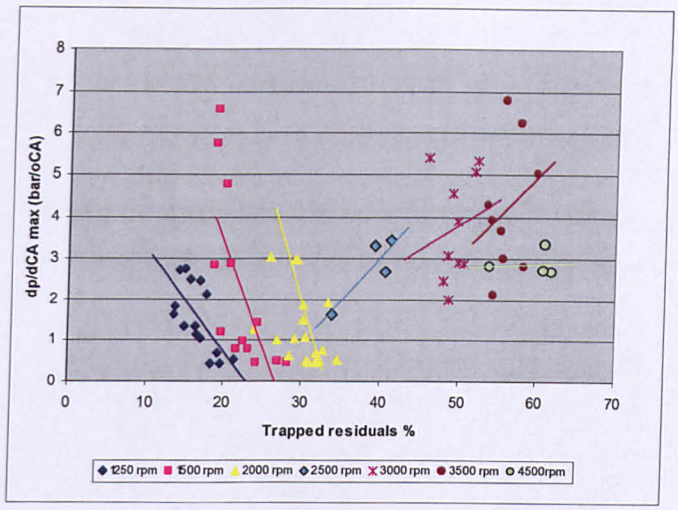

Figure 6.45 Effect of residual fraction on maximum rate of pressure rise

Figure 6.46 shows the effects of boost on maximum rate of pressure rise. It is possible to see that it has a stronger correlation with boost than with residuals, for the current set-up, regardless of being in the SI or CAI range. Again, at 4500rpm there is a change in behavior, with $dp/d^{o}CA_{max}$ falling once again, for the reasons already explained.

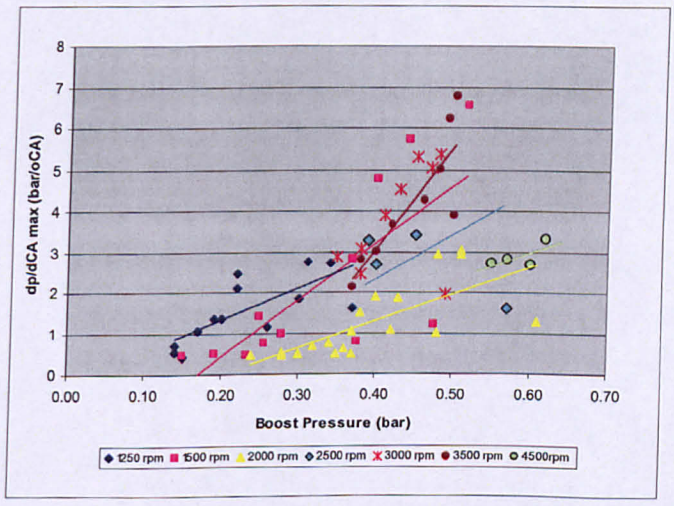

Figure 6.46 Effect of boost on maximum rate of pressure rise

It is important to notice that the values of the maximum rate of pressure rise are not very different than the ones obtained during the NA CAI test. The maximum levels were around 7 bar/°CA, which confirm that the engine was not knocking. At high speed, where

the boost is at the maximum, there is combustion noise present, but not loud enough, on a subjective analysis, to be deemed as knocking. In any case, they were below 10 bar/°CA, a value noticed and chosen to be the knock threshold.

6.13 Effects of Boost, Residuals Fraction, Pumping and Friction Losses on BSFC

Figure 6.47 shows the effects of boost on BSFC. It can be readily seen that the highest fuel consumption happens at the points of higher boost and higher speeds, i.e. BSFC gets higher as speed increases. At low speeds, BSFC is less sensitive to boost, whereas at high speeds it changes much more with boost, having a tendency to decrease with an increase in boost.

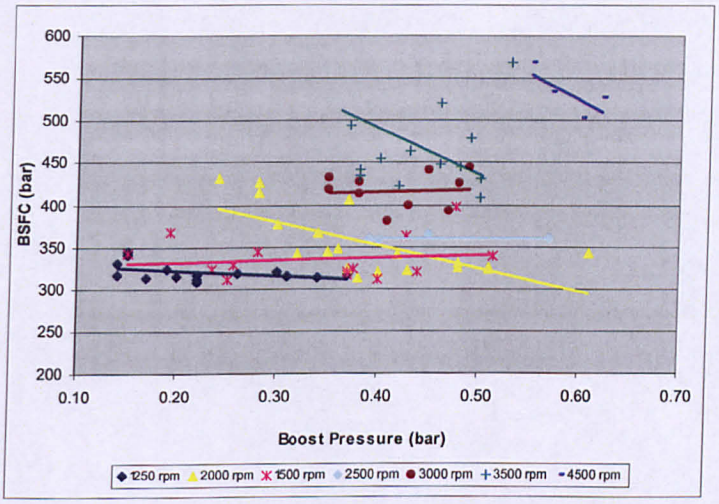

Figure 6.47 Effect of boost on BSFC

Figure 6.48 shows that ISFC increases with speed, reaching a maximum at 3500rpm and then falling again at 4500rpm. At every speed, as boost goes up, ISFC goes down. Since the difference between ISFC and BSFC can only come from the friction losses, it is apparent that at high speed frictional losses are an important source of fuel consumption. This fact can be confirmed when one looks at Figure 6.49, where it is easy to notice that the fraction of ISFC taken by the friction losses scales up with speed.

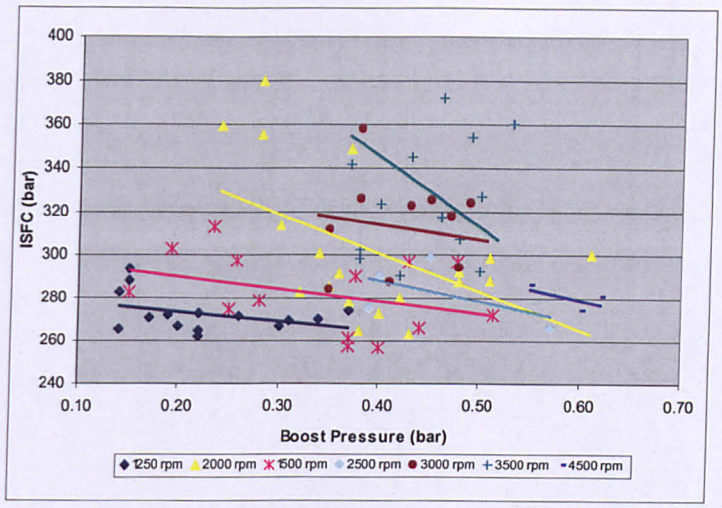

Figure 6.48 Effect of boost on ISFC

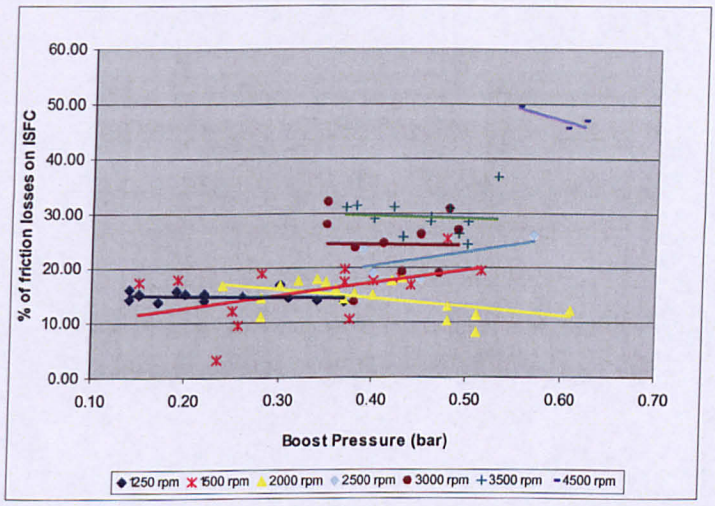

Figure 6.49 Effect of friction losses on ISFC

Similar to what happened during the NA CAI test, the fact of having the NVO strategy for achieving CAI introduces pumping losses as shown in section 5.2. Pumping losses, in turn, have a degree of dependence on the amount of trapped residuals, as shown by Figure 6.50. It can be noticed that for the SI range, pumping losses decrease as the residual fraction increases, for every speed up to 2000rpm. Pumping losses also increase with speed, in this range. For the CAI range, however, pumping losses are not so variable anymore in relation to the residual fraction.

The pumping losses seem to have a better correlation with boost, as shown in Figure 6.51, for they always increase with boost until the speed of 4500rpm. At this point, pumping losses fall. This suggests that the turbocharger may be operating in a higher efficiency zone.

This correlation with boost is expected, since for the compressor to pressurize the intake it has to take power from the turbine, which, in turn, increases the back pressure in the exhaust manifold.

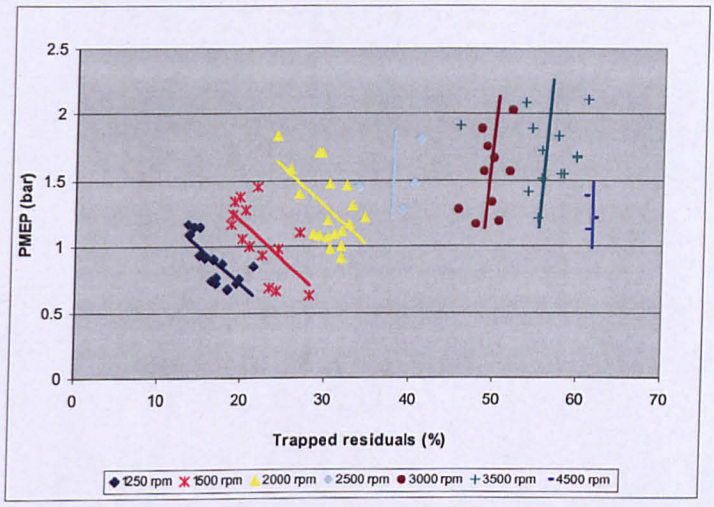

Figure 6.50 Effect of residual fraction on pumping losses

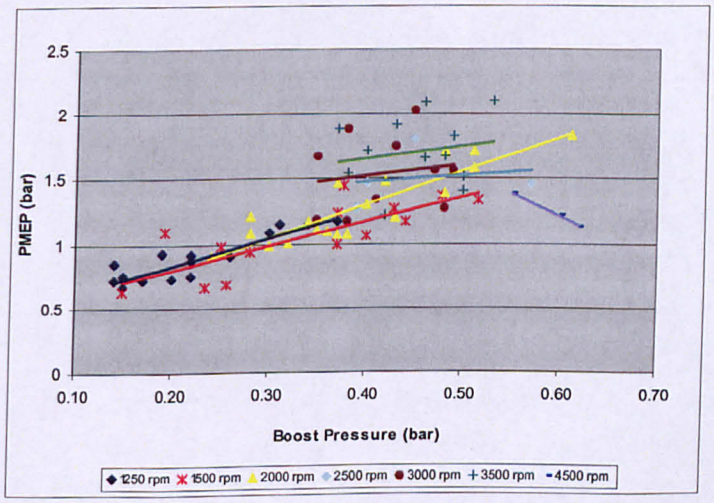

Figure 6.51 Effects of boost on pumping losses

The effect of pumping losses can be better evaluated when it is referred to ISFC, as a percentage, shown in Figure 6.52. It is very clear that pumping losses are the major source of fuel consumption in the turbocharged set-up. The only exception happens at the speed of 4500rpm, where pumping losses fall and the main source of fuel consumption becomes the frictional losses (Figure 6.49).

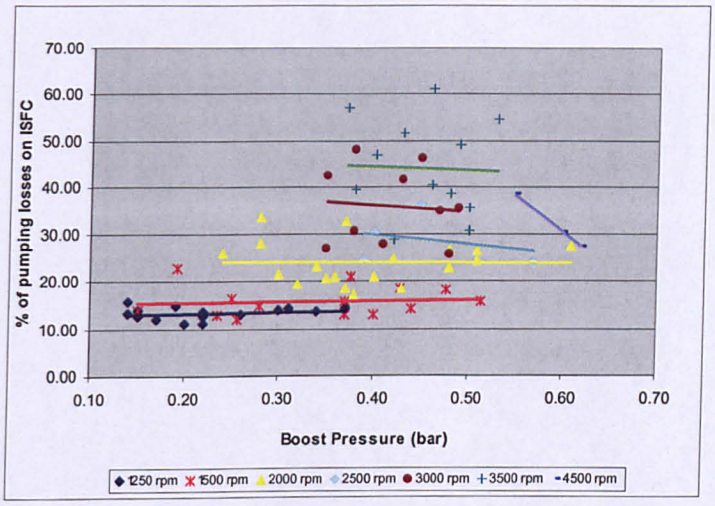

Figure 6.52 Effects of pumping losses on ISFC

Figure 6.53 shows a p-v diagram for the turbocharged CAI operation at 3500rpm and 2.43 bar boost, where it is possible to see the large pumping loop at the bottom.

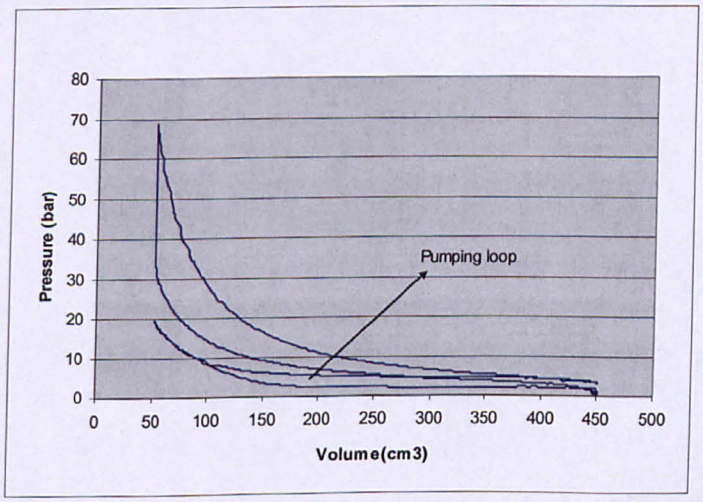

Figure 6.53 P-V diagram for the turbocharged operation at 3500rpm, λ=1.00, boost=0.53bar, BMEP=2.43bar

6.14 Summary

This section presented the results for the turbocharged operation of the CAI engine. General emissions and performance analysis was carried out, followed by the combustion and in-cylinder conditions analysis.

It was noticed that CAI could only happen at high speed. For speeds lower than 2500rpm ,only SI was present. From 2500 to 3000rpm, with more than 40% trapped residuals, CAI started to happen in spark-assisted mode and from 3000rpm to 4500rpm pure CAI was present.

Emissions of HC and CO proved to be, for most of the operational range, lower than for the standard SI engine, and NO_x emissions showed up to 98% reduction. Fuel consumption, however, was found to be higher then both the NA CAI set-up and the SI standard engine. The causes for this occurrence were investigated and it was found that pumping losses where the main cause for increasing the energy losses and, therefore, the fuel consumption.

7. Conclusions and recommendation for future work

A 4-cylinder Ford Duratec 1.6 L Ti-VCT (Twin Independent Variable Cam Timing) Gasoline Engine was commissioned and modified to operate with Controlled Auto-Ignition combustion. Two main tests were carried out and the results were compared to the ones for a standard SI production engine. The conclusions obtained from these experiments are detailed below.

7.1 Naturally Aspirated CAI/HCCI

CAI combustion has been achieved on a production type 4-stroke, 4-cylinder gasoline engine employing substantially standard components, having only the camshafts changed in order restrict the gas exchange process. CAI could be achieved over a fair range of load and speed. When in CAI operating mode, significant BSFC and emissions reduction could be achieved, especially for NOx (up to 99%). Aiming to better understand the NA CAI combustion, detailed analysis of the combustion and heat release process was carried out.

7.1.1 Effect of load, speed and residual fraction on engine performance and fuel consumption

The engine torque output was determined principally by the amount of residuals trapped in the cylinder using variable valve timing. The higher the residual fraction, the lower the torque output.

The higher load range was limited by knock at low speeds and by restrictions in the gas exchange process at high speeds. The lower load limit was determined by misfire. Measures to extend the high load limit could be the use of external, cooled EGR for the low speed part and to improve the flow at low speeds by having a more flexible valve train, allowing at least an independent control of valve opening/closing events would be necessary.

The use of trapped residuals is an effective way to control heat release. Maximum cylinder pressure and maximum rate of pressure rise decreased as the residual fraction increased.

Load had a determinant effect on CAI combustion. At high loads, CAI combustion started earlier and completes faster; combustion temperature, exhaust temperature, peak pressure and maximum pressure rise were at their maximum.

Speed had a noticeable effect as it tends to lower emissions figures and increase BSFC. At high speeds, heat losses and PMEP were lower. FMEP, however, increased and offset the advantages of the others, impairing BSFC. While BSFC increased with speed, ISFC decreased, confirming that friction was the main cause of increased fuel consumption at high speed.

Brake specific fuel consumption tended to decrease as load increased, suggesting that any increase in the load limit would be beneficial, at any speed.

The pumping losses caused by the recompression loop remained low and tended to fall with speed. This was due to lower heat losses at high speed.

To improve the CAI load range whilst still keeping the high dilution rate, forced induction via turbocharging could be a good alternative. This is because intake boost is accomplished with increased exhaust back pressure, helping to trap a larger residual fraction in the cylinder.

7.1.2 Emissions Performance

For the most of the CAI combustion range, NOx emissions were ultra-low. This was due to the low cylinder temperatures achieved by the high residuals rate. NO_x was not always low. Without the necessary residual fraction the values could be as high as for the standard SI engine. NO_x emissions tended to increase with load since lower residual rate was present. Any ways to increase load while keeping the residual fraction high would help extend CAI range while still holding NO_x emissions down.

HC levels were higher than the standard SI engine for the whole CAI range due to low combustion temperatures.

CO emissions were higher than the standard SI engine at 1000rpm, but were in general much lower at higher speeds. Improving mixture preparation at this speed could help reduce CO emissions levels.

7.1.3 Summary

The potential of CAI/HCCI for lowering emissions levels and fuel consumption was proven in a 4-cylinder NA engine with minor changes from the production unit. CAI was achieved by means of NVO strategy. It has been shown that CAI combustion is very efficient especially to control NO_x emissions. It has, however, still a limited range of operation and ways to extend it are very necessary.

7.2 Turbocharged CAI/HCCI

Similarly to the NA test, the turbocharged CAI engine relied on exhaust gas trapping using a negative valve overlap strategy to promote auto-ignition of the fresh charge. A turbocharger was added to the engine in order to provide forced induction and extend the CAI range.

Boosting via turbocharging, in conjunction with residual gas trapping, has been shown to be an effective way to raise the CAI/HCCI operation usable load range. It was possible to achieve much higher loads and increase the attainable speed.

The addition of a turbocharger and boost to the engine, together with NVO, added many more parameters for engine operation. Many secondary effects that influenced engine performance came in place. It was necessary to choose what results to aim for and optimize the parameters appropriately.

7.2.1 Emissions Performance

CO emissions showed a great dependency on AFR for both SI and CAI operation. For lean mixtures, however, CO was lower with the Turbocharged CAI than with the standard SI engine operation. It is important to point out that in this condition the Turbocharged CAI operation produced CO emissions up to 75% lower than the standard SI engine.

HC emissions were much higher with the Turbocharged CAI engine than with the standard SI engine. However, the Turbocharged CAI engine showed lower HC emissions than the NA CAI engine due to leaner mixtures and substantially higher exhaust temperatures.

NO_x emissions showed higher values in the Turbocharged CAI operation than with the NA CAI operation. Nevertheless, both cases show values extremely low when compared to the standard SI engine.

It becomes evident that the Turbocharged CAI operation is advantageous from the emissions point of view. In comparison to the standard SI engine, CO and NO_x emissions show very low figures. HC emissions, despite of being higher than the SI engine, show smaller levels than the NA CAI and could be treated by a standard 3-way catalyst.

7.2.2 Effects of AFR on engine performance

The effects of λ were more pronounced in the SI operation (below 2500rpm) than on the CAI range (above 3000rpm). Maximum cylinder temperature, load and brake specific fuel consumption tended to be more or less constant with λ in the CAI range when compared to the SI range. Nevertheless, for the CAI range, these values showed a slight decrease as λ increased.

The AFR seemed to have little effect on residuals percentage, since these were more dependent on valve timing.

There seems to be, however, an optimum λ value of 1.05 that yields low fuel consumption as well as reasonably low levels of NO_x, CO and HC emissions.

7.2.3 Effects of Spark Timing

Spark timing was found to have a strong effect over the engine's overall performance during the SI range. Since spark timing had a strong effect on exhaust temperatures, boost was highly dependent on it during SI operation (below 2500rpm). The effect became slightly less in the spark assisted CAI range and were almost inexistent in the full CAI range, i.e. above 3000rpm. This suggests that the presence of spark, at appropriate times, is a very important way to promote a seamless SI/CAI switching.

7.2.4 Effects of boost, residual fraction, pumping and friction losses on engine performance and fuel consumption

Compared to the standard SI engine, BSFC was 20% higher with the Turbocharged CAI operation. This is mainly due to the increased pumping losses caused by the turbocharger that affect engine efficiency.

BSFC has shown, however, a strong negative correlation with load, which suggests that if load could increase further, BSFC would probably decrease. At high speeds, the frictional losses reach their maximum and account for a substantial amount of the available IMEP. Since friction tends to be more dependent on speed than load, once friction has reached the maximum for a certain speed, if load increases further, BSFC will fall.

The results also suggest that the turbocharger was not operating at a good efficiency point. This implies that a better matched turbocharger would decrease pumping losses and hence fuel consumption. In addition, a better matched turbocharger would be able to provide higher boost for the same or less pumping losses, which means that the attainable load would be higher and fuel consumption would tend to fall since the overall thermal efficiency would increase.

The gas exchange process became very restricted at high speeds, therefore limiting the achievement of a potentially higher load that could contribute to decrease BSFC.

Boost increased intake air temperature. Increased air temperature limited the achievable load by lowering the knock limit and by decreasing the charge density. Measures that would tackle these effects would extend the load range and improve the overall efficiency and reduce fuel consumption, at the same time that would have the potential to decrease NO_x emissions even further.

Boost pressure increased with speed and load as more exhaust energy became available. Boost has shown a strong dependency on exhaust residuals. The higher the residual fraction, the lower the boost was.

It was possible to achieve CAI with turbocharged operation only with residual rate higher than 40%, which is similar to what happens in the NA CAI. With the turbocharged operation, the use of trapped residuals is a valuable way to control heat release. Increased residual rate tends to advance combustion phasing and make combustion faster. Values for combustion duration and maximum cylinder pressure are similar to the ones from the NA CAI operation. The latter, however, is higher than for the standard SI engine. Maximum cylinder pressure and maximum rate of pressure rise showed to be more dependent on boost than any other variable, so boost control is an effective way to limit these two quantities.

The use of residual trapping via NVO proved indeed to be a good alternative for promoting autoignition and achieving CAI. On the other hand, trapping residuals negatively affects the turbocharger operation by limiting the available exhaust energy and, therefore, boost. If there could be a way to increase boost without decreasing the percentage of trapped residuals, this would probably enable higher loads while still controlling heat release.

7.2.5 Summary

With turbocharged operation, the results seemed to be very much dependent on the set-up. The described set-up introduced high pumping losses that impaired the results for fuel consumption. Load and emissions, however, seemed to have much improved results in comparison to the standard SI engine and to the NA CAI engine. Turbocharging is, therefore, a potential way to increase even further the achievable CAI load range and to contribute for the evolution of the CAI technology.

7.3 Recommendations for Future Work

The results provided by the Turbocharged CAI Engine test unveiled some interesting characteristics as well as some areas of possible improvement by further research. The further results would give some insights that could help CAI to reach the roads and motorways in the future. It is the view of the author that the following areas could be further explored.

7.3.1 Reducing Pumping Losses

Pumping losses have to be minimized in order for the BSFC values to reach acceptable levels. This could be done by better selecting a turbocharger, i.e. finding an unit that could be a better match for the engine. In addition, it would be desirable to have a variable geometry turbocharger to operate closer to its best efficiency throughout the whole engine operating range. It would be desirable to further monitor the turbocharger operation by installing extra pressure and temperature sensors closer to the turbine and compressor inlet/outlet. Also, if possible, it would be helpful to have a rotor speed sensor to monitor the turbocharger with more precision.

7.3.2 Improving the Gas Exchange Process

The gas exchange process has to be improved in order to achieve higher loads at high speeds. This could be done by better designing the camshaft profiles. Since the engine is a research unit and does not need long-lasting camshafts, more aggressive cam profiles

could be designed, providing higher valve lifts for still short durations. The timing for the valve opening/closing events should be better studied, perhaps through simulation, in order to find more optimized figures and then to design new cam profiles based on them, if possible.

7.3.3 Expanding the Turbocharged CAI Range

The CAI range needs to be increased by expanding the upper and lower load limits. The upper load limit could be increased by the use of cooled external EGR while still using trapping residuals via NVO as well as the use of an intercooler to cool down intake air. This would avoid knocking at high loads as well as improve the charge density, contributing even further for the achievement of higher loads.

The lower load limit could be extended by lowering boost pressure by waste-gate opening. This would require an electronic control over the waste-gate. The lower load limit could be extended by increasing slightly the compression ratio. Obviously this would have an impact on the upper load limit but could be possibly counteracted by having cooled EGR and intercooler.

Instabilities at 2500rpm should be investigated and possibly counteracted. This would widen the operation at that speed.

7.3.4 Improving Mixture Preparation

Although it was not reported in this thesis, during the tests, the author observed some conditions in which mixture preparation could be improved. Injection timing could be optimized for each valve timing combination, improving mixture preparation and yielding possibly better emissions results. Particularly at low speed and low loads, when the injectors operate with very low pulse widths, their precision in metering the fuel tends to fall. At this condition smaller injectors could play a critical role.

7.3.5 Evaluating Catalyst Efficiency with CAI

Since CAI produces low exhaust temperatures, especially for the NA operation, a test should be performed to assess catalyst efficiency with CAI combustion. It should compare raw emissions with emissions downstream from the catalyst.

7.3.6 Using Ethanol as Fuel

A test having ethanol as a fuel should be performed. It's lower knock sensitivity and charge cooling effects should help extend the higher load limit. A test should be performed both in NA and boosted operation.

7.3.7 Non-symmetrical Valve Timings for NA operation

It should be performed a naturally aspirated test having valve timings not symmetrical. It should investigate the possibility to expand CAI range with this configuration and to find out optimum operating parameters.

8. References

1. Dinsdale, Jason "Environmental Facts and Figures", available from: http://www.environment-agency.gov.uk/yourenv/eff/1190084/natural_forces/climate/?version=1&lang=_e, Environmental Agency, 2007 [accessed July 2007].
2. H M Government, "Climate Change – The UK Programme 2006", available from: http://www.defra.gov.uk/environment/climatechange/uk/ukccp/pdf/ukccp06-all.pdf, March 2006 [accessed July 2007].
3. "UK Climate Change Programme: Annual Report to Parliament", Department for Environment, Food and Rural Affairs, available from: http://www.defra.gov.uk/environment/climatechange/uk/ukccp/pdf/ukcc-annrpt-07.pdf, [accessed July 2007].
4. "Kyoto Protocol to the United Nations Framework Convention on Climate Change", Available from: http://unfccc.int/resource/docs/cop3/07a01.pdf, UNFCCC Document No. FCCC/CP/1997/7/Add.1, March 1998 [accessed July 2007].
5. "Objectives of the agreements concluded with the automobile industry", European Commission, available from: http://ec.europa.eu/environment/co2/co2_agreements.htm , January 2007[accessed July 2007].
6. "The Renewable Transport Fuel Obligation Programme", Department for Transport, available from: http://www.dft.gov.uk/pgr/roads/environment/rtfo/aboutrtfo, [accessed July 2007].
7. "1990 Amendments to the Clean Air Act", US Environmental Protection Agency (EPA), obtained from http://www.epa.gov/air/caa/ , [accessed July 2007].
8. "EU Emission Standards for Passenger Cars", Dieselnet - Online information service on clean diesel engines and diesel emissions, available from: http://www.dieselnet.com/standards/eu/ld.php#stds, [accessed July 2007].
9. Robert Bosch GmbH. "Gasoline Engine Management. 3rd Edition". s.l. : Professional Engineering Ltd, June 2006. ISBN 0-470-05757-2.
10. Searles, R.A., "Emission catalyst technology – challenges and opportunities in the 21st century." International conference on 21st centurey emissions technology, IMechE, Conference Transactions 2000-2, ISBN 1-86058-322-9, 2000.

11. Zhao, Fuquan, "Automotive Gasoline Direct-Injection Engines". SAE International, May 2002. ISBN 978-0-7680-0882-1, p238.
12. Onishi, S., Hong Jo, S., Shoda, K., Do Jo, P., Kato S., "Active Thermo-Atmosphere Combustion (ATAC) – A New Combustion Process for Internal Combustion Engines", SAE Paper 790501, 1979.
13. Noguchi, M., Tanaka, Y., Tanaka, T., and Takeuchi Y., "A Study on Gasoline Engine Combustion by Observation of Intermediate Reactive Products during Combustion", SAE Paper 790840, 1979
14. "Honda readies activated radical combustion two-stroke engine for production motor-cycle", Automotive Engineering, pp.90-92, SAE Publications, January 1997.
15. Najt, P. M., Foster, D.E., "Compression-ignited homogeneous charge combustion", SAE paper 830264, 1983.
16. Christensen, M., Hultqvist, A., Johansson, B., "Demonstrating The Multi Fuel Capability of a Homogeneous Charge-Compression Ignition Engine with Variable Compression Ratio", SAE Paper 1999-01-3679.
17. Thring, R. H., Homogeneous Charge-Compression Ignition (HCCI) Engines, SAE Paper 892068, 1989.
18. Pucher, G.R., Gardiner, D.P., Bardon, M.F., Battista, V., "Alternative Combustion Systems for Piston Engines Involving Homogeneous Charge Compression Ignitions Concepts – A Review of Studies Using Methanol, Gasoline and Diesel Fuel", SAE Paper 962063.
19. Lavy, J., Dabadie, J.C., Angelberger, C., Duret, P., Willand, J., Juretzka, A., Schaflein, J., Ma, T., Lendresse, Y., Satre, A., Schulz, C., Kramer, H., Zhao, H., and Damiano, L., "Innovative Ultra-low NOx controlled auto-ignition combustion process for gasoline engines: the 4-SPACE project", SAE paper 2000-01-1873, 2000.
20. Law, D., Allen, J., Kemp D. and Williams, P., "4-Stroke Active Combustion (Controlled Auto-Ignition) Investigation using a Single Cylinder Engine with Lotus Active Valve Train (AVT)", International Conference on 21st Century Emissions Technology, C588/006/2000, IMechE, 2000.
21. Milovanovic, M., Blundell, D., Pearson, R., Turner, J., Chen, R., "Enlarging the Operational Range of a Gasoline HCCI Engine by Controlling the Coolant Temperature", SAE Paper 2005-01-0157, 2005.
22. Li J., Zhao, H., and Ladommatos, N., "Research and development of controlled auto-ignition (CAI) combustion in a four-stroke multi-cylinder gasoline engine", SAE paper 2001-01-3608, 2001.

23. Zhao, H., Li J., Ma T., Ladommatos, N., "Performance and analysis of a 4-stroke Multi-cylinder Gasoline Engine with CAI Combustion", SAE paper 2002-01-0420, 2002.
24. Zhao, F. et al., "Homogeneous Charge Compression Ignition (HCCI) engines – Key research and development issues", ISBN 0-7680-1123-X, 2003, p1.
25. Fuerhapter, A., Piock, W.F., and Fraidl G.K., "CSI – Controlled Auto Ignition – the best Solution for the fuel Consumption – Versus Emission Trade-Off?", SAE paper 2003-01-0754, 2003.
26. Christensen, M., Johansson, B., "Influence of mixture quality on premixed-charge compression ignition gasoline engine", SAE Paper 982454.
27. Oakley, A., Zhao, H., Ladommatos, H., "Experimental Studies on Controlled Auto-ignition (CAI) combustion of Gasoline in a 4-Stroke Engine", SAE Paper 2001-01-1030, 2001.
28. Oakley, A., "Experimental investigations on controlled auto ignition combustion in a four-stroke engine", PhD Thesis, Brunel University, 2001.
29. Yap, D., Megaritis, A., Wyszynsky, M., "Effect of inlet valve timing on boosted gasoline HCCI with residual gas trapping", SAE Paper 2005-01-2136, 2005.
30. Milovanovic, N., Chen, R., "Influence of Variable Valve Timing Strategy on the control of a Homogeneous Charge Compression Ignition (HCCI) Engine", SAE Paper 2004-01-1899, 2004.
31. Morikawa, H., Ishibashi, Y.,"An experimental approach to the controlled auto-ignition", SAE Paper 2007-01-0173, 2007.
32. Ohyama, Y."Simultaneous Control of Air/Fuel Ratio and Intake, Exhaust Valve Timing for HCCI Operation", SAE Paper 2003-01-1084, 2003.
33. Heywood, J., "Internal Combustion Engines Fundamentals", McGraw-Hill Book Company, 1988. ISBN 0-07-100499-8.
34. Martinez-Frias, J., Aceves S.M., Flowers, D., Smith, J.R., Dibble, R., "Equivalence Ratio-EGR Control of HCCI Engine Operation and the Potential for Transition to Spark-Ignited Operation", SAE paper 2001-01-3613, 2001.
35. Oakley, A., Zhao, H., Ladomatos, N., Ma, T., "Dillution Effects on the Controled Auto-Ignition Combustion of hydrocargon and Alcohol Fuels, SAE Paper 2001-01-3606, 2001.
36. Yelvington, P.E., Green, W.H., "Prediction of the Knock Limit and Viable Operating Range for a Homogeneous-Charge Compression-Ignition (HCCI) Engine", SAE Paper 2003-01-1092, 2003.

37. Wang, Zhi., Wang, Jian-Xin., Shuai, Shi-Jin., Tian, Guo-Hon., An, Xinlian., Ma, Qing-Jun., "Study of the Effect of Spark Ignition on Gasoline HCCI Combustion", Proceedings of the I MECH E Part D Journal of Automobile Engineering, Volume 220, Number 6, 2006, pp. 817-825.

38. Hyvonen, J., Haraldson, G., Johansson, B., "Operating Conditions Using Spark Assisted HCCI Combustion during Combustion Mode Transfer to SI in a Multi-Cylinder VCR-HCCI engine", SAE Paper 2005-01-0109, 2005.

39. Chen, R., Milovanovic, N., Turner, J., Blundell, D., "The thermal effect of internal exhaust gas recirculation on controlled auto-ignition", SAI Paper 2003-01-0751, 2003.

40. Persson, H., Pfeiffer, R., Hultqvist A., Johansson B., Ström H.," Cylinder-to-Cylinder and Cycle-to-Cycle Variations at HCCI", SAE Paper 2005-01-0130, 2005.

41. Milovanovic, M., Blundell, D., Pearson, R., Turner, J., Chen, R., "Enlarging the Operational Range of a Gasoline HCCI Engine by Controlling the Coolant Temperature", SAE Paper 2005-01-0157, 2005.

42. Stanglmaier, R., Roberts, C., "Homogeneous Charge Compression Ignition (HCCI): Benefits, Compromises and Future Engine Applications, SAE Paper 1999-01-3682, 1999.

43. Christensen, M., Johansson, B., Amneus, P., Mauss, F., "Supercharged Homogeneous Charge Compression Ignition", SAE Paper 980787, 1998.

44. Christensen, M., Johansson, B., "Supercharged Homogeneous Charge Compression Ignition (HCCI) With Exhaust Gas Recirculation and Pilot Fuel", SAE Paper 2000-01-1835, 2000.

45. Olsson, J., and Johansson, B., "Boosting for High Load HCCI", SAE Paper 2004-01-0940, 2004.

46. Olsson, J., Tunestal, P., Haraldsson, G., Johansson, B., "A Turbocharged Dual Fuel HCCI Engine", SAE Paper 2001-01-1896, 2001.

47. Olsson, J., Tunestal, P., Ulfvik, J., Johansson, B., "The The Effect of Cooled Egr on Emissions and Performance of a Turbocharged Hcci Engine", SAE Paper 2003-01-0743, 2003.

48. Yap, D., Wyszynski, M. Megaritis, A., Xu, H., "Applying boosting to gasoline HCCI operation with residual gas trapping", SAE Paper 2005-01-2121, 2005.

49. Yap, D., Megaritis, A., Wyszynski, M." Effect of Inlet Valve Timing on Boosted Gasoline Hcci With Residual Gas Trapping", SAE Paper 2005-01-2136, 2005.

50. Olsson, J., Tunestal, P., Johansson, B., "Boosting for High Load HCCI", SAE Paper 2004-01-0940, 2004.
51. Wilhelmsson, C., Tunestal, P., Johansson, B. "Operation strategy of a Dual Fuel HCCI Engine with VGT", SAE Paper 2007-01-1855, 2007.
52. Hatamura, K., "A Study on HCCI (Homogeneous Charge Compression Ignition) Gasoline Engine Supercharged by Exhaust Blow Down Pressure", SAE Paper 2007-01-1873, 2007.
53. Kaufeld H., Kolsch U., Rechs M., Ruhland H., Springer K. "The New Ford Duratec 1.6l Ti-VCT Engine". MTZ Worldwide, 2005, Vol. 66, 3.
54. Robert Bosch GmbH. "Gasoline Engine Management. 2nd Edition". s.l. : Professional Engineering Ltd, 2004. ISBN 1 8605 84349.
55. Zhao. H., and Ladommatos. N., "Engine Combustion Instrumentation and Diagnostics. First Edition". SAE International, 2001. ISBN 0-7680-0665-1.
56. Blair, Gordon P., "Design and Simulation of Four-Stroke Engines". SAE International, 1999. ISBN 0-7680-0440-3.
57. Kalian, N., "Investigation of CAI/SI Operations in a Four-cylinder Direct Injection Gasoline Engine", PhD Thesis, Brunel University, 2006.

Appendix A – CAD drawings for pressure transducer installation

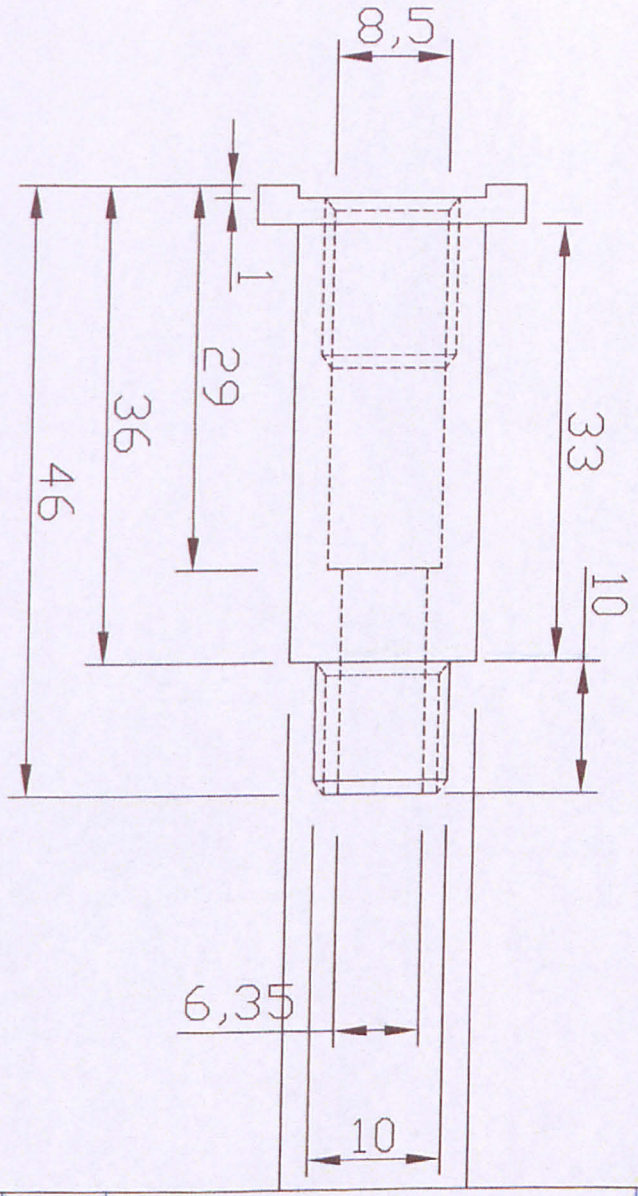

	Sleeve (mild steel)			Sheet 2/3
Mario Martins		Brunel University	13.12.2005	1:2
Cylinder head machining for pressure transducers				

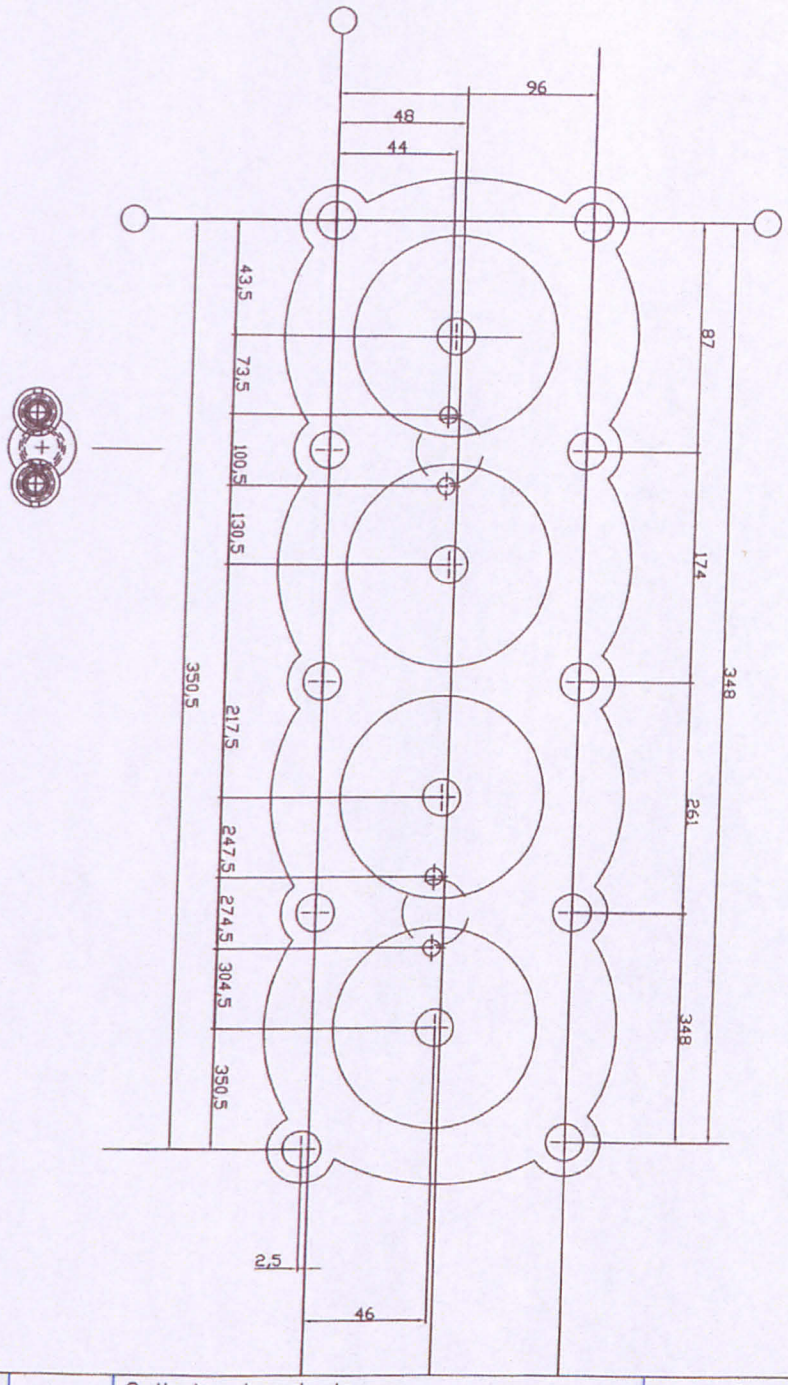

	Cylinder head view			Sheet 1/3	
Mario Martins		Brunel University		Date 13.12.2005	Scale 1:1
Cylinder head machining for pressure transducers					

Fust sleeve design
did not work and and had to
be replaced by the new
design with treaded end

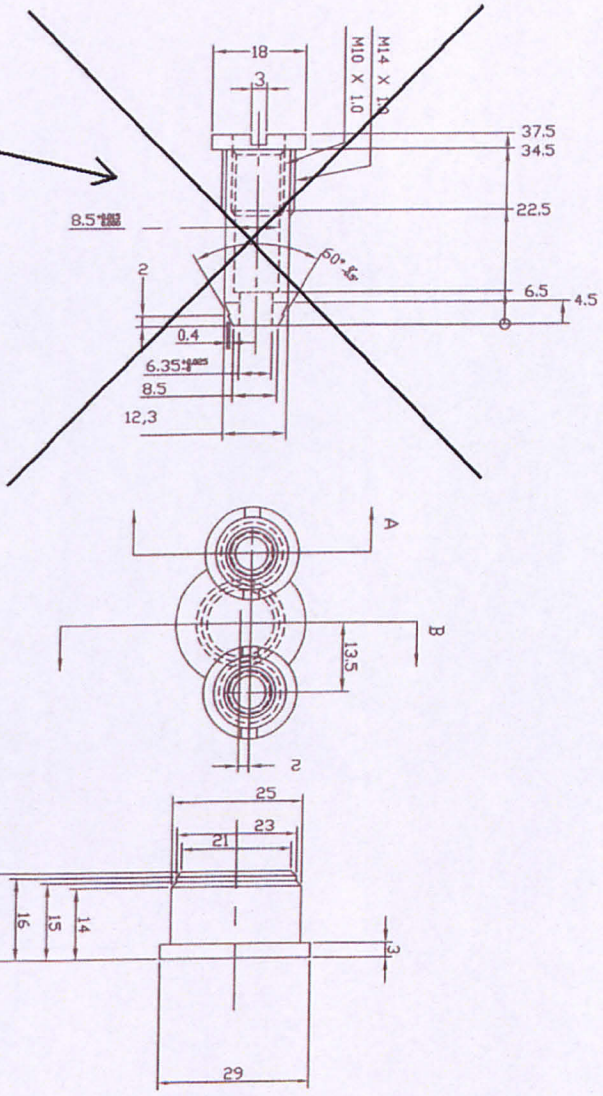

		Plug (alluminum) and sleeve (mild steel)		Sheet 3/3	
Mario Martins		Brunel University		13.12.2005	1:2
Cylinder head machining for pressure transducers					

Appendix B – MHI Turbocharger range and specifications

Specifications									
Model			TD02	TD025	TD03	TD04	TD05	TD06	TD07	TD08
Organization output (PS)			8-40	12-56	15-65	22-100	40-130	60-180	100-130	150-450
Amount of exhaust(cc)	Diesel organization		600	1,000	1,200	1,800	2,300	4,000	6,000	10,000
	Gasoline organization	Passenger car	500	750	1,000	1,500	2,000	2,600	-	-
		Two-wheeled vehicle	250	400	500	750	1,000	1,300	-	-
The highest rotation speed (rpm)			270,000	250,000	230,000	200,000	170,000	145,000	132,000	114,000
Temperature of gas allowance and the highest (Centigrade)			900	900	900	900	900	900	760	760
The maximum compression ratio			2.2	2.2	2.3	2.4	2.6	2.7	2.8	3.1
Weight (kg)			-	-	3.0	3.5	4.0	5.0	9.0	10.5
	With waist gate valve		2.0	2.3	3.5	4.0	5.0	6.5	-	-

Appendix C – MOTEC ECU M800 Series specification

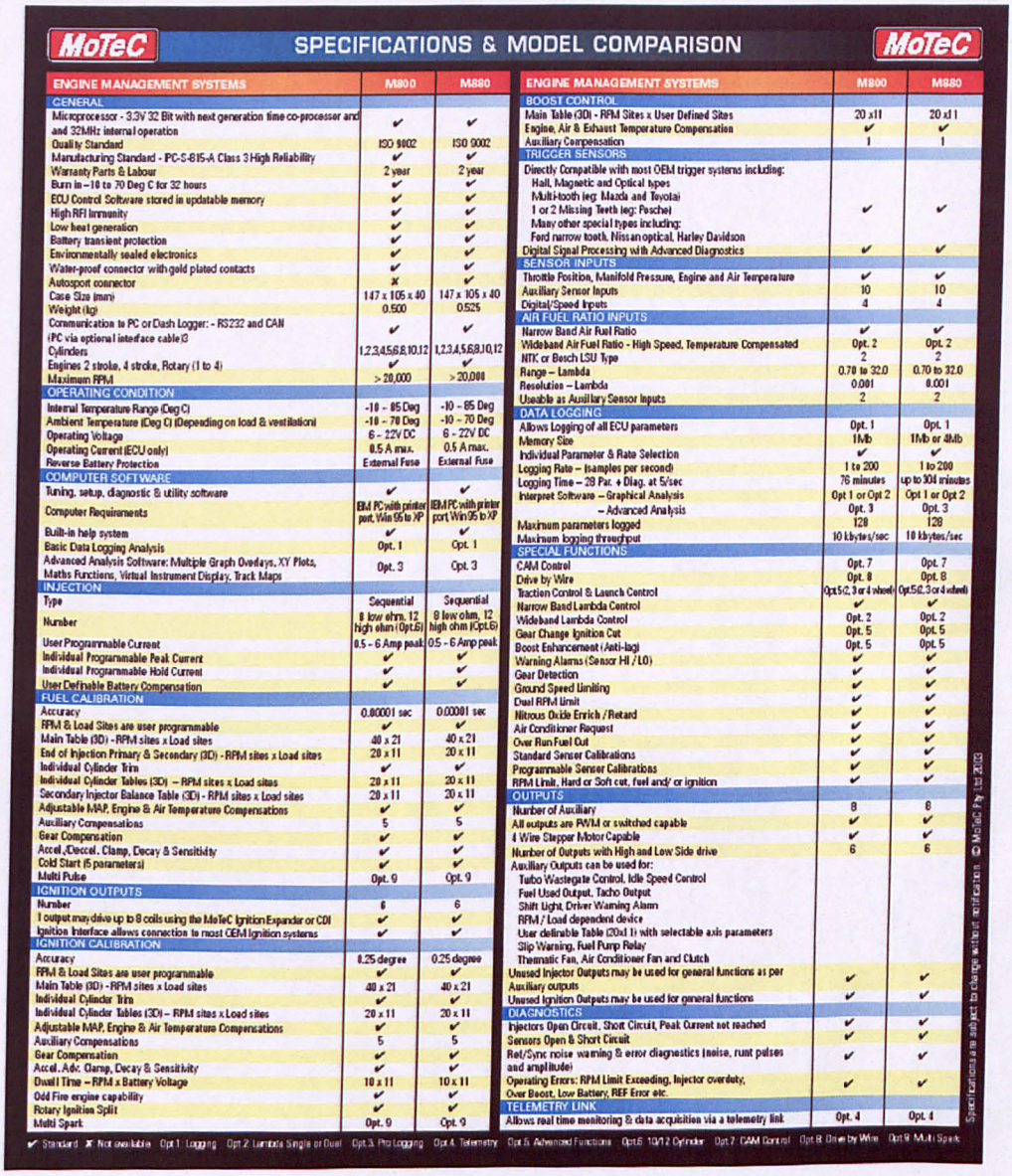

MoTeC

SPECIFICATIONS & MODEL COMPARISON

MoTeC

ENGINE MANAGEMENT SYSTEMS	M800	M880
GENERAL		
Microprocessor - 3.3V 32 Bit with next generation fine co-processor and and 32MHz internal operation	✔	✔
Quality Standard	ISO 9002	ISO 9002
Manufacturing Standard - IPC-S-815-A Class 3 High Reliability	✔	✔
Warranty Parts & Labour	2 year	2 year
Burn in – 10 to 70 Deg C for 32 hours	✔	✔
ECU Control Software stored in updatable memory	✔	✔
High RFI Immunity	✔	✔
Low heat generation	✔	✔
Battery transient protection	✔	✔
Environmentally sealed electronics	✔	✔
Water-proof connector with gold plated contacts	✔	✔
Autosport connector	✔	✔
Case Size (mm)	147 x 105 x 40	147 x 105 x 40
Weight (kg)	0.500	0.525
Communication to PC or Dash Logger: - RS232 and CAN (PC via optional interface cable)	✔	✔
Cylinders	1,2,3,4,5,6,8,10,12	1,2,3,4,5,6,8,10,12
Engines 2 stroke, 4 stroke, Rotary (1 to 4)	✔	✔
Maximum RPM	> 20,000	> 20,000
OPERATING CONDITION		
Internal Temperature Range (Deg C)	-10 – 85 Deg	-10 – 85 Deg
Ambient Temperature (Deg C) (Depending on load & ventilation)	-10 – 70 Deg	-10 – 70 Deg
Operating Voltage	6 – 22V DC	6 – 22V DC
Operating Current (ECU only)	0.5 A max.	0.5 A max.
Reverse Battery Protection	External Fuse	External Fuse
COMPUTER SOFTWARE		
Tuning, setup, diagnostic & utility software	✔	✔
Computer Requirements	IBM PC with printer port, Win 95 to XP	IBM PC with printer port, Win 95 to XP
Built-in help system	✔	✔
Basic Data Logging Analysis	Opt. 1	Opt. 1
Advanced Analysis Software: Multiple Graph Overlays, XY Plots, Maths Functions, Virtual Instrument Display, Track Maps	Opt. 3	Opt. 3
INJECTION		
Type	Sequential	Sequential
Number	8 low ohm, 12 high ohm (Opt.6)	8 low ohm, 12 high ohm (Opt.6)
User Programmable Current	0.5 – 6 Amp peak	0.5 – 6 Amp peak
Individual Programmable Peak Current	✔	✔
Individual Programmable Hold Current	✔	✔
User Definable Battery Compensation	✔	✔
FUEL CALIBRATION		
Accuracy	0.00001 sec	0.00001 sec
RPM & Load Sites are user programmable	✔	✔
Main Table (3D) - RPM sites x Load sites	40 x 21	40 x 21
End of Injection Primary & Secondary (3D) - RPM sites x Load sites	20 x 11	20 x 11
Individual Cylinder Trim	✔	✔
Individual Cylinder Tables (3D) – RPM sites x Load sites	20 x 11	20 x 11
Secondary Injector Balance Table (3D) - RPM sites x Load sites	20 x 11	20 x 11
Adjustable MAP, Engine & Air Temperature Compensations	✔	✔
Auxiliary Compensations	5	5
Gear Compensation	✔	✔
Accel./Deccel. Clamp, Decay & Sensitivity	✔	✔
Cold Start (5 parameters)	✔	✔
Multi Pulse	Opt. 9	Opt. 9
IGNITION OUTPUTS		
Number	6	6
1 output may drive up to 8 coils using the MoTeC Ignition Expander or CDI	✔	✔
Ignition Interface allows connection to most OEM ignition systems	✔	✔
IGNITION CALIBRATION		
Accuracy	0.25 degree	0.25 degree
RPM & Load Sites are user programmable	✔	✔
Main Table (3D) - RPM sites x Load sites	40 x 21	40 x 21
Individual Cylinder Trim	✔	✔
Individual Cylinder Tables (3D) – RPM sites x Load sites	20 x 11	20 x 11
Adjustable MAP, Engine & Air Temperature Compensations	✔	✔
Auxiliary Compensations	5	5
Gear Compensation	✔	✔
Accel./Adc. Clamp, Decay & Sensitivity	✔	✔
Dwell Time – RPM x Battery Voltage	10 x 11	10 x 11
Odd Fire engine capability	✔	✔
Rotary Ignition Split	✔	✔
Multi Spark	Opt. 9	Opt. 9

ENGINE MANAGEMENT SYSTEMS	M800	M880
BOOST CONTROL		
Main Table (3D) - RPM Sites x User Defined Sites	20 x 11	20 x 11
Engine, Air & Exhaust Temperature Compensation	✔	✔
Auxiliary Compensation	1	1
TRIGGER SENSORS		
Directly Compatible with most OEM trigger systems including: Hall, Magnetic and Optical types; Multi-tooth (eg: Mazda and Toyota); 1 or 2 Missing Teeth (eg: Bosche); Many other special types including: Ford narrow tooth, Nissan optical, Harley Davidson	✔	✔
Digital Signal Processing with Advanced Diagnostics	✔	✔
SENSOR INPUTS		
Throttle Position, Manifold Pressure, Engine and Air Temperature	✔	✔
Auxiliary Sensor Inputs	10	10
Digital/Speed Inputs	4	4
AIR FUEL RATIO INPUTS		
Narrow Band Air Fuel Ratio	✔	✔
Wideband Air Fuel Ratio - High Speed, Temperature Compensated	Opt. 2	Opt. 2
NTK or Bosch LSU Type	2	2
Range – Lambda	0.70 to 32.0	0.70 to 32.0
Resolution – Lambda	0.001	0.001
Useable as Auxiliary Sensor Inputs	2	2
DATA LOGGING		
Allows Logging of all ECU parameters	Opt. 1	Opt. 1
Memory Size	1Mb	1Mb or 4Mb
Individual Parameter & Rate Selection	✔	✔
Logging Rate – (samples per second)	1 to 200	1 to 200
Logging Time – 28 Par. + Diag. at 5/sec	76 minutes	up to 304 minutes
Interpret Software – Graphical Analysis	Opt 1 or Opt 2	Opt 1 or Opt 2
– Advanced Analysis	Opt. 3	Opt. 3
Maximum parameters logged	128	128
Maximum logging throughput	10 kbytes/sec	10 kbytes/sec
SPECIAL FUNCTIONS		
CAM Control	Opt. 7	Opt. 7
Drive by Wire	Opt. 8	Opt. 8
Traction Control & Launch Control	Opt.5 (2, 3 or 4 wheel)	Opt.5 (2, 3 or 4 wheel)
Narrow Band Lambda Control	✔	✔
Wideband Lambda Control	Opt. 2	Opt. 2
Gear Change Ignition Cut	Opt. 5	Opt. 5
Boost Enhancement (Anti-lag)	Opt. 5	Opt. 5
Warning Alarms (Sensor HI / LO)	✔	✔
Gear Detection	✔	✔
Ground Speed Limiting	✔	✔
Dual RPM Limit	✔	✔
Nitrous Oxide Enrich / Retard	✔	✔
Air Conditioner Request	✔	✔
Over Run Fuel Cut	✔	✔
Standard Sensor Calibrations	✔	✔
Programmable Sensor Calibrations	✔	✔
RPM Limit, Hard or Soft cut, fuel and/ or ignition	✔	✔
OUTPUTS		
Number of Auxiliary	8	8
All outputs are PWM or switched capable	✔	✔
4 Wire Stepper Motor Capable	✔	✔
Number of Outputs with High and Low Side drive	6	6
Auxiliary Outputs can be used for: Turbo Wastegate Control, Idle Speed Control; Fuel Used Output, Tacho Output; Shift Light, Driver Warning Alarm; RPM / Load dependent device; User definable Table (20x1) with selectable axis parameters; Slip Warning, Fuel Pump Relay; Thermatic Fan, Air Conditioner Fan and Clutch		
Unused Injector Outputs may be used for general functions as per	✔	✔
Auxiliary outputs	✔	✔
Unused Ignition Outputs may be used for general functions		
DIAGNOSTICS		
Injectors Open Circuit, Short Circuit, Peak Current not reached	✔	✔
Sensors Open & Short Circuit	✔	✔
Ref/Sync noise warning & error diagnostics (noise, runt pulses and amplitude)	✔	✔
Operating Errors: RPM Limit Exceeding, Injector overduty, Over Boost, Low Battery, REF Error etc.	✔	✔
TELEMETRY LINK		
Allows real time monitoring & data acquisition via a telemetry link	Opt. 4	Opt. 4

✔ Standard ✗ Not available Opt 1: Logging Opt 2: Lambda Single or Dual Opt 3: Pro Logging Opt 4: Telemetry Opt 5: Advanced Functions Opt 6: 10/12 Cylinder Opt 7: CAM Control Opt 8: Drive by Wire Opt 9: Multi Spark